Indian Geotechnical Journal, 35 (1), 2005

Engineering Aspects of Reinforced Soil*

Swami Saran†

General

Soil has been used as a construction material from times immemorial. Being poor in mechanical properties, it has been posing a challenge to civil engineers to improve its properties depending upon the requirement, which varies from site to site and the economic constraints. There are many techniques available for improving the mechanical and engineering properties of soil, and these can broadly be classified into following five major categories :

i) Soil stabilization

ii) Reinforced soil

iii) Soil nailing

iv) Texsol

v) Fibre reinforced soil or Ply soil

Attempt has been made to discuss below each method briefly.

Soil Stabilization

It is the process of improving the engineering properties of soil by mixing some binding agent thus binding the soil particles. In a broader sense, it also includes compaction, pre-consolidation and many more such processes. Soil stabilization reduces the permeability and the compressibility, improves bearing capacity and enhances its overall performance. Binding agents popularly used are lime, cement, bitumen, chemicals etc. Each one

---

* 27th Annual Lecture delivered at IGC-2004.

† Emeritus Fellow, Department of Civil Engineering, Indian Institute of Technology Roorkee, Uttaranchal, India.

has its merits and demerits. Mechanical stabilization involves altering the gradation of soil. Cement and lime stabilization employs the addition of cement or lime in specific proportion. In Bituminous stabilization, hydrocarbon of a specific grade is used. Similarly, in chemical stabilization, different chemicals are added. Thermal stabilization involves the heating or freezing of soil.

Reinforced Soil

Reinforcement in different forms is added to soil in order to improve its mechanical properties. Soils are strong in compression but weak in tension. This weak property of soil is improved by introducing reinforcing elements in the direction of tensile stress. Reinforcement material generally consists of galvanized or stainless steel strips, bars, grids or fabrics of specified material or wood, polymer and plastic etc. The reinforcement is placed more or less in the same way as steel in concrete. The end product is called reinforced soil and is very effectively used for retaining structures, embankments, footings and subgrade etc.

Soil Nailing

It is a method of reinforcing the soil with steel bars or other materials. The purpose is to increase the tensile and shear strength of the soil and restrain its displacements. The nails are either placed in drilled bore holes and grouted along their total length to form "grouted nails" or simply driven into the ground as "driven nails'. The technique permits stabilization of both the natural slopes and vertical or inclined excavations.

Texsol

It is a composite material made up of sand and continuous polyester fibres mixed together insitu to form a homogeneous construction material. The fibre content varies from 0.10% to 0.25% of dry weight of sand. The added fibres provide cohesion and impart ductility to the composite material. The sand is generally well graded and medium to coarse for good internal friction.

Substantial testing programmes have been conducted on Texsol by state agencies, universities and research institutions in France and Japan since 1984. Texsol includes high shear resistance, cohesion, low creep potential, large energy absorption capacity with respect to impact, explosions, large tolerance to differential settlements, high resistance to surface runoff and high thermal resistance (upto 600° F). Texsol also provides a suitable environment for plant roots to penetrate and seeds to germinate. Because of its remarkable feature, Texsol has been increasingly used in a variety of

engineering applications. These include earth retaining walls; specifically on soft compressible soil with a slope angle of 65° to 70° with horizontal.

In Japan, a series of shake table tests were performed on 0.4 m high earthen embankment models of loose sand under three conditions: unreinforced, reinforced with a dense sand layer and reinforced with a Texsol layer. The model was dynamically loaded and settlement of the crest was compared after 4 secs. of loading. Results revealed that a settlement of 25 mm occurred in unreinforced model whereas settlement was zero for the Texsol reinforced model. It clearly demonstrated the effectiveness of Texsol under dynamic loads.

Ply Soil

Randomly distributed fibres in soil – termed as RDFS is among the latest techniques in which fibres of a desired type and quantity are added in the soil, mixed and laid in position. The composite material is called 'ply soil'. Thus, the method of preparation of RDFS is similar to the conventional stabilization techniques.

RDFS is different from the other geosynthetic methods in its orientation. In reinforced earth, the reinforcement in the form of sheets etc., is laid horizontally at specific intervals, whereas in RDFS, the fibres are mixed randomly in soil, thus making a homogeneous mass and maintain the isotropy in strength. Improvement of soil by tree roots is similar to the work of fibres. While building the Great Wall of China, clay soil was mixed with tamarisk branches. The addition of straw of wheat locally called "turi" to the clay-mud plaster is also very popular in villages and is an ancient technique.

Experimental work by various investigators from last many years has established beyond doubt that addition of fibre in soil improves the overall engineering performance of soil. Among the notable properties that improve are, greater extensibility, small loss of post peak strength, isotropy in strength and absence of planes of weakness. Thus, RDFS has been used in many civil engineering projects in various countries in the recent past and the further research is in progress for the many hidden aspects of it.

In this paper, salient features of the work conducted on Reinforced soil at Indian Institute of Technology, Roorkee is presented.

Reinforced Soil

Reinforced soil is a composite material which is formed by the association of frictional soil and tension resistant elements in the form of sheets, strips, nets or mats of metal, synthetic fabrics or fibre reinforced

plastics and arranged in the soil mass in such a way as to reduce or suppress the tensile strain which might develop under gravity and boundary forces. It is well known that most granular soils are strong in compression and shear but weak in tension. The performance of such soils can be substantially improved by introducing reinforcing elements in the direction of tensile strains in the same way as in reinforced concrete.

The variety and the range of application of reinforced soil technique is unlimited. Jones (1978) identified several field applications, viz., retaining walls, abutments, quay walls, embankments, dams, hill roads, housing, foundations, railways, industry, pipe works, waterway structures and underground structures. Some of the field applications are illustrated in Figs. 1a to 1k.

In summary, it can be concluded that soil-reinforcement technique results in : i) a simple composite material, quick and easy to make; ii) a flexible material, able to with- stand important deformations without damage; iii) a heavy material both from the technical and architectural points of view and iv) an economical material. These merits of reinforced soil enabled its use in almost all civil engineering structures (Saran et al., 1978).

A systematic research on reinforced soil was initiated in IIT Roorkee in 1976 which continued upto 2002. It included the following:

i) Strength-deformation characteristics of reinforced soil

ii) Soil-reinforcement interface friction

iii) Reinforced earth wall

iv) Wall with reinforced backfill

v) Shallow foundation on reinforced soil slab

vi) Dynamic elastic constants of reinforced soil

vii) Frame structure – foundation – soil / reinforced soil interaction

Strength-Deformation Characteristics of Reinforced Soil

The fact that reinforcement influences the stress-strain characteristics of soil and increases its strength, can be demonstrated by the usual strength tests. Many research workers have studied the phenomenon of strength enhancement by subjecting reinforced soil samples to triaxial compression or plane-strain loading. For this purpose, reinforced soil has been assumed to be an equivalent homogeneous material and the stress-strain and strength characteristics have been investigated for samples of cohesionless soil reinforced with discs, rings or fibres of different reinforcing materials (Long

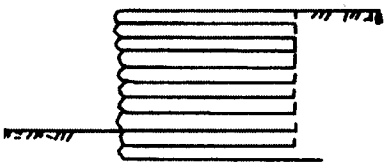

(a) For providing sharp differences of levels between two horizontal platforms

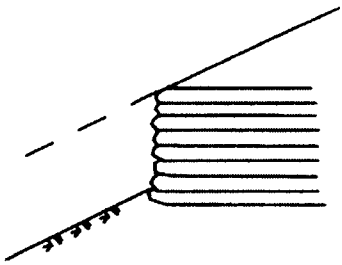

(b) For supporting and also being a boundary to a large inclined embankment

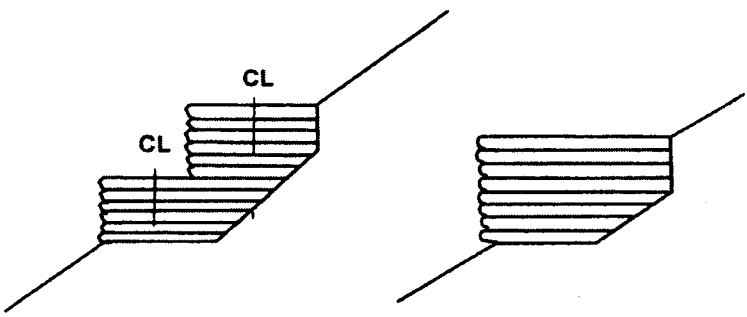

(c) For providing horizontal platforms on sloping ground

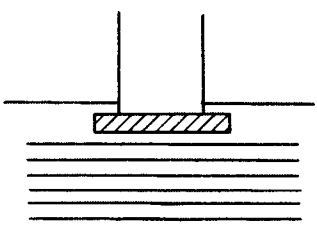

(d) As foundation slab

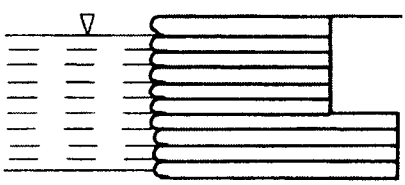

(e) As quay walls

FIGURE 1 : Uses of Reinforced Earth

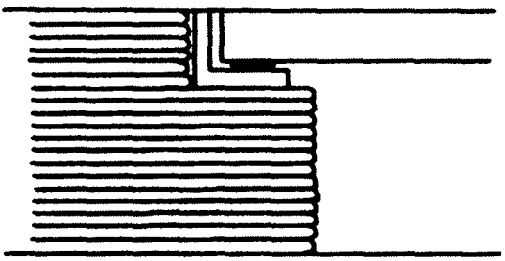

(f) As bridge abutment

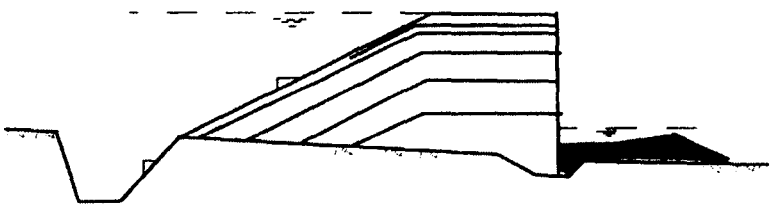

(g) As reinforced earth dam (after Cassard et al., 1979)

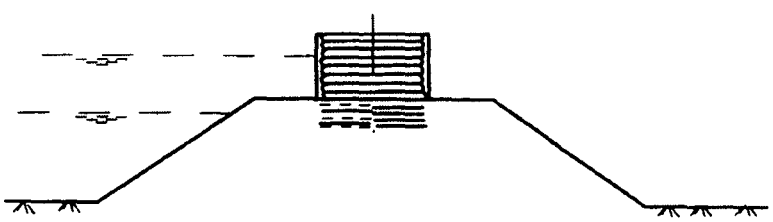

(h) For raising height of existing dam

FIGURE 1 : Continued ...

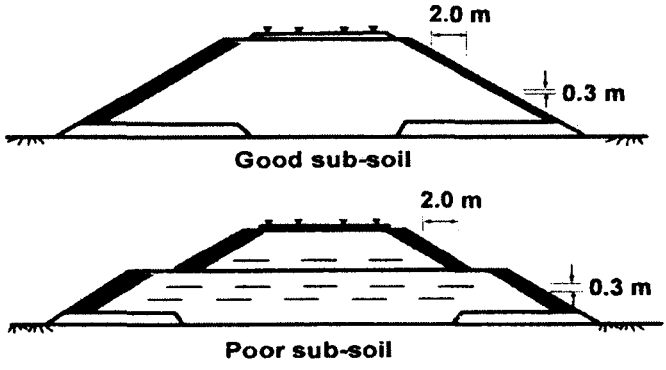

(i) As railway embankment

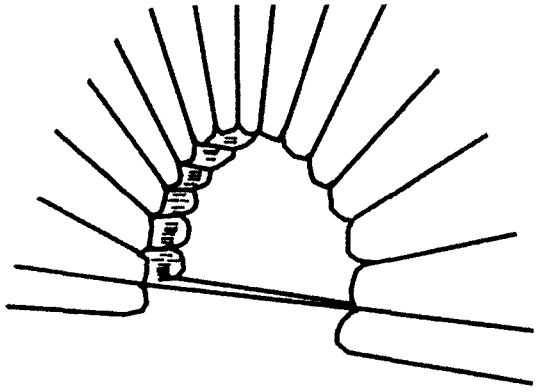

(j) As reinforced earth arch

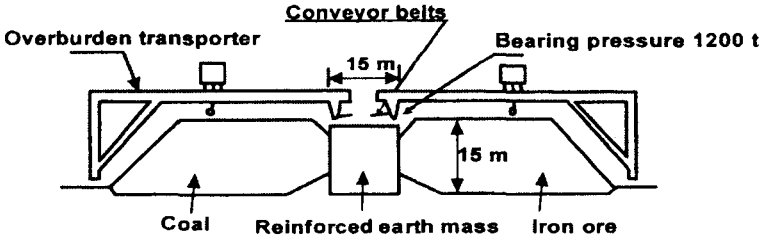

(k) For bulk storage handling

FIGURE 1 : Continued ...

et al., 1972; Yong, 1972; Hausmann, 1976; Broms, 1977; Mc.Gown and Andrawes, 1977; Verma and Char, 1978; Talwar, 1981; Saran and Talwar, 1983; Talwar et al., 1987; Garg, 1988; Garg and Saran, 1991; Singh, 1991;Youssef, 1995; Saran et al., 2004). These studies have indicated appreciable increase in the deviator stress and revealed two different patterns of failure of reinforced soil samples – one in which the failure is caused by the rupture of reinforcement and the second in which the failure is due to slippage between the soil and the reinforcement. Figure 2 shows the shape of samples in the two failure modes. The stress-strain characteristics for the two failure modes are different (Fig.3). The rupture failure mode is characterized by a well-defined peak deviatoric stress at failure and reduced failure strain as compared to the unreinforced soil. The stress-strain curves for the other failure mode (slippage failure) do not exhibit well-defined peaks and failure strains indicate a ductile behaviour for the reinforced samples in much the same way as that of unreinforced samples. Obviously, the strength in the rupture failure mode is governed by the tensile strength of reinforcing elements, whereas in the slippage mode, it is a function of the friction which develops at the soil-reinforcement interface, other conditions being the same.

The mode of failure has a profound effect on the strength envelop of the reinforced earth. Rupture failure of reinforced earth leads to a strength envelop which is virtually parallel to that of unreinforced soil but exhibits a cohesion intercept which is a function of the rupture strength of reinforcement and its distribution in the sample (Fig.4). Slippage failure, on the other hand, leads to

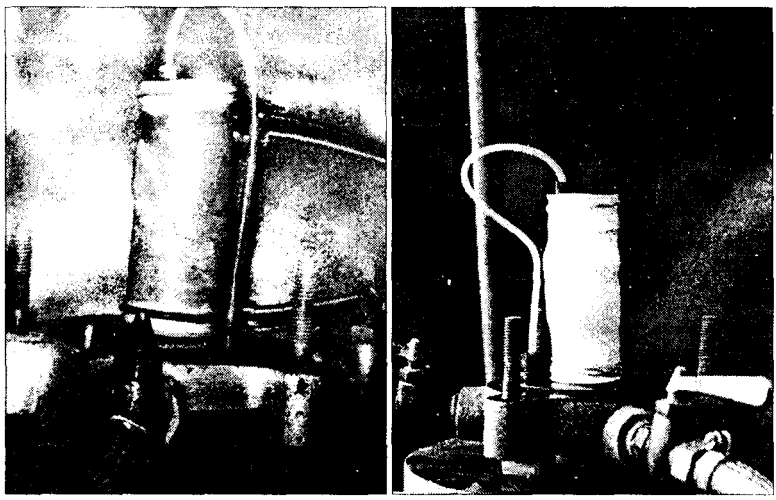

(a) Rupture Failure Mode *(b) Slippage Failure Mode*

FIGURE 2 : Condition of Failure in Triaxial Samples

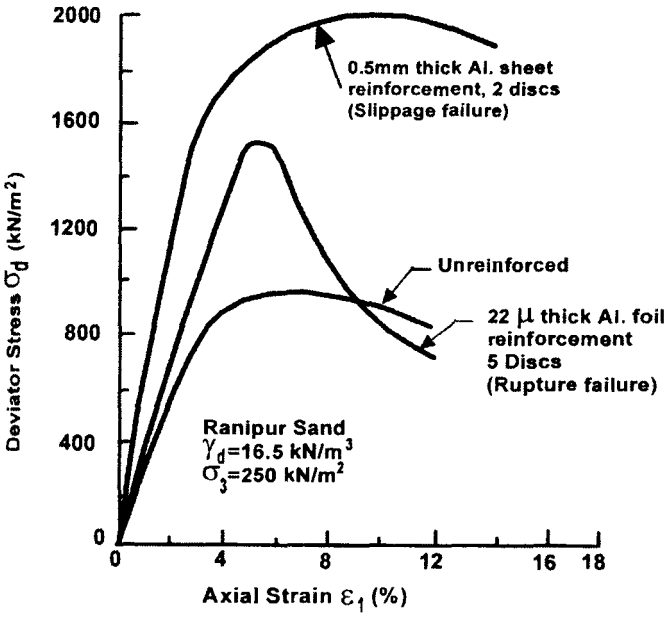

FIGURE 3 : Stress-Strain Behaviour of Reinforced and Plain Sand (Talwar, 1981)

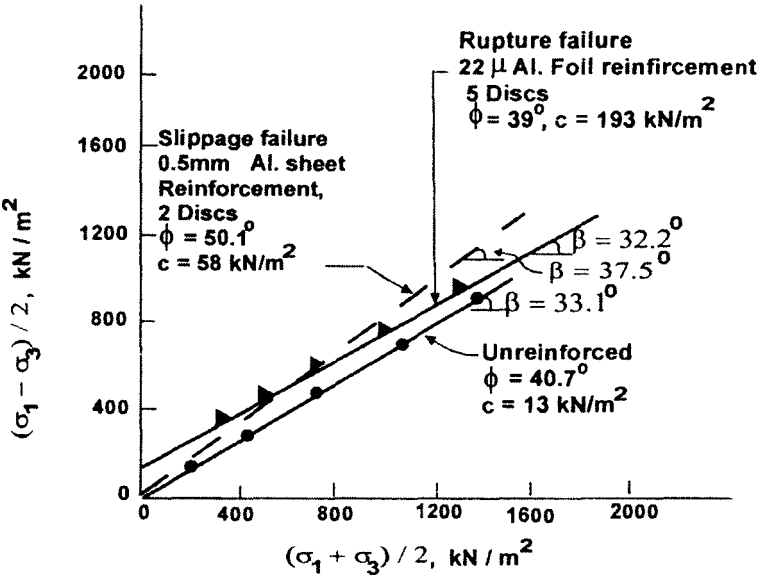

FIGURE 4 : Strength Envelops of Reinforced and Plain Sand (Talwar, 1981)

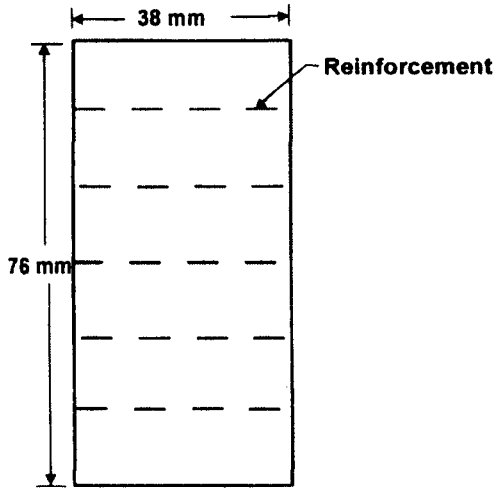

FIGURE 5 : Pattern of Reinforcement in Triaxial Sample (Talwar, 1981)

an increase in the friction angle ϕ, with little or no cohesion intercept. Thus, the experimental studies confirm the basic concepts postulated by Schlosser and Long (1970) and theoretical models developed by Hausmann (1976).

To illustrate the effect of reinforcement on the strength parameters of soil quantitatively, investigations of Saran and Talwar (1983) and Singh (1991) have been briefly summarised below :

Saran and Talwar (1983) conducted triaxial compression tests on samples of soil reinforced with discs of different materials as shown in Fig.5. The soil used was dry Ranipur sand (SP, D_{10} = 0.13 mm, C_u = 1.85). The materials for reinforcing the triaxial samples were so chosen that failure could be achieved both by rupture of reinforcement and by slippage between reinforcement and soil. The following reinforcing materials, arranged in increasing order of strength, were employed:

i) Aluminium foil 22 micron thick (R_T = 3.3 kN/m)
ii) Aluminium foil 50 micron thick (R_T = 7.5 kN/m)
iii) Fibre glass cloth 0.08 mm thick (R_T = 13.5 kN/m) and
iv) Aluminium sheet 0.5 mm thick (R_T = 71 kN/m)

The reinforcements in the form of discs of 35 mm diameter were used in five beds (Fig.5). The tests were performed on sand at two densities namely, 16 kN/m^3 and 16.5 kN/m^3 which correspond to medium dense and dense states (D_R = 67.9% and 79.5%) respectively. The tests were performed

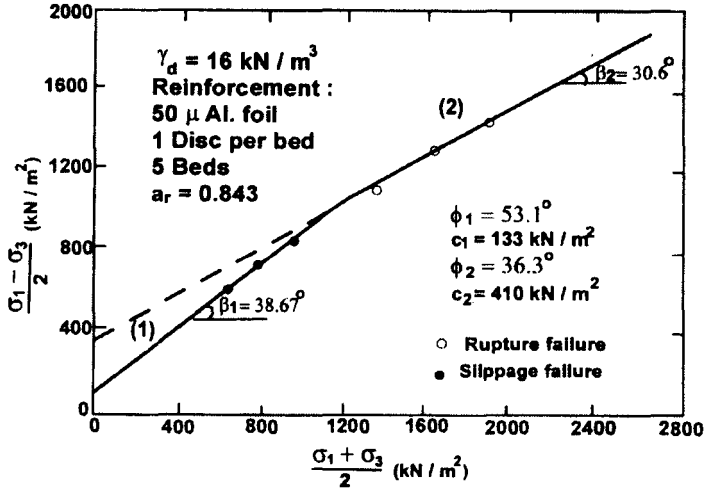

FIGURE 6 : Mohr's Envelop (Talwar, 1981)

TABLE 1 : Shear Strength Parameters of Reinforced Sand (Talwar, 1981)

Type of sample	Cohesion c, kN/m^2	Angle of Internal Friction, ϕ (Deg.)	Failure Mode	Remarks
MEDIUM DENSE SAND, D_R = 67.9%				
1. Unreinforced	10	38.5	Shear	
2. Reinforced with				
(a) 22 μm Al. foil	170	37.0	Rupture	i) Sample was reinforced as shown in Fig.5
(b) 50 μm Al. foil	133	53.0	Slippage $\sigma_3 < 100$ kN/m^2	
	410	37.0	Rupture $\sigma_3 > 100$ kN/m^2	ii) σ_3 is confining pressure
(c) Fibre glass cloth 0.08 mm thick	166	46.0	Partly rupture	
DENSE SAND, D_R = 79.5%				
1. Unreinforced	13.2	41.0	Shear	
2. Reinforced with				
(a) 22 μm Al. foil	118	40.5	Rupture	
(b) 50 μm Al. foil	80	64.2	Slippage $\sigma_3 < 100$ kN/m^2	σ_3 is confining pressure
	365	40.0	Rupture $\sigma_3 > 100$ kN/m^2	
(c) 0.5 mm Al. sheet	58	50.1	Slippage	

at different confining pressures varying from 20 kN/m^2 to 500 kN/m^2. A typical Mohr's envelop plot is shown in Fig.6. The results obtained from this study are listed in Table 1.

Singh (1991) conducted triaxial compression tests on Amanatgarh Sand (SP, D_{10} = 0.19 mm, C_u = 1.58) placed at relative density of 75%. The samples were reinforced with: i) Woven white geotextile (W) and ii) Woven black geotextile (B). The properties of the two geotextiles are given in Table 2.

The soil samples were reinforced as shown in Fig.7. The tests were performed at different confining pressures varying from 50 kN/m^2 to 500 kN/m^2. The results obtained from this study are given in Table 3.

It may be noted from Tables 1 and 3 that at higher confining pressures, mode of failure changes from slippage to rupture. This is due to the fact that dilatation of sand is reduced at higher confining pressures and so the tensile force on the reinforcing disc is not much. This leads to reduced frictional force at soil-reinforcement interface. Hence, friction angle, ϕ is not much affected at higher confinement. But at higher confinement, strength gain is a consequence of the utilization of tearing strength of the reinforcement. Since tearing strength of the reinforcement is not a function of confinement, strength of reinforced samples increases slowly with the confining pressure leading to reduced friction angle at high confinement. Further, it may be noted from the results presented in Table 3 that the strength of soil increases with the increase in the amount of reinforcement.

TABLE 2 : Properties of Different Geotextiles

S. No.	Item Description	Value	
1.	Quality No. (styles)	White (W)	Black (B)
2.	Material	100 % Polypropylene	
3.	Specific Gravity	0.91	0.91
4.	Weight/Eq. Meter in gms.	303.00	276.00
5.	Thickness in mm (@ 100 gm/cm^2)	0.78	0.68
6.	Breaking Strength: (IS:1969-1963) (5 × 10 cms)		
	Warpway (kg)	390.1	245.7
	Weftway (kg)	333.0	182.0
7.	Tear Strength: (Single rip) (ASTM-D-1982)		
	Wrapway (kg)	69.3	21.2
	Weftway (kg)	71.6	18.0

TABLE 3 : Shear Strength Parameters of Reinforced Sand (Singh, 1991)

Type of sample	Cohesion c, kN/m^2	Angle of Internal Friction, ϕ (Deg.)	Failure Mode	Remarks
1. Unreinforced	15	39	Shear	
2. Reinforced with white geotextile (Ref. Fig.7)				
(a) W_1	33	41	Rupture	
(b) W_2	50	46	Partly rupture	
(c) W_3	34	54	Slippage $\sigma_3 \leq 100$ kN/m^2	σ_3 is the confining pressure
	290	38	Rupture $\sigma_3 \geq 100$ kN/m^2	
(d) W_4	20	60	Slippage $\sigma_3 \leq 100$ kN/m^2	
	350	38	Rupture $\sigma_3 \geq 100$ kN/m^2	
3. Reinforced with black geotextile (Ref. Fig.7)				
(a) B_1	20	41.5	Rupture	
(b) B_2	35	50	Slippage $\sigma_3 \leq 100$ kN/m^2	
	240	39	Rupture $\sigma_3 \geq 100$ kN/m^2	
(c) B_3	60	54	Partly Rupture $\sigma_3 \leq 200$ kN/m^2	σ_3 is the confining pressure
	280	40	Rupture $\sigma_3 \geq 200$ kN/m^2	
(d) B_4	100	56	Slippage $\sigma_3 \leq 200$ kN/m^2	
	450	38	Rupture $\sigma_3 \geq 200$ kN/m^2	

Soil-Reinforcement Interface Friction

The friction between the earth and the reinforcement is an essential phenomenon in the reinforced soil. The traction forces developed within the soil are transmitted to the reinforcements by means of soil-reinforcement interface friction. Due to this soil-reinforcement interaction, the composite mass

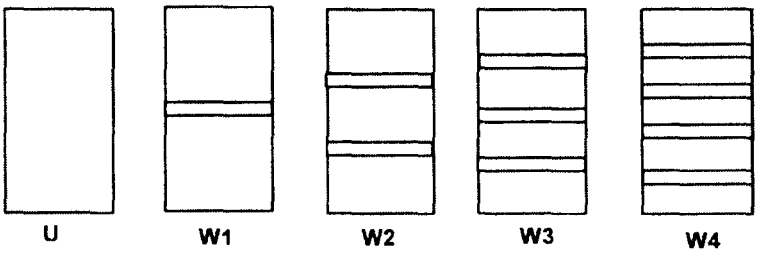

(a) Reinforced with White Geotextile

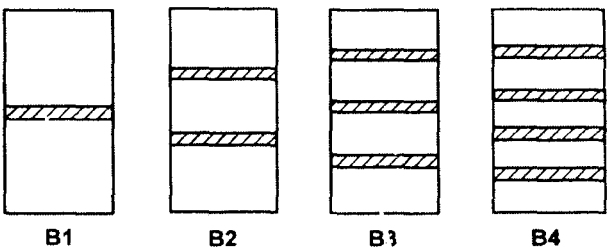

(b) Reinforced with Black Geotextile

FIGURE 7 : Pattern of Reinforcement in Triaxial Sample (Singh, 1991)

behaves as if it possessed, in the direction of the reinforcement, a cohesion proportional to the resistance of the reinforcement to tension. The mechanism of the development of interface friction between soil and the reinforcing element is a complex phenomenon and is not yet very well understood.

In order to estimate the coefficient of soil-reinforcement interface friction, normally one of the following two tests is performed : i) tests using the direct shear-box with soil in one half of the box and the reinforcing material in the other half, known as sliding shear test and ii) pull-out tests on reinforcement buried either within an embankment of soil or within a reinforced soil wall. In sliding shear tests, sliding of soil mass over a stationary reinforcement takes place and in pull-out tests, the reinforcement is pulled out of the stationary soil mass. From the mechanics point of view, the sliding test is akin to kinetic or rolling friction condition, while static friction condition prevails in pull-out tests. However, the interaction mechanisms are not so simple.

In sliding shear tests, the soil movement is minimum at the interface as the movement of soil is restrained by the reinforcement and increases with distance away from it (Fig.8a) whereas in the case of pull-out, the soil movement at the interface is maximum, since the soil resists the movement

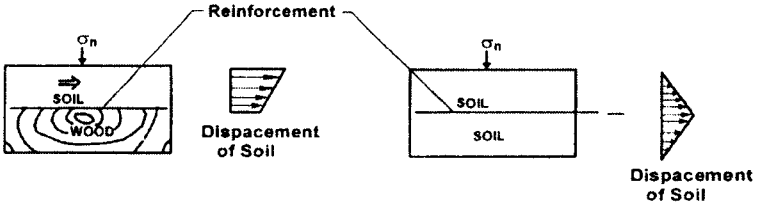

(a) Sliding *(b) Pull-out*

FIGURE 8 : Soil Movement in Mobilization of Interfacial Friction Resistance

of reinforcement and reduces away from it (Fig.8b). The above relative movements induce a near constant volume condition for pull-out tests and constant normal stress condition for sliding shear tests. In the pull-out case, an increased effective normal stress on the reinforcement is induced which is not monitored. However, in a sliding shear test, the effect of dilation is reflected in an increased shear force, which is monitored. Keeping in view the relative movements of soil and the reinforcement, it can be suggested that coefficient of apparent soil-reinforcement friction, f^* obtained from the pull out tests should be used in case of reinforced earth retaining walls, since at the time of friction failure, the reinforcement is pulled out from the stationary soil mass (resisting zone) (Fig.9a). Similar is the case of footing placed on loose to medium sand and reinforced with flexible reinforcement where punching shear occurs causing the reinforcement pullout (Fig.9b). Values of coefficient of friction, μ $(=\tan\delta)$ obtained from sliding shear tests can be used for designing a footing resting on dense sand reinforced with stiff reinforcement (Fig.9c), where soil slides past the reinforcement. However, in case of wall with reinforced backfill, both types of relative movement can occur. In the upper region the reinforcement is pulled out of the soil mass whereas in lower region, soil moves past the reinforcement (Fig.9d).

Sliding shear tests

In the past, many investigators have used a sliding shear box to obtain the coefficient of interfacial friction between soil and the reinforcement (Schlosser and Elias, 1978; Mallinder, 1978; Mckittrik, 1978a; Walter, 1978; Talwar, 1981; Miyamori et al., 1986; Haji Ali and Tee, 1988; Rao and Pandey, 1988; Kate et al., 1988; Mandal and Divshikar, 1988; Garg, 1988; Saran and Khan, 1989a; Khan, 1991). The general conclusion derived from their work was that the coefficient of sliding friction between soil and the reinforcement (μ) increases with increase in the unit weight of soil and roughness of the reinforcing material. To illustrate this aspect, work of Khan (1991) has been described briefly in the subsequent paragraphs.

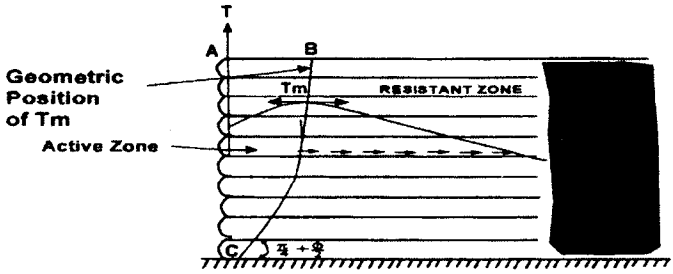

(a) Pull-out Resistance

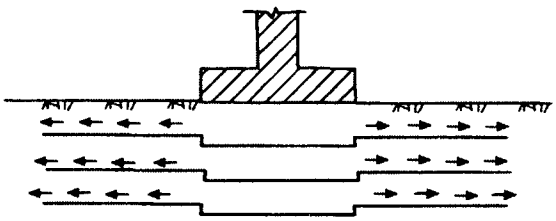

(b) Pull-out Resistance (Loose Sand)

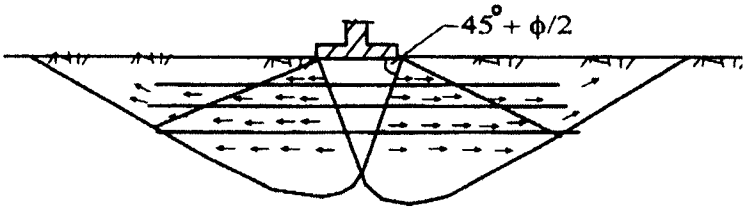

(c) Sliding Resistance (Dense Sand)

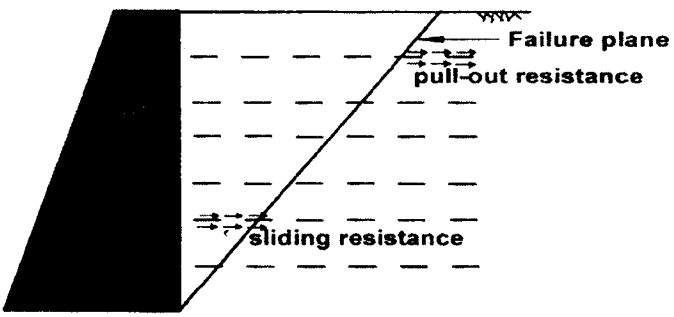

(d) Both Pull-out and Sliding Resistance

Figure 9 : Schematic Diagram Showing Sliding and Pull-out Resistance

TABLE 4 : Engineering Characteristics of Amanatgarh Sand

S. No.	Unit Weight (kN/m^3)	Relative Density D_R (%)	Angle of internal friction, ϕ (obtained from direct shear test)
1.	15.5	55	33°
2.	16.0	60	37°
3.	16.5	81	41°

Khan (1991) performed sliding shear tests on Amanatgarh Sand (C_u = 1.30 and D_{10} = 0.185 mm) placed at different relative densities. The engineering properties of the sand are given in Table 4.

Bamboo strips, Aluminium strips, Nylon niwar, Netlon CE-121, Netlon CE-131 (geogrids), Bombay dyeing geofabric PD-380B and PD-381 were used as reinforcing materials for different studies. Properties of these materials are presented in Table 5. Bamboo strips were recovered by stripping the bamboo along its outer periphery and then cut to desired size. Aluminium strips of desired sizes were cut from 0.3 mm thick aluminium sheet.

Sliding shear tests were performed in 60 mm × 60 mm and

TABLE 5 : Details of Reinforcements

S. No.	Reinforcement	Symbol used	Properties			
			Width (mm)	Thickness (mm)	Rupture Strength	
1.	Bamboo strips	R-1	20 to 30	1 to 2	1275 kg/cm	
2.	Aluminium strips	R-2	40	0.3	41.75 kg/cm	
3.	Nylon niwar	R-3	32	1.4	50 kg/cm (width)	
4.	Woven geotextile*		Breaking strength (kg) 5 × 20 cm – IS:1969-1963		Pore size in (micron)	
			Warp way	Weft way	Mean	Max
	(a) PD-381	R-4	257.7	181.9	102	230
	(b) PD-380B	R-5	247.7	182.0	25	69
5.	Netlon geogrids*		Max. Load (kN/m)	Mesh aperture size (mm)	Mesh thickness (mm)	
	(a) CE-121	R-6	7.68	8 × 6	3.3	
	(b) CE-131	R-7	5.80	27 × 27	5.2	

* Properties given by manufacturer

TABLE 6 : Sliding Shear (60 mm × 60 mm Box) Test Results

Reinforcement	Unit weight, kN/m^3			Remarks
	15.5	16.0	16.5	
	Sliding friction angle, δ			
R-1	31.0°	34.0°	36.0°	Sheared along longitudinal direction
R-1	38.0°	38.5°	42.0°	Sheared along transverse direction
R-2	23.0°	25.0°	25.5°	–
R-3	32.0°	34.0°	36.0°	–

315 mm × 315 mm size boxes. Reinforcements R-1, R-2 and R-3 were tested in a small shear box (60 mm × 60 mm). In larger shear box (315 mm × 315 mm), reinforcements R-1, R-4, R-5, R-6 and R-7 were tested. The test results obtained are summarized in Tables 6 and 7.

Table 6 shows that the angle of friction increases with increase in the density of sand for reinforcements R-1, R-2 and R-3. Further, it is interesting to note that there is a significant effect of the direction along which the reinforcement is placed. The value of friction angle for R-1 when placed in transverse direction was found to be even more than the angle of internal friction of soil. Perhaps, it is due to the additional resistance provided by the grains of R-1 material against sliding when its strip is placed in the transverse direction (Khan and Saran, 1990).

TABLE 7 : Sliding Shear (315 mm × 315 mm Box) Test Results

Reinforcement	Unit Weight, kN/m^3		
	15.5	16.0	16.5
	Sliding friction angle, δ		
R-1	29.5°	31.0°	32.5°
R-4	31.5°	32.5°	33.0°
R-5	31.0°	32.0°	32.0°
R-6	28.0°	28.5°	28.5°
R-7	27.0°	28.0°	30.0°

The results of sliding shear tests performed in a bigger box i.e. 315 mm × 315 mm (Table 7) showed a similar trend as discussed above. However, the values of friction angle were found to be lesser than those obtained in a smaller box. The reason may be attributed to the fact that as in longer strips, full friction may not be mobilized simultaneously (Khan and Saran, 1990).

Angle of interfacial friction between the sand and reinforcement was always less than the angle of internal friction of soil, except when the bamboo strip grains were in transverse direction.

Pull-out tests

Pull-out tests are performed to obtain the value of coefficient of apparent soil-reinforcement friction, f^*. These tests may be performed in a model, prototype or full scale reinforced soil wall. In these tests, reinforcing strips are pulled out from the wall and for each strip, a plot is made between the pull-out load and the corresponding displacement. From this plot, maximum pull-out load is obtained. The coefficient of apparent friction, f^* is given by:

$$f^* = \frac{T}{2\sigma_v LW} \tag{1}$$

where

T = Maximum pull-out load

σ_v = Normal pressure intensity at the reinforcing strip level = $\gamma Z + q$

γ = Unit weight of soil

Z = Depth of the reinforcing strip below soil surface

q = Intensity of uniformly distributed surcharge on the soil surface

L = Length of reinforcing strip

W = Width of reinforcing strip

The coefficient, f^* given by Eqn.1 does not take into account the actual distribution of normal stress exerted on the reinforcement, but the mean value of the overburden stress i.e. ($\gamma Z + q$).

The coefficient, f^* is a complex function of a number of parameters, e.g., height of soil above the reinforcement, length and width of the reinforcing elements, surface condition of the reinforcement and density of

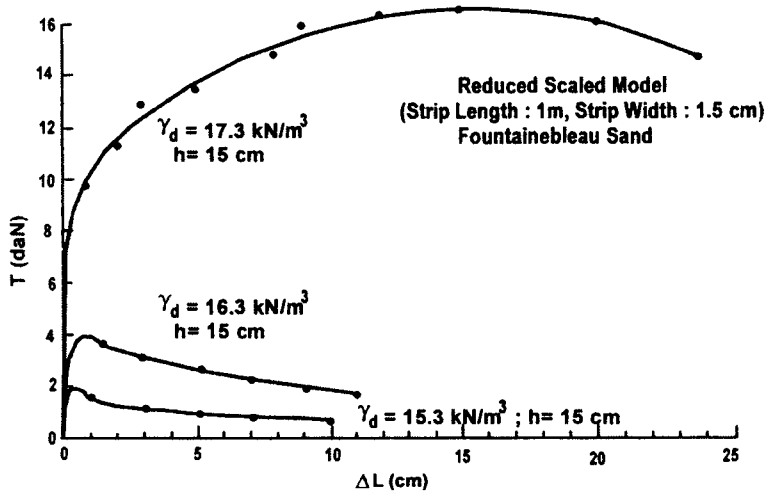

Figure 10 : Influence of the Density in Pull-out Test (After Schlosser and Elias, 1978)

soil. Schlosser and Elias (1978) demonstrated that the principal factors affecting the f^* values for the cohesionless soils are: i) the density of embankment (Fig.10), ii) the state of the surface of the reinforcements (Fig.11) and iii) the normal pressure on the reinforcements (Fig.12). These results evinced the effect of the phenomenon of dilatancy within the granular media. The shear stress generated along the reinforcement results in

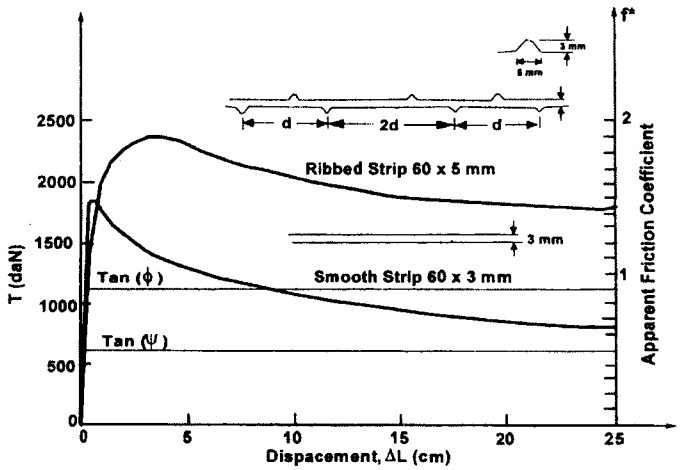

FIGURE 11 : Pull-out Test in Reinforced Earth Walls (influence of the Nature of the Strip Surface) (After Schlosser and Elias, 1978)

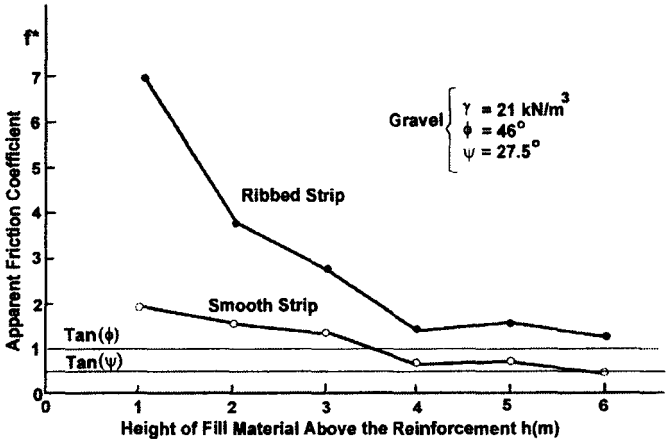

FIGURE 12 : Pull-out Tests – Apparent Friction Coefficient (After Schlosser and Elias, 1978)

increasing the normal stress σ_v. Bacot et al. (1978) explained this aspect experimentally with the help of photometric technique that pull-out load acting on the embedded reinforcing strip induces shear displacements in the zone of surrounding soil. Surface condition of the reinforcement significantly controls the volume of the dilatant zone. In a compacted granular soil around a reinforcing strip, the sheared zone tends to dilate but this volume change is restrained by the surrounding soil. This restraining effect results in an increase in the normal stress on the reinforcement (Fig.13).

Mckittrik (1978) discussed in detail the mechanism of the pull-out resistance from the point of view of shear stress relationship between the reinforcement and the soil. Varying soil-strip shear characteristics are shown

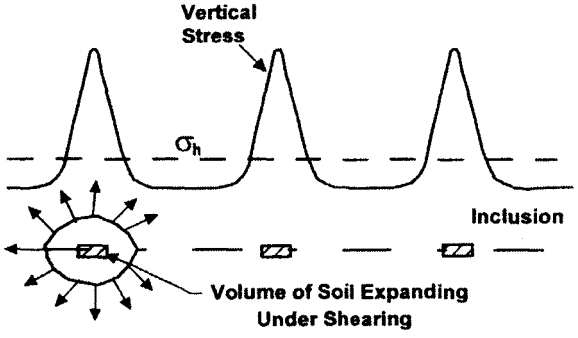

FIGURE 13 : Mechanism of Soil Inclusion Interaction in Dilatant Soil (After Bacot, 1981)

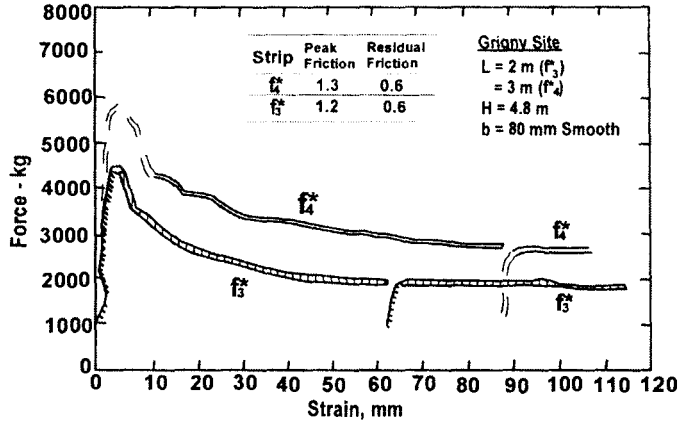

FIGURE 14 : Pull-out Force vs. Strain for Smooth Strip (Mckittrik, 1978)

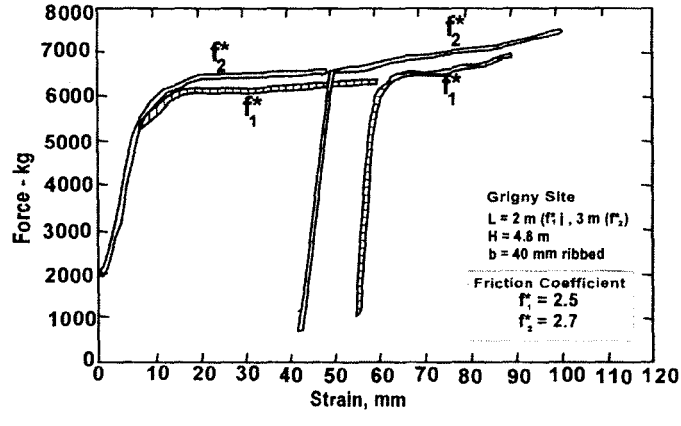

FIGURE 15 : Pull-out Force vs. Strain for Ribbed Strip (Mckittrik, 1978)

in Figs. 14 and 15. A smooth reinforcing strip exhibited peak shearing resistance and then at large strains, a residual shearing resistance which was about 50% or less of the peak value. Data collected from both the laboratory and field pull-out tests is depicted in Figs. 16 and 17. It was concluded that in the case of smooth strips, soil-strip friction characteristics control the behaviour and in the case of ribbed or roughened strips, the soil-soil characteristics control the behaviour most often.

Studies on the effect of various parameters on f^* have also been conducted at Indian Institute of Technology, Roorkee (Talwar, 1981; Garg, 1988; Saran and Khan, 1989a; Khan, 1991; Saran, 1998) using different reinforcing materials. All these investigators observed similar trends of

variation of f^* with length, width, overburden pressure and the density in the same way as the findings of earlier investigators (Bacot, 1978; Mckittrik, 1978; Schlosser and Elias, 1978). For illustration, salient features of the work done by Garg (1988) are reported herein. Garg (1988) performed tests in a wooden tank of 1.40 m × 1.40 m × 1.0 m (high). The sides and bottom of the box were made up of 30 mm thick wooden planks suitably stiffened by cast iron angles and plates. A rectangular slit of 50 mm × 5 mm was cut, 100 mm above tank bottom on one side, to facilitate the pulling of strip of reinforcing material. The close-up of the pulling device is shown in Fig.18. The strip was pulled out at the rate of 0.25 mm per minute with the help of turret gear box. The pull-out resistance and corresponding displacements were recorded by a proving ring and a dial gauge respectively. The base frame butted against the tank side, which provided reaction to the pull. The sand, classified as SP (D_{10} = 0.09 mm, C_u = 2.22), was deposited by the rainfall technique to yield a dry unit weight of 16.0 kN/m^3 in the tank. Summary of the details of pull-out tests is provided in Table 8.

Figures 19 and 20 provide the results of pull-out tests for aluminium and bamboo strips respectively. For lengths of reinforcing strips employed in the model tests, results have shown a linear increase in the value of soil-reinforcement interface friction coefficient (f^*) for each height of soil overburden. These results could be utilized in determining the value of f^* for other lengths of strips which are in the range of lengths tested. Value of f^*

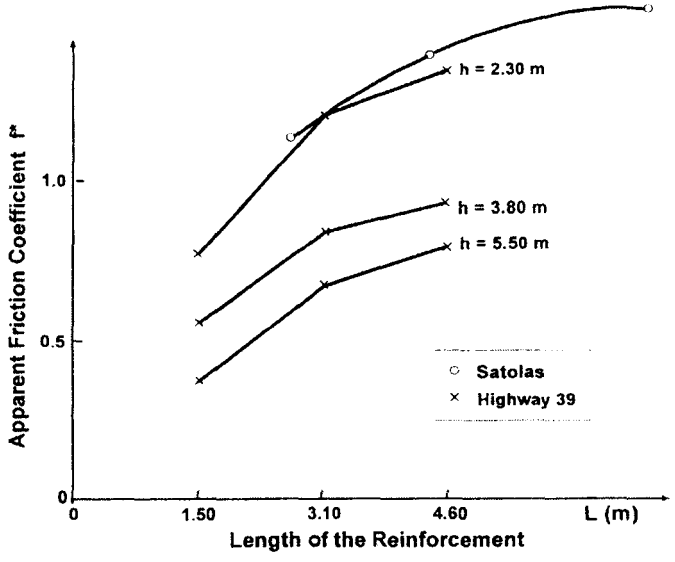

FIGURE 16 : Pull-out Tests – Apparent Friction Coefficient (Influence of the Length of the Reinforcement (After Mckittrik, 1978)

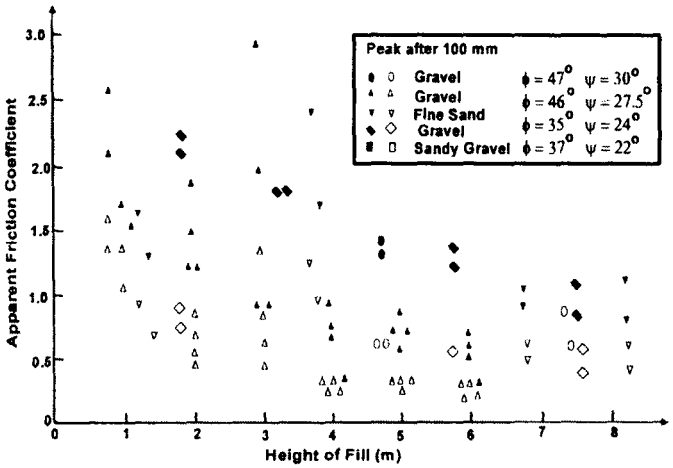

(a) Influence of the Overburden Pressure, Smooth Strips

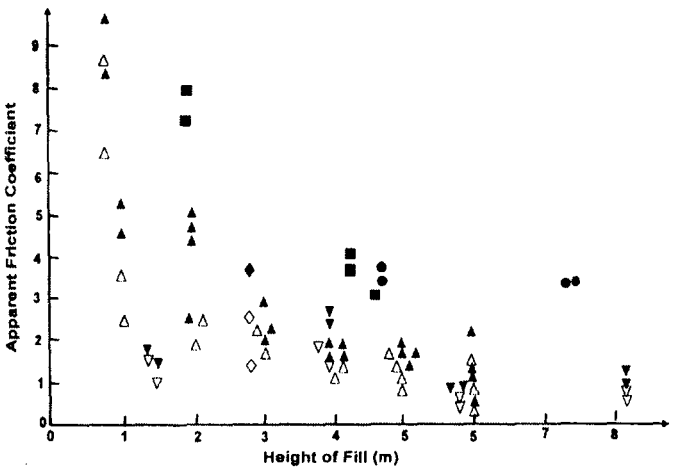

(b) Influence of the Overburden Pressure, Ribbed Strips

FIGURE 17 : Pull-out Tests – Apparent Friction Coefficient (After Mckittrik, 1978)

decreases nonlinearly with the height of overburden and tends to become asymptotic at higher values of overburden (Figs. 19 and 20). These observational trends are valid for the experimental range of heights of overburden (Garg and Saran, 1990; Kumar and Saran, 2000c).

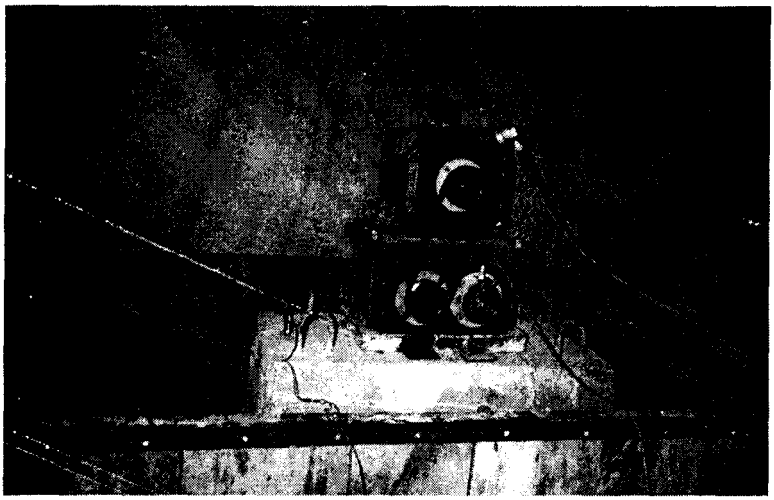

FIGURE 18 : Experimental Setup for Vertical Block Vibration Tests

Comparative evaluation of the two techniques of shear box and the pull-out test for evaluating the soil-reinforcement friction characteristics was presented by Ingold (1984). Three geotextiles (two fabrics + one geogrid) were used in the experimental study. Soil used was coarse to medium sand. The investigation included i) the 60 mm × 60 mm and 300 mm × 300 mm fixed shear box tests in which the geotextile was fixed to a rigid spacer block inserted in the lower half of the shear box with soil in the upper half; ii) the 300 mm × 300 mm free shear box tests wherein geotextile was clamped at one end of the shear box and the soil was deposited in both the halves of shear box; iii) the pull-out tests in a box of size 285 mm × 500 mm. The consolidated drained tests were run with a uniform speed of 1 mm/min on all the samples. The difficulty in interpreting the pull-out test data, because of the extensibility of the geotextile, was discussed. Test-results reported (Fig.21) showed a marked difference in the values of shear stress obtained from different tests. The need was emphasized for further research on the effect of geotextile extensibility on its reinforcing capability.

TABLE 8 : Summary of Pull-out Tests

S. No.	Material of Strip	Height of Overburden (mm)	Width of strip (mm)	Length of Strip (mm)
1.	Aluminium	200, 400, 600, 800	40	250, 500, 750, 920
2.	Bamboo	200, 400, 600, 800	22	250, 500, 750, 1000

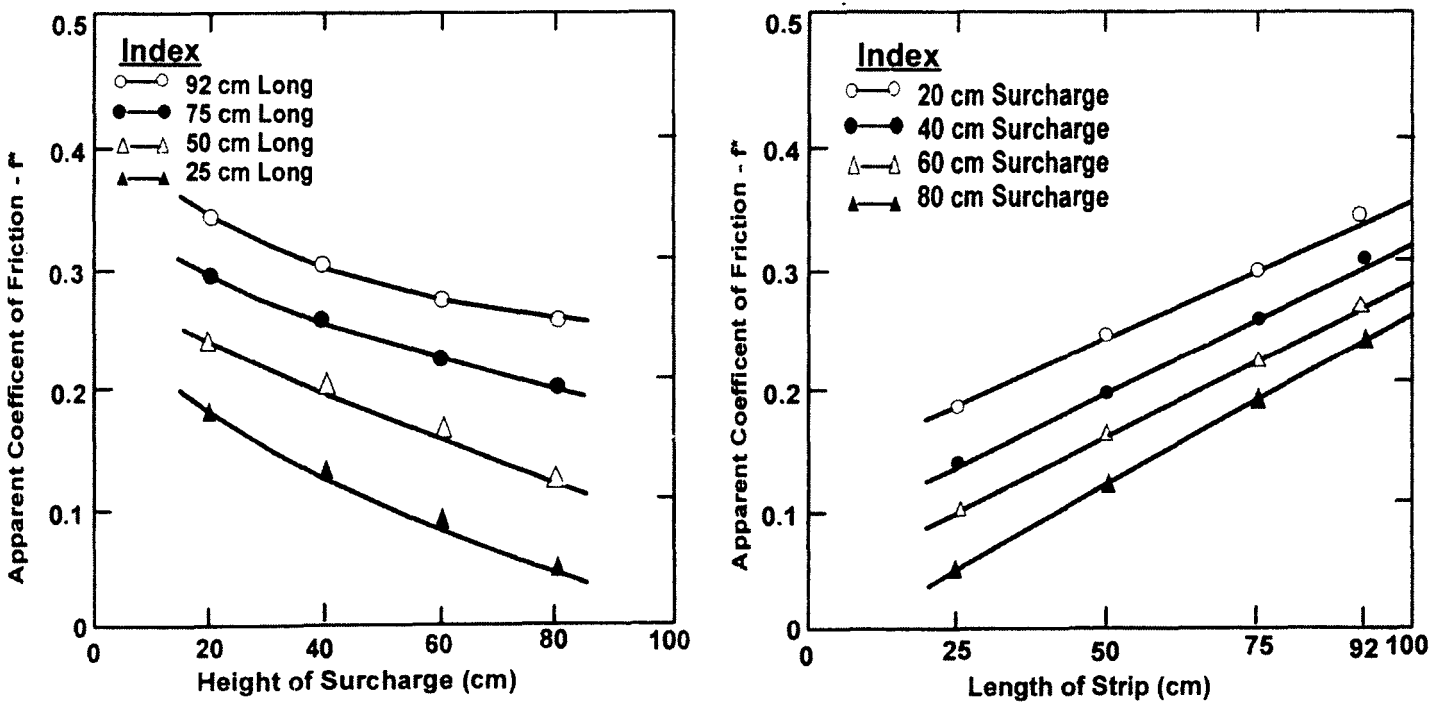

FIGURE 19 : Variation of Apparent Coefficient of Friction with Height of Observation and Length of Strip (Aluminum) (After Garg, 1988)

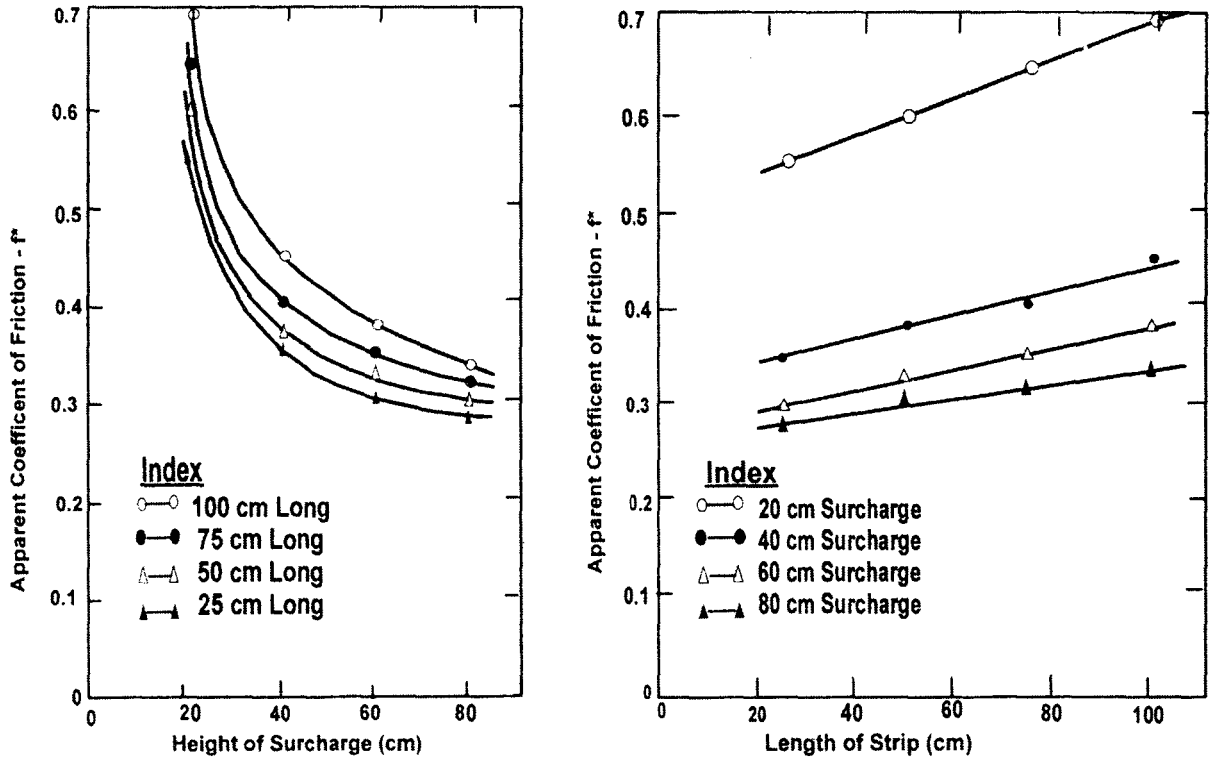

FIGURE 20 : Variation of Apparent Coefficient of Friction with Height of Observation and Length of Strip (Bamboo) (After Garg, 1988)

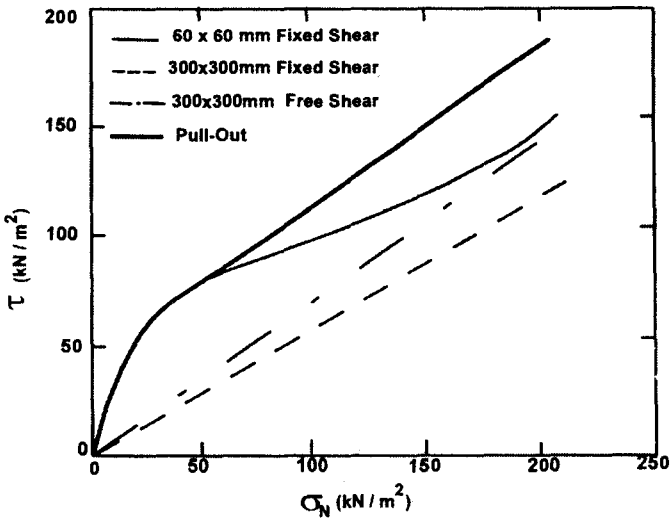

FIGURE 21 : Comparison of Test Results – Geogrid (After Ingold, 1984)

Sridharan and Singh (1988) studied the effect of soil type, density, moisture content and pull-out speed on apparent friction coefficient, f^*. Pull-out tests were conducted in a box of size 305 mm × 76 mm × 102 mm (high). 12 mm dia. smooth and tor mild steel bars were used in the study. It was found that grain size of sand does not affect the value of f^* significantly, however, the use of coarse grained soil for good drainage was recommended. Further, apparent friction coefficient was found to increase with increase in unit weight and the pull out speed. Deformation at maximum pull-out force was found to be more in smooth bar than tor steel bars. So the deformation of the structure will be less for reinforcing elements having higher friction coefficient.

Reinforced Earth Wall

Reinforced soil has found the greatest application in the construction of earth retaining structures. Several thousand retaining walls and abutments constructed all over the world in the last 3-4 decades bear the testimony to the soundness of the concept of reinforced earth and the rationality of design. Reinforced earth walls possess certain definite advantages over other conventional types of walls. They are generally more economical if the wall heights are large or when the sub-soil conditions are poor. They can be rapidly constructed and require relatively simple equipment for construction. Since the soil forms the bulk of their volume, they can be considered as flexible structures with greater ability to withstand differential settlement than the rigid retaining walls. Due to large base to height ratio, stress distribution

beneath the foundation is nearly uniform with little stress concentration at the toe. This enables the construction of high retaining structures, the height being limited practically by the overburden stress, which the base soil can bear.

The internal stability of reinforced earth retaining walls depends upon the strength characteristics of soil and length, cross-sectional area and spacing of the reinforcement. Reinforced earth structures should possess adequate safety against failure due to rupture of reinforcement as well as against slippage between soil and the reinforcement. The safety against rupture of reinforcement is ensured by providing sufficient reinforcement of adequate strength. The safety against a reinforcement pullout failure is achieved by providing reinforcement of adequate length. Greater attention has, nevertheless, been paid to the study of rupture failure mode than the pullout failure. This paper presents the results of an experimental investigation on a model reinforced earth retaining wall, which was tested to failure due to failure of reinforcing strips (Narain et al., 1981).

Test program

Ranipur sand (D_{10} = 0.13 mm, D_{50} = 0.25, C_u = 1.85, e_{min} = 0.57, e_{max} = 0.88) was used for the construction of panels and the backfill in the model. The central section of the wall was instrumented to measure horizontal and the vertical stresses in soil behind the skin and variation of tension in the strips. In addition, the lateral deformation of the wall was measured by dial gauges under surcharge loading conditions.

Deflecting diaphragm type pressure cells were used for measurement of stresses in soil. The variation of tension in the reinforcing strips was monitored by electrical resistance strain gauges pasted on the reinforcing strips. The number of gauge stations varied with the length of strip – their number being 5 for the longest strip of length 2.0 m (1.33 H) and 2 for the shortest strip of 0.6 m (0.4 H). The first gauge station was located at 100 mm from the fixed end of strip and other(s) at intervals of 350 mm.

A set of instrumentation consisting of one cell each for the measurement of vertical and horizontal soil stresses and the instrumented strip was installed at six locations along the vertical at elevations of 125, 375, 625, 875, 1125 and 1375 mm above the base in the instrumented section. Three dial gauges for the measurement of lateral movement of the wall were fixed at 250, 750 and 1250 mm above base.

Test procedure

The construction procedure was much the same as adopted in actual

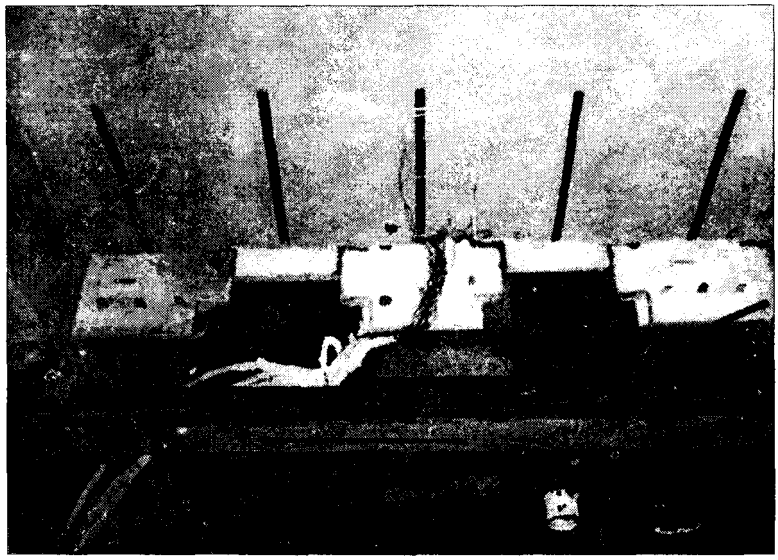

FIGURE 22 : Position of Reinforcing Strips and Pressure Cells

field construction. The first row of panels consisting of 3 full-sized and two half-sized panels was assembled, aligned and set in plumb. The sides of the pit were then covered with plastic sheets to reduce the side friction. 10 mm wide open vertical joints at either end of the wall were closed by interposing folds of the plastic sheets between the pit wall and the side panels. Sand was deposited behind the skin panels by rain fall technique with the help of a perforated box carried by a trolley, which gave uniform sand deposit of dry unit weight of 16.2 kN/m^3 corresponding to a relative density of 84.5 per cent. The first bed of reinforcing strips and monitoring devices was installed at an elevation of 125 mm. The initial zeros of these devices were noted. The level of backfill was raised by 250 mm and changes in the readings of the monitoring devices were recorded before installation of the next set of strips and devices. The changes in the readings of instrumented strips and pressure cells were thus recorded for every 250 mm increase in height of the backfill till the full height of wall was reached. In between, other skin panels were carefully placed in position over the first set of panels as and when it became necessary. A surcharge load of 8.83 KPa was applied over the wall and the backfill. Figure 22 shows a view of the reinforcing strips and pressure cells at an elevation of 1125 mm above base.

In all, nine tests were performed on reinforced earth retaining wall and one on skin panel wall (without reinforcement). The latter test was performed to determine the influence of self weight of panels and side effects in the performance of the wall. Complete details of the tests performed are given

TABLE 9 : Summary of Tests Performed

Test no.	L/H Ratio	Horizontal spacing of strip (m)	No. of gauge station on instrumented strip	Length of pullout strips (m)	Remarks about wall failure
1	1.33	0.27	5	1.80	No failure
2	1.33	0.55	5	1.80	No failure
3	1.05	0.27	5	1.575	No failure
4	1.05	0.55	5	1.575	No failure
5	0.85	0.55	4	1.275	No failure
6	0.60	0.27	3	0.900	No failure
7	0.60	0.55	3	0.900	No failure
8	0.40	0.27	2	0.600	No failure
9	0.40	0.55	2	0.600	Incipient failure
10*	–	–	–	–	Failure by overturning

* Wall failed when backfill height was 0.72 m

elsewhere (Talwar, 1981). A summary of the tests performed is given below in Table 9.

Test results and interpretations

i) Tension in-strips

The data obtained from instrumented strips for test no. 1 are presented in Fig.23. Plots show nonlinear variation of tension along the strip length. Maximum tension occurs either at the face of wall or close to it. Strips embedded at shallow depth show peak tension at a greater distance from the face of the wall than those buried at greater depth. Almost similar trends were observed in other tests. Slope of the tension versus distance curves tended to increase with reduction in the length of strips indicating greater mobilization of soil-tie friction. The loci of points of maximum tension in different strips corresponding to full surcharge loading for tests nos. 1, 5 and 8 are shown in Fig.24. The active zone defined by the locus and the wall face has a tendency to shrink with decrease in the length of strips. For very short strips, the active zones were nearly rectangular in shape. Plots between the ratio of maximum tension T_{max} to overburden versus L/H for full surcharge loading are shown in Fig.25. It shows a large scatter but a general trend can be observed which indicates a decrease in T_{max}/Overburden ratio with increase in the strip length.

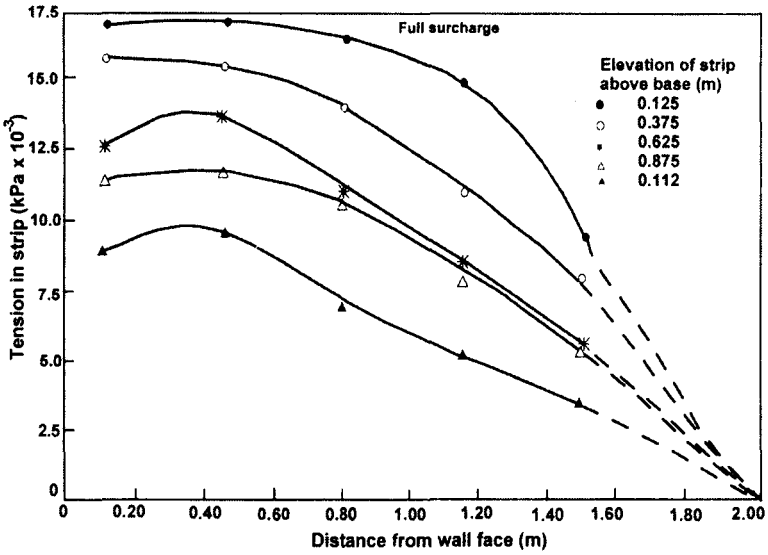

FIGURE 23 : Variation of Tension in Reinforcing Strip (Test No. 1)

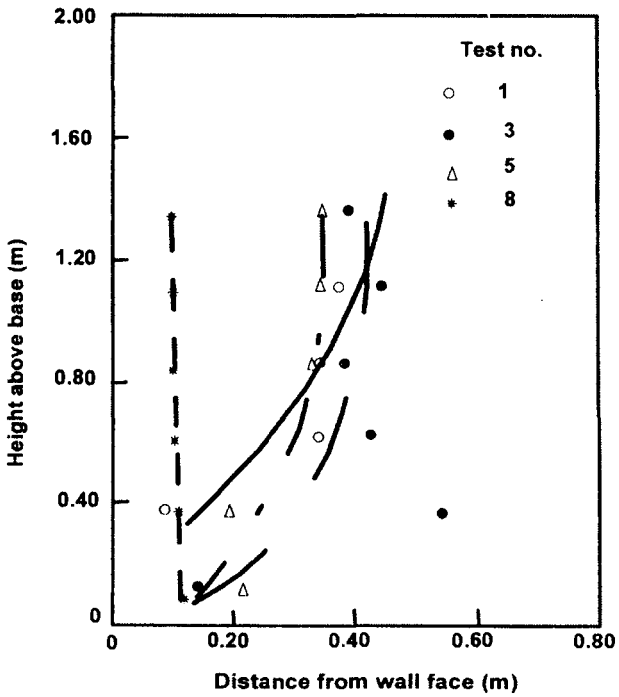

FIGURE 24 : Locus of Points of Maximum Tension

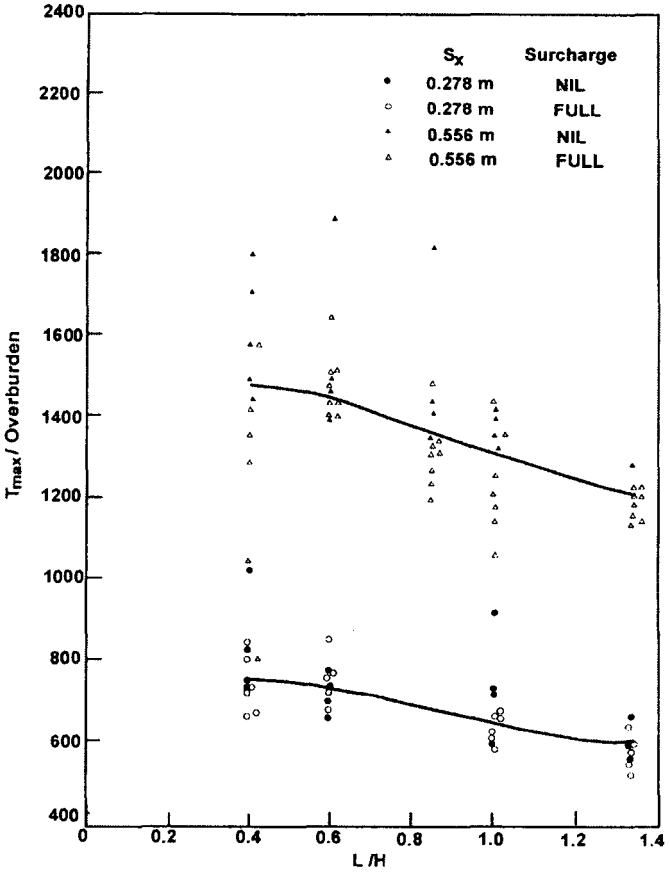

FIGURE 25 : T_{max} /Overburden vs. L/H

ii) State of stress in soil

Figures 26a, b show the measured vertical soil stresses as recorded by pressure cells for tests Nos. 1 to 5. The line representing the theoretical overburden is also drawn. Corresponding measured horizontal stresses are plotted in Fig.27. The vertical stresses are reasonably in agreement with the values of overburden. The observed values of horizontal stresses in the soil lie between at-rest and Rankine active states.

Similar studies were also undertaken by Saran and Khan (1989) and Khan (1991) on 1.0 m high and 4.0 m high walls. The results of these investigations confirm the observations given above in this paper.

It will be appropriate to mention here that Saran and Khan (1990)

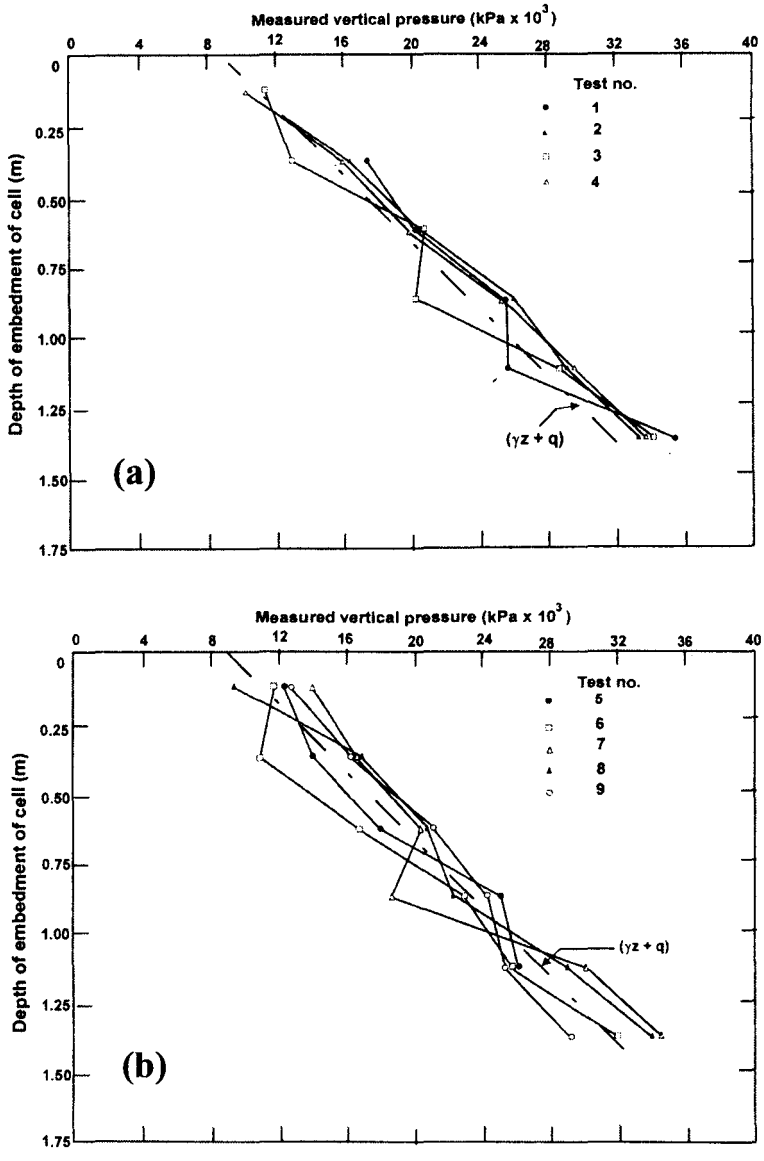

FIGURE 26 : Measured Vertical Stresses, σ_v

suggested a procedure for carrying out seismic design of reinforced earth wall. The results have been presented in the form of non-dimensional plots to obtain the factors of safety against sliding and overturning, minimum and maximum base pressures and checking the safety for pullout and tension failure of reinforcements. The details are given elsewhere (Saran and Khan, 1990; Khan, 1991).

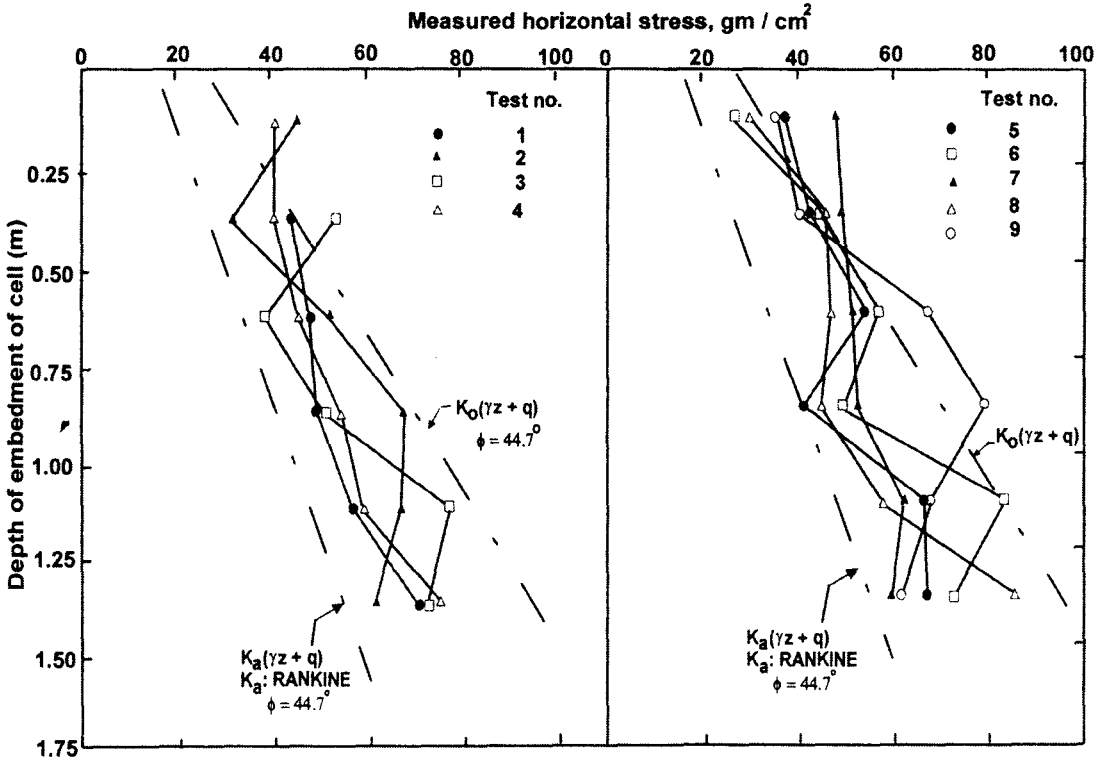

FIGURE 27 : Measured Horizontal Stress, σ_h

Wall with Reinforced Backfill

The usefulness of the patented reinforced earth retaining wall of Vidal has been proved economical by thousands of such structures constructed all over the world. But situations can be met where reinforced earth walls may not provide ideal solution. This can be true for a location with limited space behind the wall (Fig.28) or for narrow hill roads on unstable slopes, which may not permit the use of designed length of reinforcement (Fig.29). In such circumstances a rigid wall with reinforced backfill may appear more appropriate. Backfill is reinforced with unattached horizontal strips/mats/nets laid normal to the wall (Fig.30).

Pasley (1822), based on field trials, demonstrated that substantial reduction occurs in the magnitude of lateral earth pressure on the wall by reinforcing its backfill. Broms (1977, 1987) and Hausmann and Lee (1978) performed model tests on rigid retaining walls with reinforced backfill and reported that considerable reduction in moments occur at the base of the wall. Saran et al. (1979), Talwar (1981) and Saran and Talwar (1983)

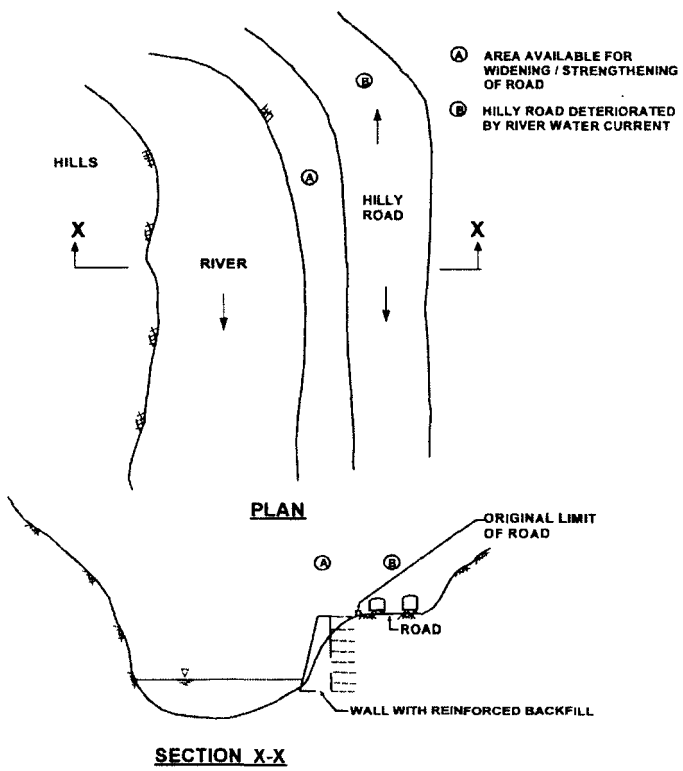

FIGURE 28 : An Example of Suitability of Wall with Reinforced Backfill

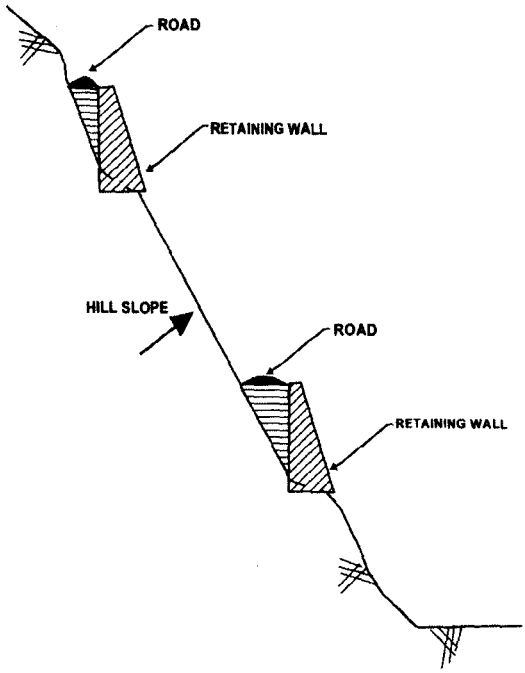

FIGURE 29 : Possible Situation for Application of Retaining Wall with Reinforced Backfill

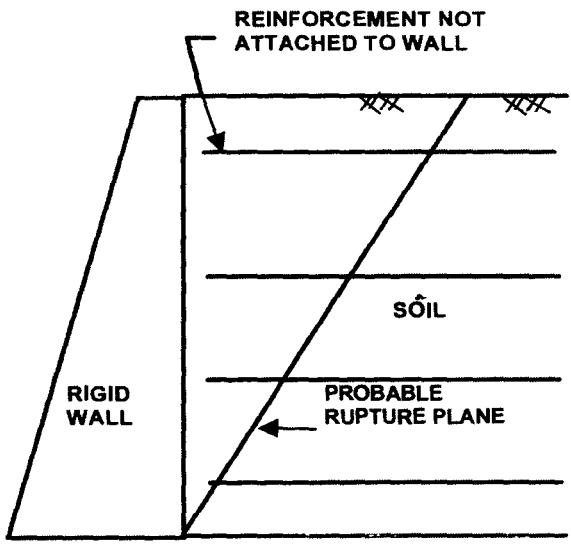

FIGURE 30 : Rigid Wall with Reinforced Backfill

developed theoretical analysis for obtaining earth pressure and its point of application in vertical wall with reinforced backfill. The results were presented in the form of non-dimensional charts. Garg (1988) and Saran et al. (1992) extended the work of Talwar (1981) for uniformly distributed surcharge on the backfill. Saran and Khan (1988, 1989b) and Khan (1991) presented theoretical analysis for the inclined retaining wall with reinforced backfill and having a uniformly distributed and line load surcharge on the backfill. The analyses by Talwar (1981), Garg (1988) and Khan (1991) were based on the limit equilibrium approach and the soil in the backfill was considered as cohesionless. Mittal (1998) extended the analysis of Khan (1991) for cohesive-frictional soil. The results of all the above analyses were presented in the form of non-dimensional charts to determine the value of the total earth pressure and the height of the point of application from the base of wall. Further, the analytical findings were validated by carefully conducted model tests (Talwar, 1981; Garg, 1988; Garg and Saran, 1989; Khan, 1991; Mittal, 1998; Saran et al., 2001).

Pseudo-static analysis of retaining wall has been carried out to determine the seismic pressures and their point of application (Saran and Talwar, 1981a, 1982; Saran, 1998). The results of these analyses indicated that provision of the reinforcement in the backfill reduces the seismic pressures significantly.

All the above studies illustrated the effectiveness of unattached reinforcement in reducing the earth pressure on a rigid wall. To highlight the salient features of the methodology adopted by above mentioned investigators, the work of Saran et al. (1992) has been described here briefly.

Analysis

The analysis was developed for a retaining wall of height H with vertical back face retaining cohesionless backfill having dry density γ_d and an angle of internal friction ϕ. The backfill which carries a uniform surcharge of intensity q is reinforced with unattached horizontal strips of length L and width W, placed at a vertical spacing of S_z and a horizontal spacing of S_x. A failure plane BC, making an angle θ with the vertical, passes through the heel of the retaining wall (Fig.31).

The frictional resistance offered by a reinforcing strip will be located in the shorter portion of the strip, which moves relative to the failure plane. The shorter portion of the strip is referred as the effective length. For example, if strip DF is cut by failure plane at E, then the effective length will be either DE or EF. In the case in which the portion of the strip length within the wedge DE < EF, then EF will not move out of the soil mass. DE will come out of the wedge as the latter moved away from the stationary

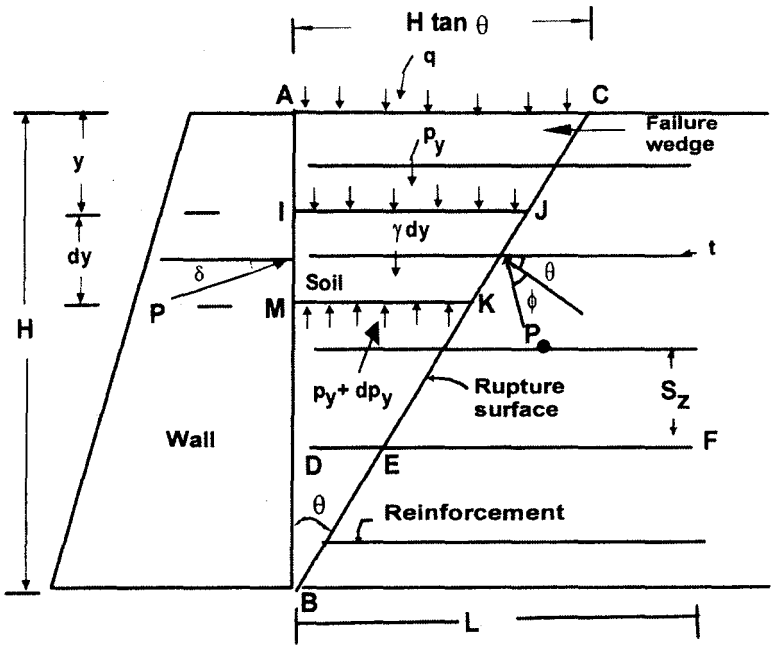

FIGURE 31 : Failure Wedge and Various Intensities of Forces Keeping Element IJKM in Equilibrium

portion of the backfill. If EF < DE, the strip will move with the failure wedge, pulling length EF out of the stationary mass of backfill. Therefore, the effective length of the strip will be the smaller of DE or EF. A reinforcing strip, located completely within the moving wedge, will not contribute any frictional resistance to the movement of the wedge.

An element IJKM (Fig.31) of the failure wedge of thickness dy, located at a distance y from the top of the wedge, is in equilibrium under the following intensities of forces:

p_y = pressure intensity acting uniformly on IJ in the vertical direction due to the self-weight of the backfill lying above IJ and the uniform surcharge q;

$(p_y + dp_y)$ = uniform reaction intensity acting upward on KM in the vertical direction;

p_θ = reaction-intensity on JK acting at an angle ϕ to the normal on JK;

p = pressure-intensity on IM acting at an angle δ to the normal on IM;

σ_n = vertical stress due to the weight of an element IJKM acting downward, or

$\sigma_n = \gamma \cdot dy$, and

t = (T/S_z) = intensity of tension in the reinforcing strip, which is assumed to be transmitted uniformly to the soil layers of thickness S_z encompassing the strip.

Neglecting second-order and higher order terms, the static equilibrium of an element IJKM ($\sum H = 0$, $\sum V = 0$ and $\sum M = 0$) of failure wedge ABC (Fig.31) finally yields the following expression:

$$\frac{dp}{dy} = -C_1 \frac{p}{H-y} + C_2\gamma - C_3 \frac{dt}{dy} \tag{2}$$

where,

$$C_1 = \frac{2\sin\delta\cos(\theta+\phi)}{\sin(\theta+\phi-\delta)} \tag{3}$$

$$C_2 = \frac{\tan\delta\cos(\theta+\phi)}{\sin(\theta+\phi-\delta)} \tag{4}$$

$$C_3 = \frac{\sin(\theta+\phi)}{\sin(\theta+\phi-\delta)} \tag{5}$$

Tension T at the limiting equilibrium can be taken as

$$T = \frac{2Wf^* \sigma_v l'}{S_x} \tag{6}$$

where

l′ = effective length of strip, and

$$\sigma_v = \gamma\left(y + \frac{dy}{2}\right) + q \tag{7}$$

l′ will vary for each reinforcing strip, depending on the wedge angle θ and the length L of the strip as shown in Fig.32.

Case 1: $H\tan\theta \leq L/2$

$$l' = (H-y)\tan\theta$$

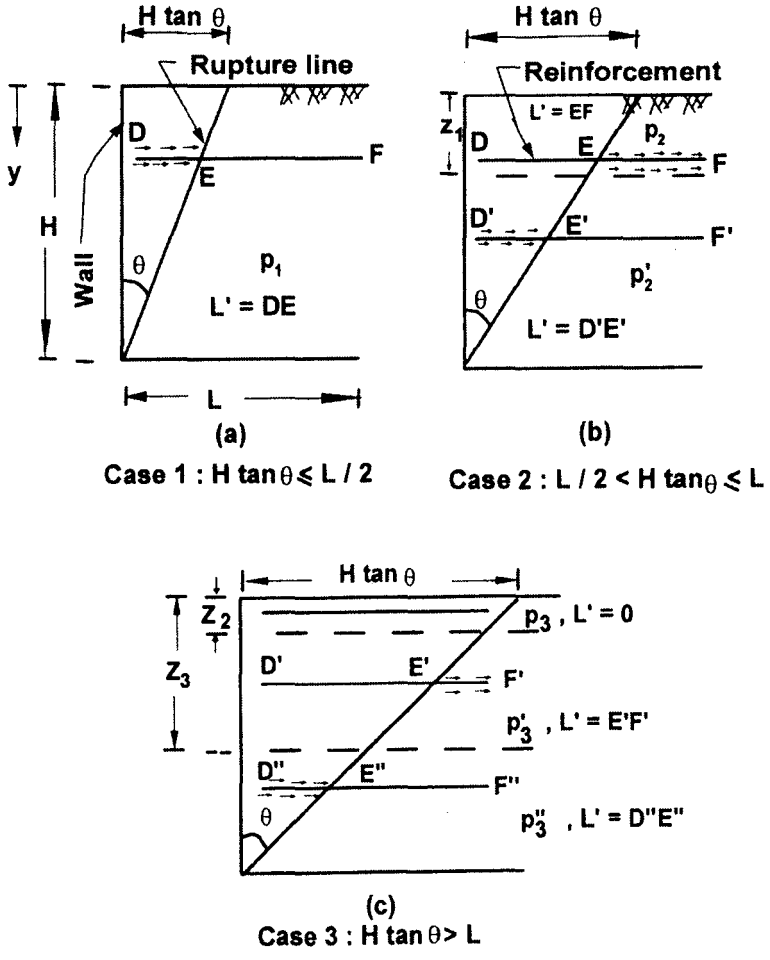

FIGURE 32 : Effective Length Criteria of Reinforcing Element

Case 2: $L/2 \leq H\tan\theta \leq L$

$$l' = L-(H-y)\tan\theta \qquad \text{for } y \leq Z_1$$

$$l' = (H-y)\tan\theta \qquad \text{for } y > Z_1$$

$$Z_1 = H-L/2\cot\theta$$

Case 3: $H\tan\theta > L$

$$l' = 0 \qquad \text{for } y \leq Z_2$$

$$l' = L-(H-y)\tan\theta \qquad \text{for } Z_2 \leq y \leq Z_3$$

$$l' = (H-y)\tan\theta \qquad \text{for } y > Z_3$$

$$Z_2 = H-L\cot\theta$$

$$Z_3 = H-L/2\cot\theta$$

The differential equation (Eqn.2) is solved for these three cases separately by substituting appropriate boundary conditions. For presenting the results in non-dimensional form, lateral earth pressure p is considered to consist of two parts: i) lateral earth pressure due to backfill only, p_γ and ii) lateral earth pressure due to only surcharge load, p_q i.e.

$$p = p_\gamma + p_q \tag{8}$$

Expressions for pressure intensities $p_{1\gamma}$ and p_{1q} (Fig.32a) for Case 1, $p_{2\gamma}$, $p'_{2\gamma}$, p_{2q} and p'_{2q} (Fig.32b) for Case 2, and $p_{3\gamma}$, $p'_{3\gamma}$, $p''_{3\gamma}$, p_{3q}, p'_{3q}, p''_{3q} (Fig.32c) for Case 3 were obtained.

Expressions for pressure intensities are integrated over their respective domains to obtain the resultant earth pressure. The distance of the point of application of the resultant earth pressure is first obtained from the top of wall by integrating the moment of pressure intensity in each case and dividing it by the respective resultant earth pressure. The height of the point of application of the resultant earth pressure above the base of wall is obtained by substracting this distance from the total height of the wall.

The resultant earth pressure and the height of its point of application above the base of the wall in each case is expressed in non-dimensional form as follows:

For Case 1:

$$K_\gamma = \frac{P_{1\gamma}}{(1/2)\gamma H^2} = \frac{\int_0^H p_{1\gamma}dy}{(1/2)\gamma H^2} \tag{9}$$

$$\frac{H_\gamma}{H} = 1-\frac{\int_0^H p_{1\gamma}y\,dy}{H\int_0^H p_{1\gamma}\,dy} \tag{10}$$

$$K_q = \frac{P_{1q}}{qH} = \frac{\int_0^H p_{1q}dy}{qH} \tag{11}$$

$$\frac{H_q}{H} = 1 - \frac{\int_0^H p_{1q}y\,dy}{H\int_0^H p_{1q}\,dy} \tag{12}$$

In Case 2:

$$K_\gamma = \frac{P_{2\gamma}}{(1/2)\gamma H^2} = \frac{\int_0^{Z_1} p_{2\gamma}dy + \int_{Z_1}^H p'_{2\gamma}dy}{(1/2)\gamma H^2} \tag{13}$$

$$\frac{H_\gamma}{H} = 1 - \frac{\int_0^{Z_1} p_{2\gamma}y\,dy + \int_{Z_1}^H p'_{2\gamma}y\,dy}{H\left(\int_0^{Z_1} p_{2\gamma}dy + \int_{Z_1}^H p'_{2\gamma}dy\right)} \tag{14}$$

$$K_q = \frac{P_{2q}}{qH} = \frac{\int_0^{Z_1} p_{2q}dy + \int_{Z_1}^H p'_{2q}dy}{qH} \tag{15}$$

$$\frac{H_q}{H} = 1 - \frac{\int_0^{Z_1} p_{2q}y\,dy + \int_{Z_1}^H p'_{2q}y\,dy}{H\left(\int_0^{Z_1} p_{2q}dy + \int_{Z_1}^H p'_{2q}dy\right)} \tag{16}$$

In Case 3 :

$$K_\gamma = \frac{P_{3\gamma}}{(1/2)\gamma H^2} = \frac{\int_0^{Z_2} p_{3\gamma}dy + \int_{Z_2}^{Z_3} p'_{3\gamma}dy + \int_{Z_3}^H p''_{3\gamma}dy}{(1/2)\gamma H^2} \tag{17}$$

$$\frac{H_\gamma}{H} = 1 - \frac{\int_0^{Z_2} p_{3\gamma}y\,dy + \int_{Z_2}^{Z_3} p'_{3\gamma}y\,dy + \int_{Z_3}^H p''_{3\gamma}y\,dy}{H\left(\int_0^{Z_2} p_{3\gamma}dy + \int_{Z_2}^{Z_3} p'_{3\gamma}dy + \int_{Z_3}^H p'_{3\gamma}dy\right)} \tag{18}$$

$$K_q = \frac{P_{3q}}{qH} = \frac{\int_0^{Z_2} p_{3q}dy + \int_{Z_2}^{Z_3} p'_{3q}dy + \int_{Z_3}^H p''_{3q}dy}{qH} \tag{19}$$

$$\frac{H_q}{H} = 1 - \frac{\int_0^{Z_2} p_{3q}y\,dy + \int_{Z_2}^{Z_3} p'_{3q}y\,dy + \int_{Z_3}^H p''_{3q}y\,dy}{H\left(\int_0^{Z_2} p_{3q}dy + \int_{Z_2}^{Z_3} p'_{3q}dy + \int_{Z_3}^H p''_{3q}dy\right)} \tag{20}$$

It should be mentioned here that the closed-form solutions of these equations have been obtained. The details of the derivations are available elsewhere (Garg, 1988). The expressions of K_γ, K_q, H_γ/H and H_q/H have following two non-dimensional coefficients describing the reinforcement characteristics:

(i) Spacing coefficient, $D_p = \dfrac{f^* WH}{S_x S_z}$ for strip type reinforcement (21a)

$= \dfrac{f^* H}{S_z}$ for mat type reinforcement (21b)

(ii) Length coefficient $= L/H$ (22)

Parametric study

The earth pressure coefficient K_γ and K_q, and the height of the point

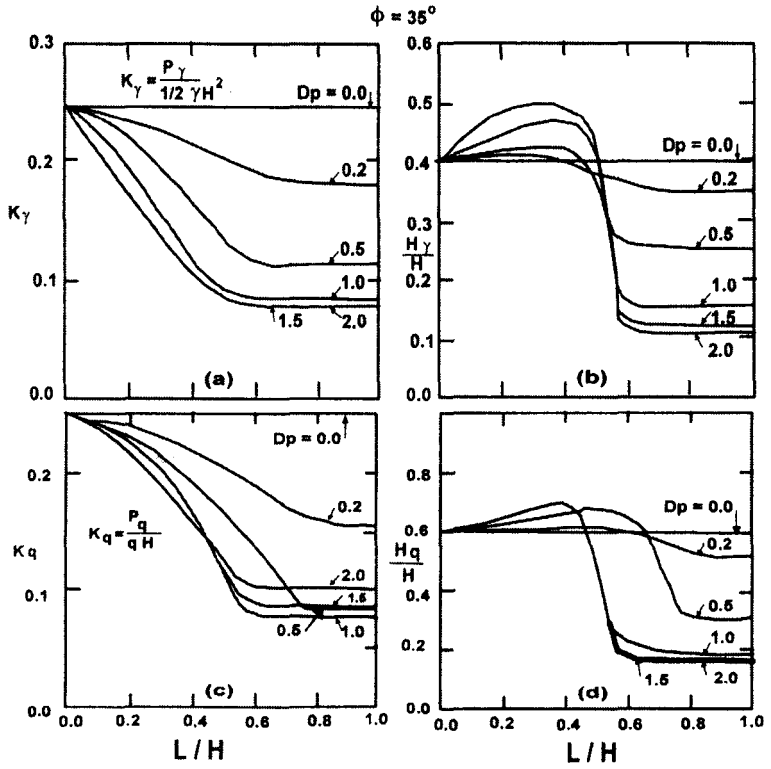

FIGURE 33 : Non-dimensional Chart for Resultant Pressure and Height of Point of Application – (a) and (b) Due to Backfill; (c) and (d) Due to Surcharge Loading (ϕ = 35°)

of application, H_γ/H and H_q/H were evaluated for ϕ equal to 30°, 35° and 40°, L/H ratio for a range 0.0 to 1.0 at interval of 0.2 and D_p with a range 0.2 to 2.0 at variable intervals. One such typical set of design charts for ϕ = 35° is provided in Fig.33. The non-dimensional pressure coefficients, K_γ and K_q reduce with an increase in L/H upto 0.6 and thereafter these are almost constant. K_γ and K_q also reduce with an increase in non-dimensional coefficient D_p upto about 1.0 beyond which the reduction is insignificant. Variation of H_γ/H and H_q/H with L/H shows that point of application

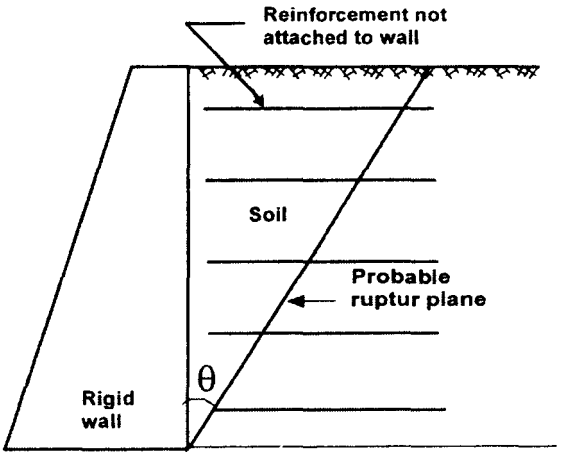

(a) Normal Placement of Reinforcement (NPR)

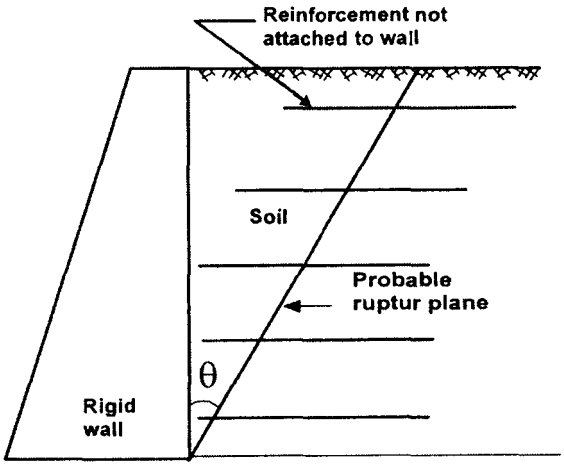

(b) Effective Placement of Reinforcement (EPR)

FIGURE 34 : Section of Rigid Wall with Reinforced Backfill

of the resultant earth pressures (P_γ and P_q) moves towards the bottom of the wall for $L/H > 0.6$.

Investigations reported so far have considered the laying of reinforcement right from the backface of the wall, i.e., NPR case (Fig.34a). In this case the reinforcing elements, lying totally within the failure wedge of retained soil, will not provide any relief in the lateral earth pressure on the wall. Therefore, it was considered to place the reinforcement in such a

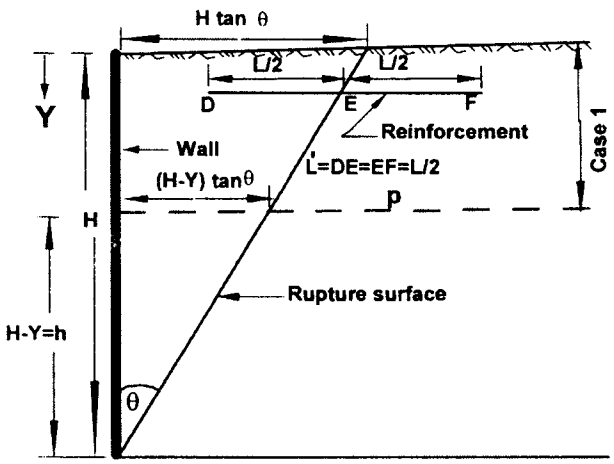

(a) Case 1 – $(H-Y)\tan\theta \geq L/2$

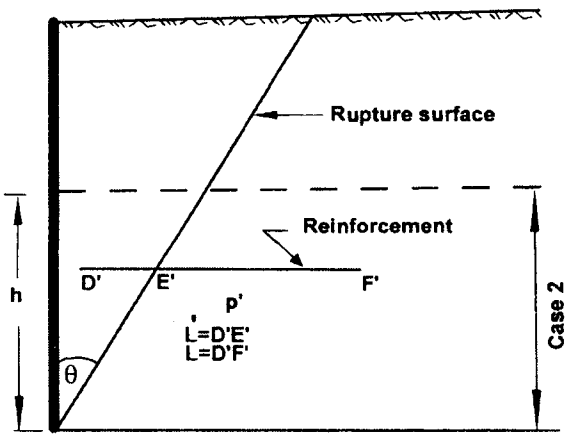

(b) Case 2 – $(H-Y)\tan\theta < L/2$

FIGURE 35 : Effective Length Criteria of Reinforcement

way that it is effective in reducing the active earth pressure on the wall right from its top most layer. In this case the reinforcing elements are considered to be laid across the hypothetical (rupture surface, extending half of its total length on either side of the rupture surface (Fig.34b). This placement of reinforcement is considered upto a depth (from top of wall) in which $(H - y) \geq L/2$. For the sake of clarity this method of placement of reinforcement in the backfill has been termed as Effective Placement of Reinforcement (EPR).

The procedure of stability analysis remains the same as discussed for NPR above. In this case the effective length of reinforcement, for the depth of wall in which $(H-y)\tan\theta \geq L$, will be $L/2$, where H, y, θ and L are as shown in Fig.35a, and for the remaining depth in which $(H-y)\tan\theta < L$, effective length will be $(H-y)\tan\theta$ as considered earlier also in case of NPR (Fig.35b). Non-dimensional design charts have been developed for this case (EPR) also on the same pattern as discussed for NPR above. One such typical set of non-dimensional design charts is provided in Fig.36.

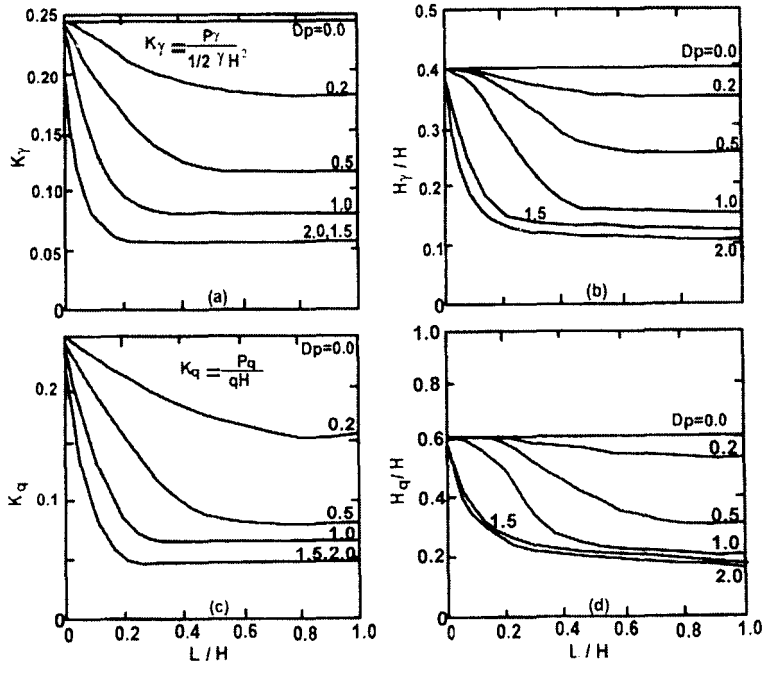

FIGURE 36 · Non-dimensional Charts for Resulting Pressure and Height of Point of Application – (a) and (b) Due to Backfill; (c) and (d) Due to Surcharge Loading (ϕ = 35°)

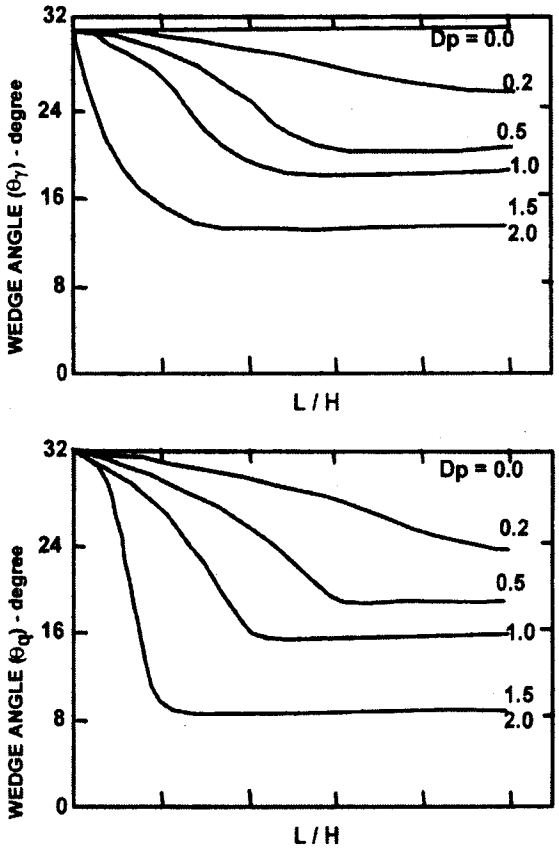

FIGURE 37 : Critical Wedge Angles θ_γ and θ_q (ϕ = 35°)

In case of EPR a designer need to know in advance the critical rupture surface to decide upon the placement of reinforcement in the fill at appropriate locations. That is possible with the knowledge of critical rupture wedge angle θ_{cr}. Series of curves are presented in Fig.37, which provide a relationship between wedge angles (θ_γ and θ_q) and L/H ratio for different values of D_p for ϕ = 35°. Similar charts are available elsewhere for other values of ϕ (Garg, 1988; Garg and Saran, 1997). Normally, there is not much difference in the values of θ_γ and θ_q. Therefore, it is suggested that an average value (θ_γ + θ_q) should be taken as the critical rupture wedge angle, θ_{cr}.

Model tests

Verification of the analytical findings was attempted through model experiments on a 12 mm thick mild steel wall (L = 865 mm and H = 990 mm) in a tank with dimensions shown in Fig.38. A locally available uniform

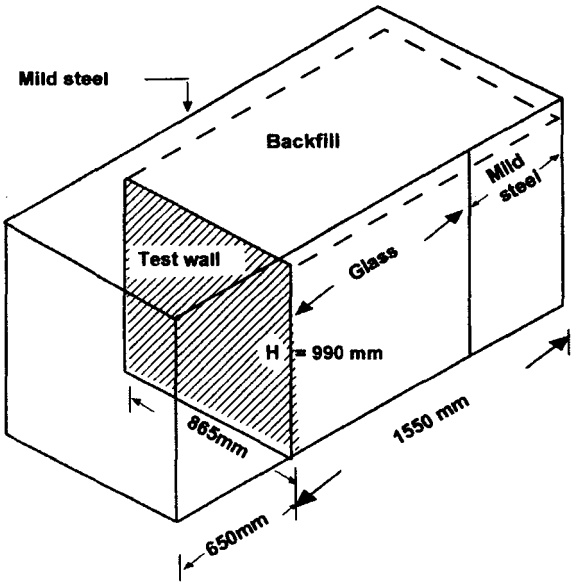

FIGURE 38 : Dimensional Sketch of Test Tank

sand (SP) was used. Strips of Aluminium (width = 4.00 cm, thickness = 0.03 cm) and Bamboo (width = 2.20 cm, thickness = 0.103 cm) were used as reinforcement. The angles of sliding friction between the reinforcement and sand, determined from laboratory box shear tests, were found to be 30° and 34° respectively for aluminium and bamboo. The intensity of surcharge load was varied from 25 kN/m^2 to 200 kN/m^2. A section of one side of the tank was constructed of a 12 mm thick glass sheet to allow observation of the rupture surface. A typical set of results is shown in Fig.39. It may be noted that the results are presented in the form of moments, obtained by multiplying the observed lateral thrust by the moment arm of 450 mm (height of the screw jack above the base of wall).

The experimental and the net theoretical moments (net theoretical moment = total theoretical moment − total friction moment on the two adjoining sides of the tank) of active earth pressure on the test wall compare well (Fig.40), suggesting that the proposed analytical approach is valid for designing rigid walls with reinforced fill that supports surcharge loading on its surface.

Guidelines for practical application

The following steps may be followed for designing a retaining wall using the proposed theory:

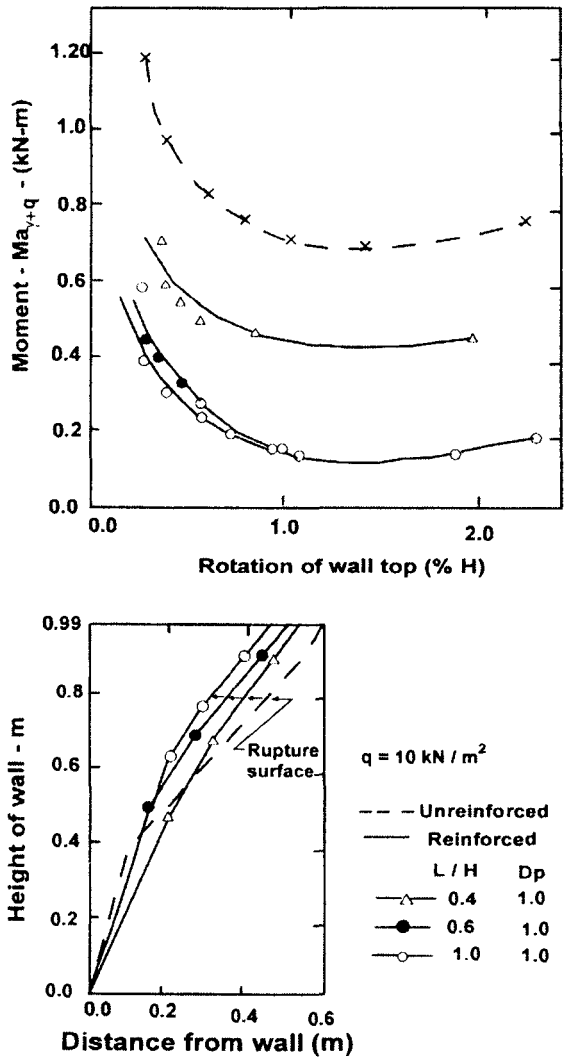

FIGURE 39 : Typical Results of Model Tests for Reinforced Backfill with Surcharge

(a) Normal placement of reinforcement (NPR)

(1) Collect the data for which the wall is to be designed: height of the wall H, and the density γ and the angle of internal friction ϕ of the fill material; the coefficient of base friction μ; the allowable soil pressure q_a and the intensity of the surcharge load q on the fill.

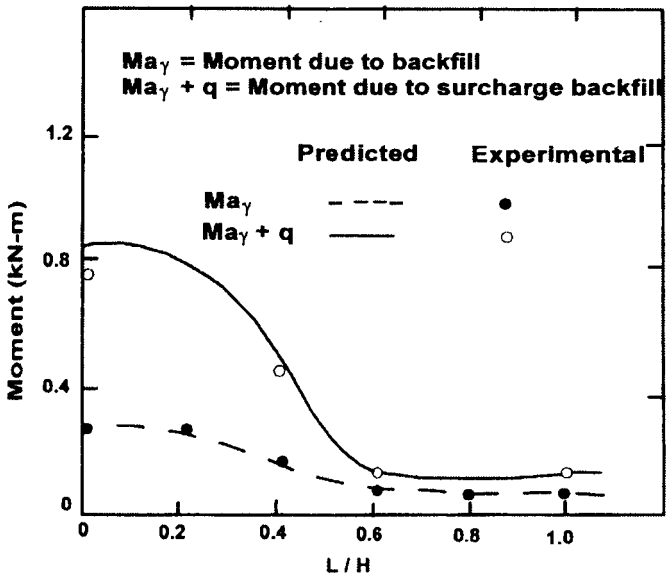

FIGURE 40 : Comparison of Analytical and Experimental Results

(2) Choose an appropriate reinforcing material and obtain its frictional characteristics f^* and allowable tensile stress σ_t.

(3) Assume suitable values of L/H and D_p. For an economical design, it is recommended to adopt L/H between 0.4 to 0.6 and D_p between 0.5 to 1.0.

(4) Using relevant non-dimensional design chart (Garg, 1988), obtain K_γ, H_γ/H, K_q and H_q/H for the design value of ϕ and the assumed values of L/H and D_p.

(5) Select suitable reinforcing strip dimensions, b and W, b being the thickness of the strip. The horizontal (S_x) and vertical (S_z) spacings of the reinforcing strips may be kept equal and worked out as given below:

$$S_x S_z = \frac{f^* WH}{D_p} \qquad (23)$$

(6) Tension (T_B) in the bottom most strip will be maximum and is obtained by :

$$T_B = \left[\gamma H\left(K_{\gamma 0} - K_\gamma\right) + q\left(K_{q0} - K_q\right)\right] S_x S_z$$

Where, $K_{\gamma 0} = K_{q0}$ are Coulomb's active earth pressure coefficient for unreinforced backfill and is obtained from non-dimensional design charts for L/H = 0. For safe design, $T_B \leq \sigma_t \cdot b \cdot w$, i.e., the allowable tensile strength of the reinforcing strip.

(7) Check the stability of the section of the wall against sliding, overturning and bearing failure for resultant earth pressure values (P_γ and P_q) and their corresponding points of application H_γ and H_q.

The proposed method is also applicable for mat-type reinforcement, i.e. using geotextile or geogrid, with some modifications as given below:

$$D_p = \frac{f^* H}{S_z} \quad \text{and} \tag{24}$$

$$T_B = \left[\gamma H\left(K_{\gamma 0} - K_\gamma\right) + q\left(K_{q0} - K_q\right)\right] S_z \tag{25}$$

Usually in this case, the value of D_p will be more than 2.0. Values of the earth pressure coefficients may be obtained from non-dimensional design charts corresponding to $D_p = 2.0$, since values of $D_p > 2.0$ do not significantly affect the K_γ and K_q.

(b) Effective placement of reinforcement (EPR)

Steps (1) to (7) are same as for NPR.

(8) To get the probable location of theoretical rupture surface, obtain θ_{cr} for the design value of ϕ and the assumed values of L/H and D_p. Compute the height (h) from bottom of wall to the point, along the height of wall, at which $h \tan\theta = L$.

(9) Place the reinforcing elements in the fill upto height 'h' from the bottom as shown in Fig.34a.

(10) Between heights h and H along the wall, the reinforcing elements are laid across the failure surface by extending half of its length on either side of the rupture surface (Fig.34b).

Field application

Border Roads Organisation (BRO) constructed a 11.0 m high and 19.50 m long retaining wall at Byasi which is about 30 km from Rishikesh towards Badrinath in Garhwal Himalaya along the National Highway (NH-58). The purpose of construction of the retaining wall was to increase the width of road. The site lies in the Krol-belt sequence of the lesser Garhwal Himalaya. The rocks exposed, along the road near the wall site are mainly limestone of Infrakrol-Krol sequence. The limestones are highly fractured, crushed, well jointed and interbedded with greyish green shales and sometimes traversed by calcite veins. The rocks exposed in the vicinity of the retaining wall exhibit bedding planes dipping at 45°-50° towards NE to SE. Geological map of the area is shown in Fig.41.

The wall was designed by Garg (1998) using the methodology and the concept of reinforcing the backfill (Garg, 1988) given in the paper. Adopting the following data:

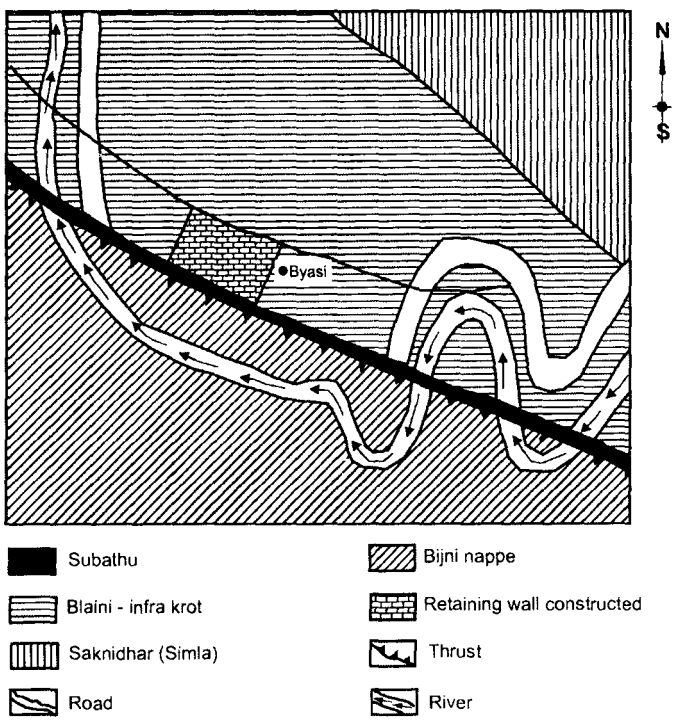

FIGURE 41 : Geological Profile of the Area in the Vicinity of Proposed Retaining Wall

Angle of internal friction of compacted backfill, ϕ	=	35°
Unit weight of backfill soil	=	18.0 kN/m^3
Unit weight of R.R. masonry	=	22.0 kN/m^3
Intensity of surcharge on the backfill, θ	=	20.0 kN/m^2
Coefficient of wall base friction, μ	=	0.5
Allowable soil pressure at the base of wall, q_a	=	300 kN/m^2
Reinforcing materials: Geogrids CE-121 and CE-131 having 6.0 kN/m and 4.5 kN/m permissible tensile strengths respectively.		
Soil-reinforcement interface friction coefficient, f^*	=	0.45

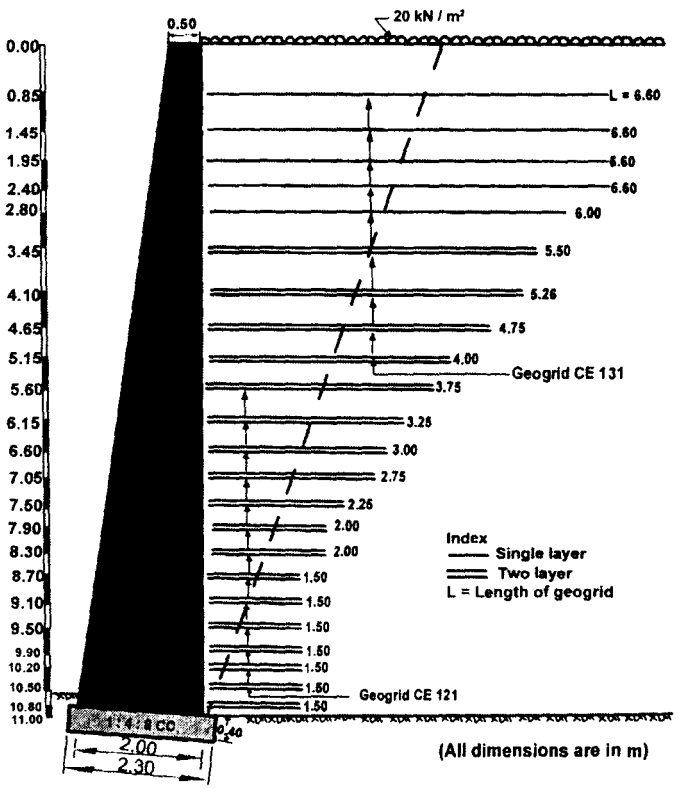

FIGURE 42 : Cross-section of 11 m High Wall Retaining Geogrid Reinforced Cohesionless Backfill

Factor of safety against sliding	=	1.5
Factor of safety against overturning	=	2.0

Design

Adopting D_p = 1.0; L/H = 0.60; angle of wall friction $\delta = 2/3\phi$ and referring to Fig.33, we get,

K_γ	=	0.085;	H_γ	=	0.15 H
K_q	=	0.078;	H_q	=	0.24 H

The section of the wall, shown in Fig.42, was checked for its stability against sliding, overturning and bearing failure and was found to be safe. Stability checks yielded the following:

F.O.S. (against sliding)	1.62
F.O.S. (against overturning)	2.64
Max. pressure transmitted to the ground below	220 kN/m^2

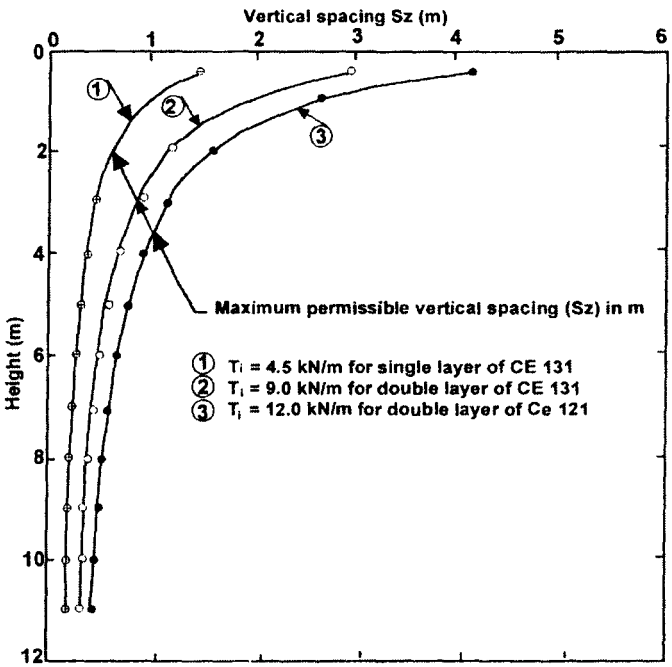

FIGURE 43 : Permissible Vertical Spacing (S_z) of Geogrid

Vertical spacing of geogrid reinforcement in the earth backfill was worked out using the following equation:

$$T = \left[\gamma h_i \left(K_a - K_\gamma\right) + q\left(K_a - K_q\right)\right] S_z$$

where, T = Permissible tensile strength/m length of geogrid
6.0 kN/m in case of Netlon geogrid CE121
4.5 kN/m in case of Netlon geogrid CE 131
h_i - Depth at which spacing is required
K_a - Coulomb's active earth pressure coefficient

Figure 43 shows the permissible spacing along the height of wall for the two types (CE 121 and CE 131) for geogrid used in the wall backfill.

Monitored performance of wall

Four observation points (O.P.) were fixed in the body of the wall at its top (Fig.44) to monitor the lateral movement of wall top away from the backfill. These observations were taken with the help of an electronic distance meter (E.D.M.) at some interval of time for a period of about 36 months. An average trend of lateral movement of wall with time is shown in Fig.45. It can

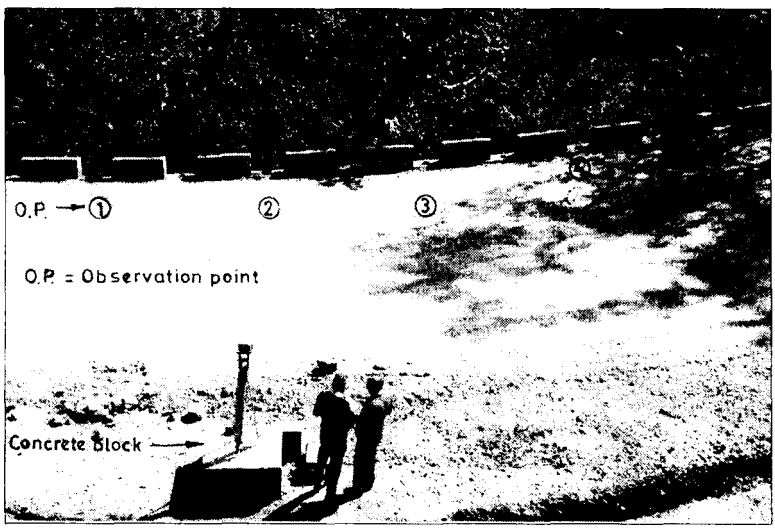

FIGURE 44 : View Showing Electronic Distance Meter (EDM) and Observation Points on the Wall

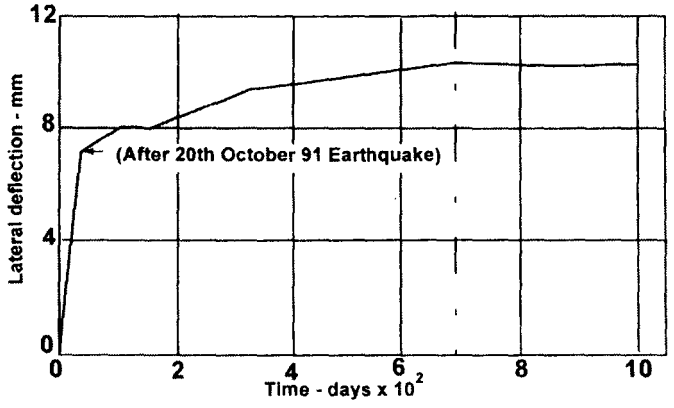

FIGURE 45 : Average Lateral Deflection of the Wall with Time

be observed from the latter that the retaining wall alongwith its reinforced backfill has attained almost stable equilibrium beyond 700 days of its construction in this case. Furthermore, major part of the total lateral movement (60% to 70%) has taken place within a short span of 45 days. A logical reason for this may be the additional active earth pressure that was exerted on the wall due to ground shaking by the Uttarkashi earthquake of 20th October 1991. The total observed maximum horizontal movement of wall, at any point along its length, was almost 0.1 percent of height of wall and was just sufficient to bring the retaining wall and its reinforced backfill to full active state.

The cost of construction of the retaining wall with reinforced fill was only about 79 percent of the cost of the retaining wall with conventional earth fill.

Footings on Reinforced Sand

Due to the meager availability of good construction sites, a foundation engineer today frequently comes across the problem of erecting the structures on low bearing capacity deposits. The traditional solutions to such situations have been – deep foundations placed through the loose soil, excavation and replacement with suitable soil, stabilizing with injected additives or applying the techniques for densification of soil. All of these methods have a certain degree of applicability, but all suffer from being either expensive or time consuming. The newly emerging alternate method is to remove the existing weak soil up to a shallow depth and replace it by the soil reinforced with horizontal layers of high tensile strength reinforcement. In recent years, geosynthetics like- geotextiles or geogrids and metal strips have replaced the traditional materials in reinforcing the soils for improvement of bearing capacity and the settlement of soil beds (Saran, 1998).

In the following section, a method of analysis for calculating the pressure intensity corresponding to a given settlement of the footings resting on reinforced soil foundation has been presented for the following cases: i) Isolated strip footings, ii) Isolated rectangular footings, iii) Closely spaced strip footings and iv) Closely spaced rectangular footings subjected to central-vertical load. However, on similar lines, the analysis has also been extended to strip, square, rectangular and ring footings subjected to eccentric-vertical loads. The process has been simplified by presenting non-dimensional charts for the various terms used in the analysis, which can be directly used by practicing engineers. An approximate method has been suggested to find out the ultimate bearing capacity of footing on reinforced soil for each of the above cases. The results have been validated with small and large-scale model tests. In addition to the coefficient of friction between the reinforcement and the soil in pull out, there are other parameters affecting the behaviour of strip footings on reinforced sand. The parametric study has been carried out for a number of layers of reinforcement, depth of first layer of reinforcement, vertical spacing between the layers of reinforcement, length of reinforcement, depth of reinforcement, tensile strength of reinforcement and the size of footing.

Discussion on laboratory model tests performed to study the bearing capacity, settlement and the tilt characteristics of closely spaced strip and square footings resting on sand reinforced with horizontal layers of geogrid reinforcement are also presented. Interference effects on the bearing capacity and settlement of closely spaced square footings on reinforced sand were almost insignificant in comparison to the isolated footings on reinforced sand whereas, a significant improvement in the tilt of adjacent square footings has been observed by providing continuous reinforcement layers in the foundation soil under the closely spaced footings. A considerable improvement in the bearing capacity, settlement and the tilt of adjacent strip footings has been observed by providing continuous reinforcement layers in the foundation soil under the closely spaced strip footings.

Many investigators have studied experimentally the behaviour of isolated footings resting on reinforced earth (Binquet and Lee, 1975a; Akinmusuru and Akinbolade, 1981; Saran and Talwar, 1981b; Fragszy and Lawton, 1984; Saran et al, 1985; Guido et al, 1985,1986; Dembicki et al, 1986; Sridharan et al, 1988; Sreekantiah, 1990; Samatni et al, 1989; Huang and Tatsuoka, 1990; Mandal et al, 1990,1992; Shankariah, 1991; Dixit and Mandal, 1993; Khing et al., 1992, 1993,1994; Rao et al., 1994; Yetimoglu et al., 1994; Adams and Collin, 1997).

Binquet and Lee (1975b) were perhaps the first who proposed an analytical approach for getting the pressure on an isolated strip footing resting on reinforced sand corresponding to a given settlement, which was further modified by Murthy et al., (1993). In this paper, an analysis has been

presented for a strip footing resting on reinforced sand. Attempt has been made to overcome the shortcomings in the Binquet and Lee (1975b) approach for isolated strip footings, modifying the assumptions made by them to more realistic ones and it was further extended to isolated rectangular footings and closely spaced strip, square and rectangular footings subjected to central-vertical loads (Saran and Kumar, 1996; Kumar, 1997; Kumar and Saran, 2000a; 2001a; 2001b; 2001c; 2003a; 2003b; 2003c; 2004a). Analysis was further extended to strip, square, rectangular and ring footings subjected to eccentric-inclined loads (Al-Smadi, 1998; Saran and Galav, 1998; Kumar and Saran, 2002; Saran and Al-Smadi, 2002). Binquet and Lee (1975b) assumed the soil-reinforcement friction angle as constant for all the layers of reinforcement. Whenever, reinforcement is embedded in the soil, soil-reinforcement frictional resistance depends upon the mobilization of friction between soil and the reinforcement, which in turn depends on relative vertical movement of soil at different depths. As the relative movement of soil will be different at different depths, it is not reasonable to assume the angle of interfacial friction constant for all layers of reinforcement. Further, it was also assumed that the force developed in any reinforcement layer is inversely proportional to the number of layers of reinforcement. As the development of force in the reinforcement will be in different proportions at different layer levels, this assumption also does not seem to be reasonable. Accordingly, these assumptions have been modified.

Pressure ratio

For convenience in expressing and comparing the data, a pressure ratio term has been introduced and is defined as:

$$p_r = q/q_0$$

where q_0 = the average contact pressure of a footing on unreinforced soil, at a given settlement, and

q = the average contact pressure of the same footing on reinforced soil, at the same settlement.

It may be mentioned here that the pressure intensity of the footing on unreinforced soil at a given settlement can be obtained using standard penetration test data or standard plate load test data or using a method developed by Prakash et al. (1984) and Sharan (1977).

Aanalysis of isolated strip footings

Consider a strip footing of size, B. If the footing is loaded with uniformly distributed load of q, then normal and shear stresses can be

calculated at any depth Z using the theory of elasticity (Poulos and Davis, 1974). The analysis is based on the following assumptions:

(1) The central zone of soil moves down with respect to outer zones. The boundary between the downward moving and outward moving zones has been assumed as the locus of points of maximum shear stress at every depth, Z. The location of separating planes can only be inferred from the location of broken ties (Binquet and Lee, 1975a) and deformation pattern of reinforcement after failure (Kumar, 1997; Kumar and Saran, 2001a).

(2) At the plane separating the downward and lateral movements, the reinforcement is assumed to undergo two right angles bend around two frictionless rollers and T_D is vertically acting tensile force (Fig.46). In

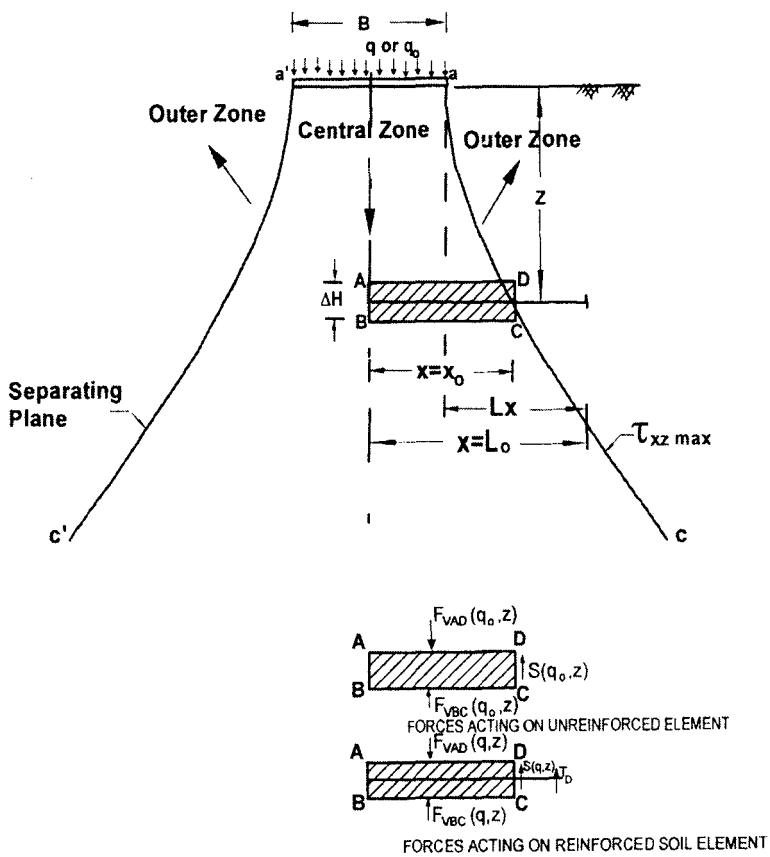

FIGURE 46 : Assumed Separating Plane and Components of Forces for Pressure Ratio Calculation of Isolated Strip Foundation on Reinforced Soil

a reinforcing layer embedded within the soil, the kink will form due to the relative movement along the plane separating the downward and lateral flow. The relative vertical movement decreases at larger depths, the right angle kink in reinforcement will not form. As the reinforcement placement at depths beyond the footing width will not be feasible from economic and construction considerations, assuming a right angle kink for reinforcements placed within this depth is reasonable. Further, from the basic mechanics, tension in reinforcement can be considered equally effective in the vertical direction at right angle bends.

(3) The mobilization of friction is dependent on the relative movement of soil and reinforcement. As the settlement of the footing at the surface causes a vertical settlement of different magnitude at different layer levels, settlement in this investigation has been assumed to vary in proportion to vertical stress at that point. This concept results in 30% of surface settlement at depth B and negligible settlement at depth 2B (Fig.47). Therefore, soil-reinforcement friction coefficient, f^*, has been assumed to vary with depth as per the following equation:

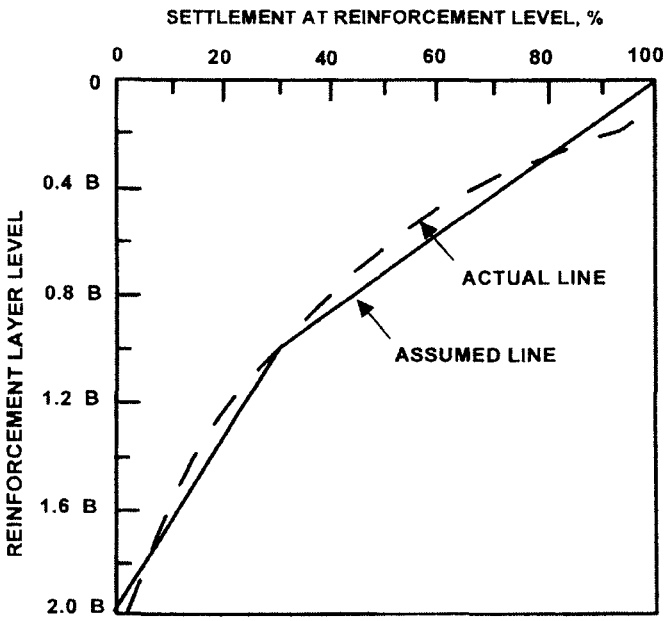

FIGURE 47 : Effective Settlement at Different Reinforcement Layer Level (After Murthy et al., 1993)

$$f^* = m \cdot f \tag{26}$$

where

$$m = \left[(1 - Z/B)0.7 + 0.3\right] \text{ for } Z/B \leq 1.0 \tag{26a}$$

$$m = \left[(2 - Z/B)0.3\right] \text{ for } Z/B > 1.0 \tag{26b}$$

$f = \tan\phi_f$, ϕ_f is soil-reinforcement friction angle (26c)

The variation of m with depth is shown in Fig.47.

(4) As the normal force on the lower layers of reinforcement gets affected by the load carried by the upper layers, for N_R layers of reinforcement provided in the foundation soil, the normal force responsible for the development of reinforcement force has been assumed to vary in proportion of $r_1 : r_2 : r_3 : \ldots : r_{NR}$, such that $r_1 + r_2 + r_3 + \ldots + r_{NR} = 1$ and failure has been assumed for various combinations of reinforcement pull out and breakage at different layer levels.

(5) The forces evaluated in the analysis are for the same size of footing and for the same settlement for a footing on reinforced and unreinforced soil.

(6) Elastic theory has been applied to estimate the stress distribution inside the soil mass, as no stress equations are available for anisotropic non-homogeneous material like reinforced sand. However, it has been demonstrated later that results are not affected by this assumption.

Failure mechanism

Three modes of failure are possible for the foundations on reinforced soil as depicted in Fig.48.

(i) Shear failure of soil above the uppermost layer of the reinforcement is possible if the depth to the top most layer of reinforcement is sufficiently large. Since, significant improvements can be obtained at lower cost, by providing the reinforcement at shallow depths, this possible mode of failure is unlikely in practice.

(ii) Reinforcement pullout failure, which may occur for reinforcement placed at shallow depths beneath the footing with insufficient anchorage.

(iii) Reinforcement rupture failure, which occurs in case of long and shallow reinforcement for which the frictional pullout resistance is more than the rupture strength.

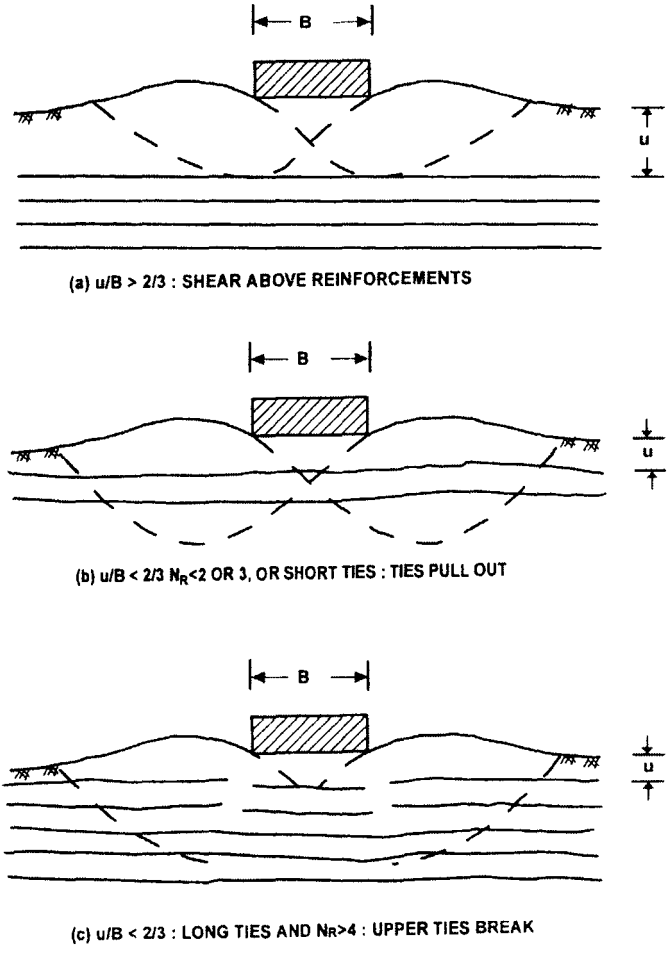

FIGURE 48 : Three Modes of Failure (After Binquet and Lee, 1975)

To evaluate the two likely failure modes, we need the expressions for driving force and resisting forces. In the discussions, hereafter, we describe the method to compute the driving force and reinforcement pullout resistance force.

Computation of force developed in reinforcement (T_D)

To evaluate the force developed in the reinforcement due to applied load on the footing, it was assumed that the plane separating the downward and lateral flow is the locus of points of maximum shear stress, τ_{xzmax} at every depth, Z. In Fig.46, ac and a'c' are assumed separating planes. Consider an element ABCD at depth, Z (Fig.46), which is the volume of soil

lying between two vertically adjacent layers of reinforcement. The forces acting on the element are shown in Fig.46 for unreinforced and reinforced foundation soil. The force developed in the reinforcement, T_D may be expressed in terms of pressure ratio as under

$$T_D = \left[J_Z B - I_Z \Delta H\right] q_0 (p_r - 1) \tag{27}$$

in which

$$J_Z = \frac{\int_0^{X_0} \sigma_z dx}{(q \text{ or } q_0) B} \tag{27a}$$

$$I_Z = \frac{\tau_{xz\,max}}{q \text{ or } q_0} \tag{27b}$$

T_D is the force developed in the reinforcement, if there is only one layer of reinforcement in the foundation soil and that is placed at depth Z. The value of X_0/B, J_Z and I_Z corresponding to Z/B values can be taken from non-dimensional chart (Kumar, 1997 and Kumar and Saran, 2001a). ΔH is taken equal to vertical spacing between the horizontal layers of reinforcement, if layers are at equal vertical spacing and is equal to the average of two adjacent layers, if layers are at different vertical spacing. The stress equations have been solved by numerical integration.

Computation of reinforcement-pull-out frictional resistance (T_f)

The pull out frictional resistance shall be due to the vertical normal force on the length of the reinforcement, which is outside the assumed plane separating the downward and the outward flow (Fig.46). The normal force consists of two components, one due to the applied bearing pressure and the other, due to the normal overburden pressure of soil.

The reinforcement pull out frictional resistance per unit length of the strip footing is, given by

$$T_f = 2f^* LDR\left[M_Z B q_0 p_r + \gamma (L_0 - X_0)(Z + D_r)\right] \tag{28}$$

where

T_f = pull out frictional resistance per unit length of strip footing at depth Z, developed due to the reinforcing length beyond the assumed plane ac.

D_f = depth of footing below ground level.

$$L_0 = 0.5B + L_X \tag{28a}$$

L_X = Extension of reinforcement beyond the either edge of footing.

LDR = Linear density of reinforcement

= Plan area of reinforcement/Total area of reinforced soil layer

= 1, for geogrid or other geosynthetic sheets covering the total soil layer

f^* = Soil-reinforcement friction coefficient

$$M_Z = \frac{\int_{X_0}^{L_0} \sigma_z dx}{qB} \tag{28b}$$

Non-dimensional charts have been prepared for M_Z at different Z/B values for L_X/B values of 0.5, 1.0, 1.5, 2.0, 2.5 and 3.0 (Kumar, 1997 and Kumar and Saran, 2001a). The stress equations have been solved by numerical integration.

Analysis of isolated rectangular footings

An attempt has been made to extend that approach to an isolated rectangular footing resting on reinforced sand (Kumar and Saran, 2003a).

Computation of driving force (T_D)

Consider a rectangular footing of length, L and width, B. Figure 49 shows the plan and section of the assumed planes separating the downward and the outward flow, which are loci of points of maximum shear stress at every depth, Z. The location of the separating planes can only be inferred from the location of broken ties (Binquet and Lee, 1975a) and the deformation pattern of reinforcement after failure (Kumar, 1997).

The driving force in the x-direction is given by

$$T_{Dx} = \left[J_{xz}BL - I_{xz}L\Delta H\right]q_0\left\{p_r - 1\right\} \tag{29}$$

in which,

$$J_{xz} = \frac{\sum_{i=1}^{i=n}\int_0^{X_i} \sigma_z(q, x, y, Z)dx\delta y}{(q \text{ or } q_0)BL} \tag{29a}$$

and $$I_{xz} = \frac{\sum_{i=1}^{i=n} \tau_{xz}(q, X_i, Z)\delta y}{(q \text{ or } q_0)BL} \quad (29b)$$

X_i is the horizontal position of peak shear stress at the i^{th} element. Equations are solved by numerical integration and/or by summation. The Interval, X_i is divided into small units of size 0.01B and the length of reinforcement $(L+2L_y)$ is divided into 'n' parts, each of size δy = 0.01B. L_y = extension of reinforcement beyond the edge of the footing in the y-direction.

Similarly, the driving force in the y-direction is given by:

$$T_{Dx} = \left[J_{yz}BL - I_{yz}B\Delta H\right]q_0\{p_r - 1\} \quad (30)$$

where J_{yz} = total non-dimensional force due to applied pressure on area g'h'k'j'g' marked as 'A_2', Fig.49, and

I_{yz} = total non-dimensional shear force along g'h'.

If the footing is loaded with a uniformly distributed load, q, then these components will be:

$$J_{yz} = \frac{\sum_{k=1}^{k=p} \int_0^{Y_k} \sigma_z(q, x, y, Z)dy\delta x}{qBL} \quad (30a)$$

$$I_{yz} = \frac{\sum_{k=1}^{k=p} \tau_{yz}(q, Y_k, Z)\delta x}{qB} \quad (30b)$$

Y_k is the horizontal position of peak shear stress at the k^{th} element. The stress equations are solved by numerical integration and/or by summation. The interval, Y_k is divided into small units of size 0.01B and the length of reinforcement $(B+2L_x)$ is divided into 'p' parts, each of size, δx = 0.01B. L_x = extension of reinforcement beyond the edge of footing in x-direction.

Computation of reinforcement-pull-out frictional resistance (T_f)

Considering both components over the whole area, A_{xz}, outside the

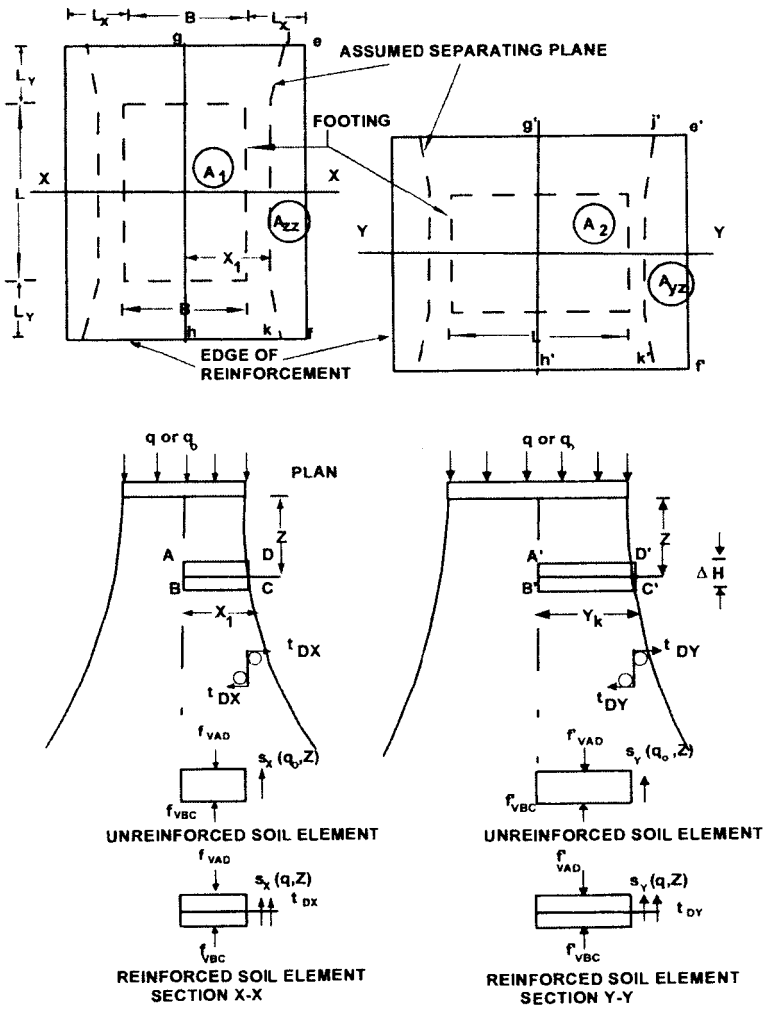

FIGURE 49 : Plan and Section of Assumed Separating Plane and Components of Forces for Pressure Ratio Calculation

separating plane, we get reinforcement pull out frictional resistance in x-direction at depth, Z, for a footing placed at depth, D_f as:

$$T_{fx} = 2f_e LDR\left[M_{xz} q_0 p_r + \gamma A_{xz}\left(Z + D_r\right)\right]BL \tag{31}$$

where,
$$M_{xz} = \frac{\sum_{i=1}^{i=n} \int_{X_i}^{(0.5B+L_x)} \sigma_z(q, x, y, Z)\,dx\delta y}{qBL} \tag{31a}$$

$$A_{xz} = \frac{\sum_{i=1}^{i=n}(0.5B + L_x - X_i)\delta y}{BL} \tag{31b}$$

Similarly,

$$T_{fy} = 2f_e LDR\left[M_{yz} q_0 p_r + \gamma A_{yz}(Z + D_r)\right]BL \tag{32}$$

where, M_{yz} is a non dimensional frictional resistance factor due to the vertical normal force on the plan area of reinforcement, j'e'f'k'j', marked as A_{xz}, which is outside the assumed plane separating the downward and the outward flow (Fig.49) and A_{yz} in non-dimensional form is:

$$M_{yz} = \frac{\sum_{k=1}^{k=p}\int_{Y_k}^{(0.5L+L_y)} \sigma_z(q, x, y, Z)\,dy\delta x}{qBL} \tag{32a}$$

and $$A_{yz} = \frac{\sum_{k=1}^{k=p}(0.5L + L_y - Y_k)\delta x}{BL} \tag{32b}$$

The forces T_{Dx}, T_{Dy}, T_{fx} and T_{fy} are the forces in x and y directions only. As the reinforcement would be pulled out simultaneously from all the directions with the application of load on the footing, the direction giving an average value of pressure ratio has been adopted. Thus, the direction making an angle of 45° with x or y direction gives the average value and has been adopted for the calculation of pressure ratio, which coincidentally gives the results obtained by adding the forces in the x and y directions. Total driving force is, therefore, given by

$$T_D = T_{Dx} + T_{Dy} = \left[(J_{xz} + J_{yz})BL - (I_{xz}L + I_{yz}B)\Delta H\right] q_0 (p_r - 1)$$

$$= \left[(J_z)BL - (I_{xz}L + I_{yz}B)\Delta H\right] q_0 (p_r - 1) \tag{33}$$

where $$J_z = J_{xz} + J_{yz} \tag{33a}$$

The total pull-out frictional resistance T_f is, therefore, given by:

$$T_f = T_{fx} + T_{fy}$$

$$= 2f_e LDR\left[\left(M_{xz} + M_{yz}\right)q_0 p_r + \gamma\left(Z + D_f\right)\left(A_{xz} + A_{yz}\right)BL\right]$$

$$= 2f_e LDR\left[\left(M_z\right)q_0 p_r + \gamma\left(Z + D_f\right)\left(A_z\right)BL\right] \quad (34)$$

where $M_z = M_{xz} + M_{yz}$, and

$A_z = A_{xz} + A_{yz}$

Charts have been prepared for J_{xz}, J_{yz}, I_{xz}, I_{yz}, M_{xz}, M_{yz}, A_{xz} and A_{yz} corresponding to different Z/B values for various values of L_x or L_y and for L/B ratio of 1, 2 and 3 (Kumar, 1997; Kumar and Saran, 2003a).

Analysis of closely spaced strip footings

Due to heavy loads and non-availability of good construction sites, engineers have to place the footings at closer spacing. Therefore, the footings in the field generally interfere with each other to some extent and are rarely isolated (Stuart, 1962; Myslivee and Kysela, 1973; Singh et al., 1973; Saran and Agarwal, 1974; Siva Reddy and Mogaliah, 1996; Khadlikar and Verma, 1977; Deshmukh, 1978; Dembicki et al., 1981; Dash, 1981,1982; Patankar and Khadlikar, 1981; Das and Larbi-cherif, 1983; Graham et al., 1984; Pathak and Dewaikar, 1985; Verma and Saran, 1987; Saran and Amir, 1992; Siva Reddy and Manjunatha, 1996).

As a lot of research work in the area of isolated footings on reinforced soil suggests a considerable improvement in their bearing capacity and settlements, the study of closely spaced footings on reinforced soil is of paramount practical significance. Al-Ashou et al. (1994) studied experimentally the effect of number of layers of reinforcement on the bearing capacity of closely spaced square and strip footings resting on reinforced sand. They have reported that interference between adjacent square footings on reinforced sand is insignificant contrary to the unreinforced sand, but it has a pronounced effect on the bearing capacity of adjacent strip footings.

An analytical method has been presented for determining the pressure corresponding to a given settlement for the closely spaced strip footings resting on reinforced sand (Kumar, 1997; Kumar and Saran, 2003b).

Computation of driving force in reinforcement (T_D)

Consider two strip footings, each of size, B and placed at a clear spacing of S. Let both the footings be loaded simultaneously with uniformly

distributed load, q. The normal and shear stresses can be calculated at any depth Z using the theory of elasticity (Poulos and Davis, 1974) by superimposing the stresses induced by adjacent footings. Figure 50 shows the distribution of shear stresses beneath the interfering footings at a certain depth Z. Let X_0 be the horizontal position of zero shear stress and X_1, X_2 be the shear stress peaks as shown in Fig.51. With the change in spacing between the footings and depth beneath the footing, values of X_0, X_1 and X_2 change. The loci of points of maximum shear stress have been assumed as the surface separating the downward and lateral flow (Fig.50). The location of the separating planes can only be inferred from the location of broken ties (Binquet and Lee, 1975a) and deformation pattern of reinforcement after failure (Al-Ashou et al., 1994; Kumar, 1997). For the reinforcement layer placed at a depth lower than that corresponding to level c', the failure of reinforcement can take place along aa' or bb' or dc' or cc'. At higher depths, there will be only one shear stress peak obtained from the superposition of shear stresses under the interfering footings as shown at level C (Fig.50) and the reinforcement can break only along aa' or bb' (Fig.50). The driving force T_D is given by:

$$T_D = \left[J_z B - I_z \Delta H\right] q_0 \left(p_r - 1\right) \tag{35}$$

where $T_D = T_{D1} + T_{D2}$ (T_{D1} and T_{D2} are shown in Fig.51.) (35a)

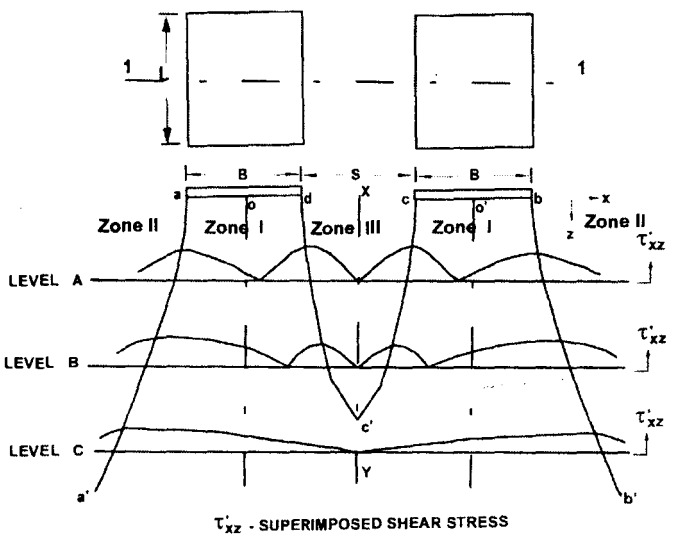

FIGURE 50 : Shear Stress Distribution between Interfering Footings (Section 1-1)

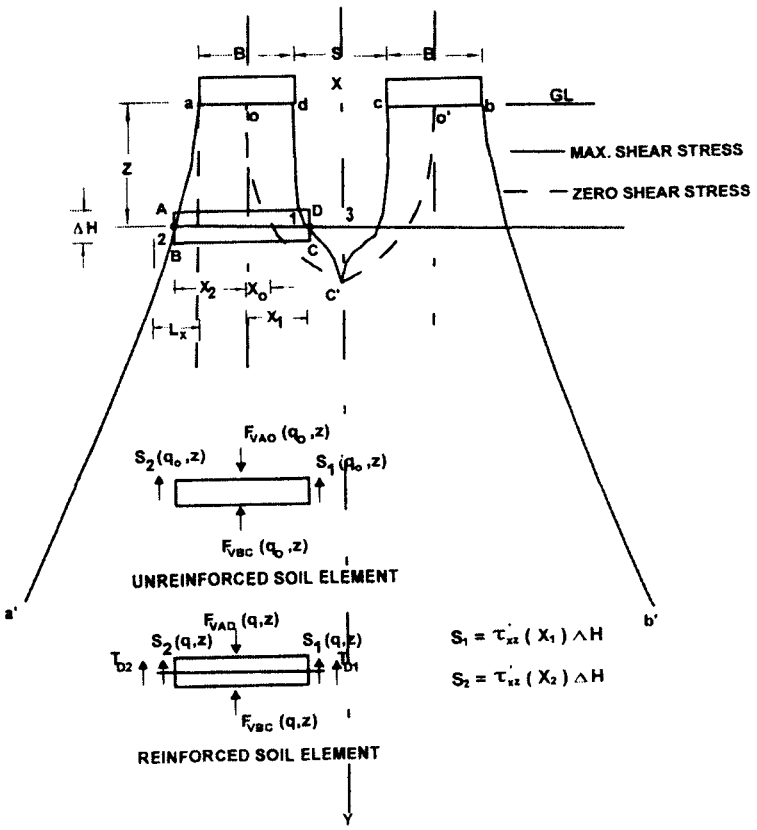

FIGURE 51 : Assumed Separating Plane and Components of Forces for Pressure Ratio Calculation of Adjacent Strip Footing on Reinforced Soil

T_{D1} and T_{D2} are shown in Fig.51.

$$I_Z = I_{Z1} + I_{Z2}$$

$$I_{Z1} = \frac{\tau'_{xz}\left(\frac{X_1}{B}, \frac{Z}{B}\right)}{q} \qquad (35b)$$

$$I_{Z2} = \frac{\tau'_{xz}\left(\frac{X_2}{B}, \frac{Z}{B}\right)}{q} \qquad (35c)$$

$$Jx = \frac{\int_{-X_2}^{X_1} \sigma'_z dx}{qB} \qquad (35d)$$

where, σ'_z and τ'_{xz} are the normal and shear stresses obtained after superposition of stresses of interfering footings and q is the applied load.

The values of X_0/B, X_1/B, X_2/B, J_Z and I_Z have been presented in the form of non-dimensional charts for various depths, expressed as Z/B and for S/B equal to 0.5, 1.0, 2.0, 3.0 (Kumar, 1997; Kumar and Saran, 2003b).

Computation of reinforcement-pull-out frictional resistance (T_f)

The pull out frictional resistance shall be due to the vertical normal force on the length of the reinforcement, which is outside the assumed plane separating the downward and the outward flow. The normal force consists of two components. One is due to the applied bearing pressure and the other is due to the normal overburden pressure of the soil.

The reinforcement pull out frictional resistance per unit length of the strip footing placed at depth D_f is, given by:

$$T_{f1} = 2f_e LDR\left[M_{z1}Bq_0p_r + \gamma(L_1 - X_1)(Z + D_f)\right] \tag{36}$$

$$T_{f2} = 2f_e LDR\left[M_{z2}Bq_0p_r + \gamma(L_2 - X_2)(Z + D_f)\right] \tag{37}$$

where T_{f1} = pull out frictional resistance per unit length of the strip footing at depth, Z, developed due to the reinforcing length beyond the assumed plane, dc′ and

T_{f2} = pullout frictional resistance per unit length of the strip footing at depth, Z, developed due to reinforcing length beyond the assumed plane aa′.

$$M_{z1} = \frac{\int_{X_1}^{L_1} \sigma'_z dx}{qB} \tag{37a}$$

$$M_{z2} = \frac{\int_{X_2}^{L_2} \sigma'_z dx}{qB} \tag{37b}$$

where σ'_Z = superimposed normal stress at depth Z and q is the applied load

$$L_2 = 0.5B + L_x \tag{37c}$$

$L_1 = 0.5B + L_x$, for discontinuous reinforcement (37d)

$= (S+B)/2$ for continuous reinforcement, (37e)

S = clear spacing between the footings

L_x = Extension of reinforcement beyond the edge of footing on either side of footing, if the reinforcement is discontinuous.

= Extension of reinforcement beyond the outer edge of footing, if the reinforcement is continuous.

f_e = mobilized friction coefficient.

Non-dimensional charts have been prepared for M_{z1} and M_{z2} at different Z/B values for S/B equal to 0.5, 1.0, 1.5, 2.0 and 3.0 for continuous reinforcement, for L_x/B values as 0.5, 1.0 and 1.5. Non-dimensional charts have also been prepared for discontinuous reinforcement for S/B values of 2.0 and 3.0 for L_x/B values of 0.5 and 1.0 (Kumar, 1997; Kumar and Saran, 2003b). The stress equations have been evaluated by numerical integration.

Analysis of closely spaced rectangular footings

Kumar and Saran (2003a) approach for isolated rectangular footings has been extended to closely spaced rectangular footings. Consider two rectangular footings, each of length, L and width, B placed close to each other at a clear spacing of S. When both the footings are loaded simultaneously, the footing and the soil beneath moves in the downward direction associated with lateral flow of soil on either side. The downward moving zone (Zone I, Fig.50) yields the value of the driving force. That driving force is compared with the rupture strength and soil-reinforcement frictional resistance of strip length in the outward moving zones (Zone II and III, Fig.50) so as to determine the pressure ratio in rupture and pull out failure respectively. The reinforcement layer can be continuous or discontinuous under the two closely spaced footings.

Computation of driving force in reinforcement (T_D)

Let each footing be loaded with uniformly distributed load, q. Then normal and shear stresses can be calculated at any point (x, y, z) using the theory of elasticity (Poulos and Davis, 1974) by superimposing the stresses induced by the adjacent footing. When the load on the footing increases, the central zone of soil moves down with respect to outer zones. The boundary between the downward moving and outward moving zones has been assumed as the locus of points of maximum shear stress at every depth, Z. The

location of separating planes can only be inferred from the location of broken ties (Binquet and Lee, 1975a) and the deformation pattern of reinforcement after failure (Al Ashou et al., 1994; Kumar, 1997).

Let X_i and X'_i be the horizontal positions of shear stress peaks as shown in Fig.52. With change in spacing between the footings at different depth levels, the value of X_i and X'_i changes. The loci of points of maximum shear stress have been assumed as the plane separating the downward and lateral flow (Fig.52) and accordingly, there will be three zones (downward moving Zone, I and outward moving Zones, II and III). At depth level

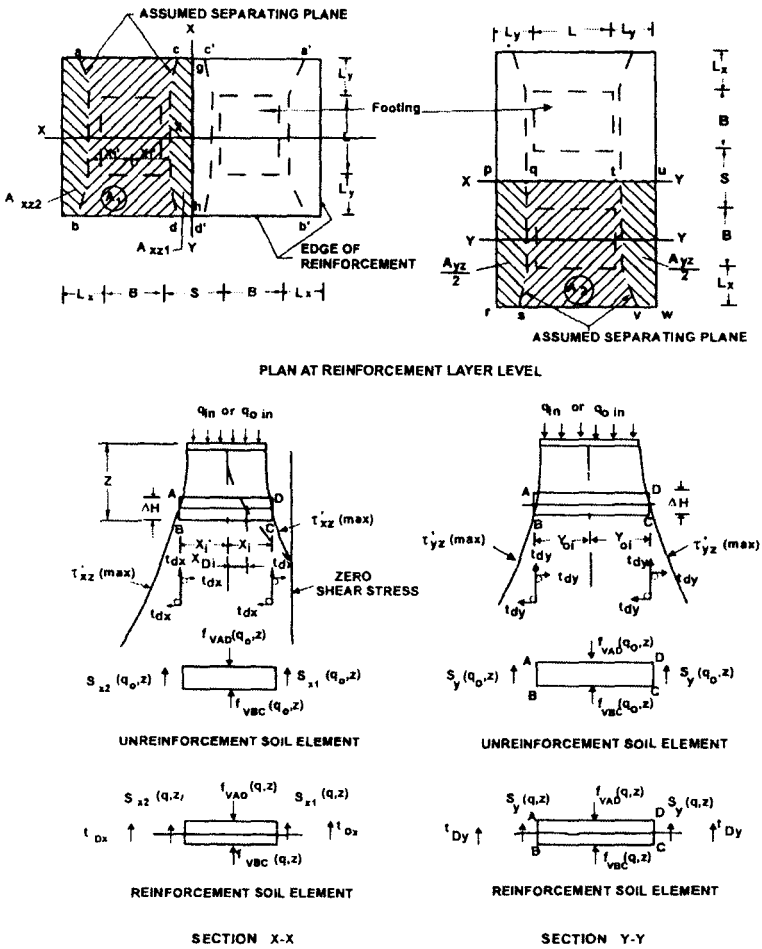

FIGURE 52 : Plan and Section of Assumed Separating Plane and Components of Forces for Pressure Ratio Calculation of Adjacent Rectangular Footing on Reinforced Soil

corresponding to point c′ shown in Fig.50 and lower than level of c′, there will be two zones (downward moving Zone I and outward moving Zone II). This depth is approximately 1.25B and 1.75B for S/B equal to 0.5 and 1.0 respectively for L/B equal to 1, 2 and 3 and is greater than 2B for S/B equal to 2.0. These depth values correspond to level c′ at and beyond which there will be only one shear stress peak obtained from superposition of shear stresses under the interfering footings.

The driving force in x-direction, T_{Dx} may be written as:

$$T_{Dx} = \left[J_{xz}BL - I_{xz}\Delta HL\right]q_0\left(p_r - 1\right) \tag{38}$$

where, $p_r = q/q_0$ and T_{Dx} represents the driving force in x-direction when only one layer of reinforcement ($N_R = 1$) is provided up to depth Z,

$$I_{xz} = I_{xz1} + I_{xz2} \tag{38a}$$

$$J_{xz} = \frac{\sum_{i=1}^{i=n}\int_{-X_i}^{X_i}\sigma'_z(q, x, y, Z)\,dx\delta y}{qBL} \tag{38b}$$

$$I_{xz1} = \frac{\sum_{i=1}^{i=n}\tau'_{xz}(X_i, Z)\delta y}{qL} \tag{38c}$$

$$I_{xz2} = \frac{\sum_{i=1}^{i=n}\tau'_{xz}(X'_i, Z)\delta y}{qL} \tag{38d}$$

where σ'_Z = normal stress obtained after superposition of stresses of interfering footings

τ'_{xz} = shear stress obtained after superposition of stresses of interfering footings and

q = applied load.

The interval $(X_i + X'_i)$ is divided into small units of size 0.01B. The length of reinforcement, $(L + 2L_y)$ is divided into n intervals, each of width $\Delta y = 0.01B$. Here, L_y is the extension of reinforcement beyond the edge of footing in y-direction.

Similarly, the driving force in reinforcement in the y-direction is given by:

$$T_{Dy}(Z) = \left[J_{yz}BL - I_{yz}\Delta HB\right]q_0(p_r - 1) \tag{39}$$

$T_{Dy}(Z)$ represents the driving force in the y-direction when only one layer of reinforcement is provided upto depth, Z'

$$J_{yz} = \frac{\sum_{i=1}^{i=n} \int_{-Y_{0i}}^{Y_{0i}} \sigma'_z(q, x, y, Z)\,dy\delta x}{qBL} \tag{39a}$$

$$I_{yz} = 2 \cdot \frac{\sum_{i=1}^{i=n} \tau'_{yz}(Y_{0i}, Z)\delta x}{qB} \tag{39b}$$

Equations have been solved by numerical integration. The interval Y_{0i} is divided into small units of value 0.01B. The width of reinforcement, L_{x0} is divided into n intervals, each of width Δx = 0.01B. The normal force component, J_{yz} is the stress area A_2 shown hatched in Fig.52.

L_{x0} = B + $2L_x$, for discontinuous reinforcement

= B + L_x + 0.5S, for continuous reinforcement

L_x = Extension of reinforcement beyond either edge of the footing in x-direction, if the reinforcement is discontinuous.

= Extension of reinforcement beyond the outer edge of footing in x-direction, if the reinforcement is continuous.

Y_{0i} = The value of y at the i^{th} element corresponding to maximum value of τ'_{yz}

τ'_{yz} = Superimposed shear stress

The values of J_{xz}, J_{yz} and I_{xz}, I_{yz} have been presented in the form of non-dimensional charts for various depths, expressed as Z/B, for S/B equal to 0.5, 1.0 and 2.0, for L/B = 1, 2 and 3, for various L_x and L_y values (Kumar, 1997; Kumar and Saran, 2004a). ΔH is taken equal to vertical spacing between the horizontal layers of reinforcement, if layers are at equal vertical spacing and is equal to the average of two adjacent layers, if layers are at different vertical spacing. The total driving force is, therefore, given by:

$$T_D(Z) = T_{Dx}(Z) + T_{Dy}(Z) \tag{40}$$

Computation of pull-out frictional resistance (T_f)

The pull out frictional resistance shall be due to the vertical normal force on the area of the reinforcing layer that is outside the assumed plane separating the downward and outward flow. The normal force consists of two components. One is due to the applied bearing pressure and the other, due to the normal overburden pressure of the soil.

Total pull out frictional resistance in x-direction is, therefore, given by:

$$T_{fx} = 2f_e LDR\left[M_{xz} q_0 p_r + \gamma A_{xz}\left(Z + D_f\right)\right]LB \tag{41}$$

where $T_{fx} = T_{fx1} + T_{fx2}$

T_{fx1} = pull out frictional resistance at depth, Z, developed due to the reinforcing area beyond the assumed separating plane cd

T_{fx2} = pullout frictional resistance at depth Z; developed due to reinforcing area beyond the assumed plane ab

f_e = mobilized friction coefficient.

$$M_{xz} = M_{xz1} + M_{xz2} \tag{41a}$$

$$A_{xz} = A_{xz1} + A_{xz2} \tag{41b}$$

$$M_{xz1} = \frac{\sum_{i=1}^{i=n} \int_{X_i}^{L_1} \sigma'_z(q, x, y, Z)\,dx\delta y}{qBL} \tag{41c}$$

$$M_{xz2} = \frac{\sum_{i=1}^{i=n} \int_{X'_i}^{L_2} \sigma'_z(q, x, y, Z)\,dx\delta y}{qBL} \tag{41d}$$

$$A_{xz1} = \frac{\sum_{i=1}^{i=n} (L_1 - X_i)\delta y}{LB} \tag{41e}$$

$$A_{xz2} = \frac{\sum_{i=1}^{i=n} (L_2 - X'_i)\delta y}{LB} \tag{41f}$$

Equations have been solved by numerical integration. The interval $(L_1 - X_i)$ and $(L_2 - X'_i)$ is divided into small units of value 0.01B. The width of reinforcement, L_{y0} is divided into n intervals, each of width $\delta y = 0.01B$.

Similarly

$$T_{fy} = 2f_e LDR\left[M_{yz} q_0 p_r + \gamma A_{yz}\left(Z + D_f\right)\right] LB \tag{42}$$

$$M_{yz} = 2 \cdot \frac{\sum_{i=1}^{i=n} \int_{Y_{0i}}^{(0.5L+L_y)} \sigma'_z(q, x, y, Z)\, dy \delta x}{qBL} \tag{42a}$$

$$A_{yz} = 2 \cdot \frac{\sum_{i=1}^{i=n} \left(0.5L + L_y - Y_{0i}\right) \delta x}{LB} \tag{42b}$$

Equations have been solved by numerical integration. The interval Y_{0i} is divided into small units of value 0.01B. The width of reinforcement, $(L_1 + L_2)$ is divided into n intervals, each of width, $\delta x = 0.01B$.

Non-dimensional charts have been prepared for M_{xz1}, M_{xz2}, M_{yz}, , A_{xz1}, A_{xz2} and A_{yz} at different Z/B values for S/B equal to 0.5, 1.0 and 2.0 for L/B ratio equal to 1.0, 2.0 and 3.0 (Kumar, 1997; Kumar and Saran, 2004a).

The forces T_{Dx}, T_{Dy}, T_{fx} and T_{fy} are the forces in x and y directions only. As the reinforcement would be pulled out simultaneously from all the directions with the application of load on the footing, the direction giving an average value of pressure ratio has been adopted. Thus, the direction making an angle of 45° with x or y direction gives the average value and has been adopted for the calculation of pressure ratio, which coincidentally gives the results obtained by adding the forces in x and y directions. Total driving force is, therefore, given by:

$$T_D = T_{Dx} + T_{Dy} = \left[\left(J_{xz} + J_{yz}\right) BL - \left(I_{xz} L + I_{yz} B\right) \Delta H\right] q_0 \left(p_r - 1\right)$$

$$= \left[\left(J_z\right) BL - \left(I_{xz} L + I_{yz} B\right) \Delta H\right] q_0 \left(p_r - 1\right) \tag{43}$$

where $$J_z = J_{xz} + J_{yz} \tag{43a}$$

The total pull-out frictional resistance, T_f is, therefore, given by:

$$T_f = T_{fx} + T_{fy}$$

$$= 2f_e LDR\left[\left(M_{xz} + M_{yz}\right)q_0 p_r + \gamma\left(Z + D_f\right)\left(A_{xz} + A_{yz}\right)BL\right]$$

$$= 2f_e LDR\left[\left(M_z\right)q_0 p_r + \gamma\left(Z + D_f\right)\left(A_z\right)BL\right] \quad (44)$$

where $M_z = M_{xz} + M_{yz}$, and

$A_z = A_{xz} + A_{yz}$

Pressure ratio calculation

T_D is the driving force in the reinforcement, if there is only one layer of reinforcement provided in the foundation soil at depth, Z. When, N_R layers of reinforcement are provided in the foundation soil, the load carried by the upper layers affects the normal force on the lower layers of reinforcement. For N_R layers of reinforcement, let the load be distributed in proportion of $r_1 : r_2 : r_3 : \ldots : r_{NR}$ such that $r_1 + r_2 + \ldots + r_{NR} = 1$. Therefore, the driving force at different layer levels has been assumed to vary in proportion of $r_1 : r_2 : r_3 : \ldots : r_{NR}$ such that $r_1 + r_2 + \ldots + r_{NR} = 1$. After calculation of driving force and soil-reinforcement frictional resistance and tensile or breaking strength of reinforcing material, the value of p_r is computed by applying the following conditions:

i) The driving force in any reinforcing layer should not exceed the soil-reinforcement frictional resistance in that layer, i.e. $r_j T_{Dj} \leq T_{fj}$ where, j varies from 1 to N_R.

ii) The driving force in any reinforcing layer should not exceed allowable breaking strength, i.e., $r_j T_{Dj} \leq T_R$ where, $T_R = T_{Rx} + T_{Ry}$

Distribution factors, r_j's are assumed for distribution of driving force in N_R layers.

iii) $r_1 + r_2 + r_3 + \ldots + r_{NR} = 1$

A check is applied to various combinations of reinforcement pull-out and breaking failures, each giving one value of p_r. The smallest value is the critical p_r.

Ultimate bearing capacity of reinforced soil

With the help of proposed analysis, one can compute the pressure intensity of footing on reinforced soil at a settlement, Δ, corresponding to the given pressure intensity of the same footing on unreinforced soil for the

same settlement Δ. Therefore, the pressure-settlement values of a footing on reinforced soil can be computed only up to the ultimate bearing capacity of the same footing on unreinforced soil. The experimental results show that this does not give the ultimate bearing capacity of the footing on reinforced soil. The studies by Singh (1988), Huang and Tatsuoka (1990) and Kumar (1997) show that the bearing capacity of an isolated footing increases by reinforcing the soil zone immediately beneath the footing with footing size reinforcing layers up to depth, d_R and with a vertical spacing between the adjacent layers not exceeding 0.25B and the effect is similar to that of an unreinforced sand loaded with rigid deep footing having the same depth, $D_f = d_R$ and is the case of $D_f = d_R$ up to 1.0B. In the proposed analysis, pressure ratio (p_r) becomes unity when reinforcement does not extend beyond the edge of footing. It shows that the effect of footing size reinforcement beneath the footing has not been included in the calculation of p_r. Therefore, the following empirical equation is proposed for calculating the ultimate bearing capacity of an isolated footing on reinforced soil:

$$q_{ur} = q_r + \gamma d_R N_q \tag{45}$$

where q_r and q_{ur} are as shown in Fig.53, d_R is the depth of lower most layer of reinforcement and N_q is Terzaghi's bearing capacity factor.

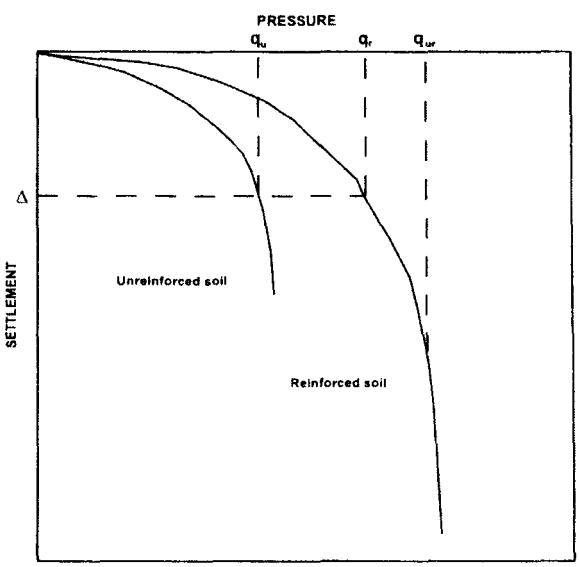

FIGURE 53 : General Nature of Pressure-Settlement Curves for Unreinforced and Reinforced Sand Supporting a Footing

The above equation has been validated with the model test results of Singh (1988), Youssef (1995), Kumar (1997), Adams and Collin (1997) and Kumar (2002).

Similarly, for closely spaced footings, if q_r (Fig.53) is the pressure intensity of the adjacent footings on reinforced soil at a settlement corresponding to ultimate bearing capacity of adjacent footings on unreinforced soil, q_u, then ultimate bearing capacity of adjacent footings on reinforced soil, q_{ur} (Fig.53) can be obtained from:

$$q_{ur} = q_r + \gamma d_R N_q \xi_q \tag{46}$$

where d_R is the depth of lower most layer of reinforcement, N_q is Terzaghi's bearing capacity factor and ξ_q is interference factor after Stuart (1962).

The theoretical results have been validated with the model test results of Kumar (1997) and Kumar and Saran (2003c). The values calculated match well with the experimental results.

Parametric study of footings resting on reinforced sand

In addition to the coefficient of friction between reinforcement and the soil in pull out, there are other parameters affecting the behaviour of footings on reinforced sand. The various parameters which have been studied are: number of layers of reinforcement, depth of first layer of reinforcement, vertical spacing between the layers of reinforcement, length of reinforcement, depth of reinforcement, tensile strength of reinforcement, size of footing and interference effects. Parametric study has been carried out on field size foundations using the analytical approach proposed by Kumar and Saran (2001c, 2002, 2004b). Field tests on prototype foundations give more realistic results in any geotechnical engineering problem. However, economic considerations and other practical difficulties either eliminate the prototype tests completely or restrict their scope to a greater extent. Thus, the findings of such an analytical study provide useful quantitative data, which can be subsequently used to study the effect of important variables through prototype tests.

The study has been carried out in terms of pressure ratio, p_r. Method based on non-linear constitutive laws of soil, suggested by Prakash et al. (1984) and Sharan (1977), has been used to determine the pressure at a given settlement for an isolated footing on unreinforced soil. For interfering footings on soil, the same method (Prakash et al., 1984) extended by Amir (1992), Saran and Amir (1992) and Kumar and Saran (2003d), has been used to determine the pressure at a given settlement for footing on unreinforced

soil. Drained triaxial shear tests were conducted on sand at a relative density of 60%, for determining the parameters of constitutive laws. The angle of internal friction of sand was obtained as $\phi = 37°$. The soil-reinforcement-friction angle, $\phi_f = 22°$, as obtained through pullout tests, has been used for the parametric study.

The various parameters, which have been studied, are:

(i) Depth of first layer of reinforcement (U/B)

If the depth of first layer of reinforcement is kept too large, failure of the soil may take place above the uppermost layer of reinforcement. When the first layer of reinforcement is placed at too shallow a depth, friction failure will reach early due to very low normal force on the reinforcement. Hence, there exists an optimum position for the placement of first layer of reinforcement.

It has been observed that, for isolated strip footings, the optimum range of U/B is 0.25 to 0.40 if more than one layer of reinforcement is provided and for single layer of reinforcement, its value is 0.7 and for isolated square footings the optimum range of U/B is 0.25 to 0.40 if more than one layer of reinforcement is provided and for single layer of reinforcement, its value is 0.6.

For interfering strip footings, it can be observed that the optimum range of U/B is 0.25 to 0.50 if more than one layer of reinforcement is provided and for single layer of reinforcement its value is 0.7 and from the variation of p_r with U/B for different number of layers of reinforcement, for interfering rectangular footings, it can be observed that the optimum range of U/B is 0.25 to 0.50.

(ii) Vertical spacing of layers of reinforcement (S_V/B)

The variation of p_r with S_V/B for isolated strip footings clearly indicates that the optimum range of vertical spacing between the horizontal layers of reinforcement is 0.10 to 0.25 and for isolated square footings, the optimum range of vertical spacing between the horizontal layers of reinforcement up to four layers of reinforcement is 0.15 to 0.25 whereas, for 5 layers of reinforcement, optimum value is 0.15B.

In case of interfering strip and rectangular footings, the optimum range of vertical spacing between the horizontal layers of reinforcement is 0.15 to 0.25. The vertical spacing of reinforcement also affects the p_r value because of the variation of the normal force on the reinforcement and due to lesser mobilization of friction as we go further down.

(iii) Length of reinforcement beyond the edge of footing (L_x/B)

With the increase in length of reinforcing layer, the frictional force increases due to increase in total normal force on the reinforcement. With the increase in L_x/B value beyond 2.5, the rate of increase of p_r is very small up to three layers of reinforcement. For four layers of reinforcement, pressure ratio increases even beyond 2.5B. It is the increase in overburden pressure on the reinforcing layers, which increases the, soil-reinforcement frictional resistance. However, to get this benefit for field size foundations, very high strength reinforcement is required. Further, it was observed that for field size foundation, for B greater than 1.0 m, p_r doesn't change with increase in length of reinforcement beyond the edge of footing for $L_x/B > 0.5$. This is due to the rupture failure of the reinforcement, which takes place before earlier than reaching the full benefit of frictional resistance which is developed due to increased length of reinforcement. So, the length of reinforcement beyond the edge of footing shouldn't be taken more than 1B so as to get the maximum benefit.

In case of interfering strip footings, with the increase in L_x/B value beyond 1.0, the rate of increase of p_r is very small both for $S/B = 1$ and 2. It is the increase in overburden pressure on reinforcing layers, which increases the soil-reinforcement frictional resistance. But, to get this benefit for field size foundations, very high strength reinforcement is required. Further, it was observed that for field size foundation i.e., for B greater than 1.0m, p_r doesn't change with increase in length of the reinforcement beyond the edge of footing for $L_x/B > 0.5$. This is due to the rupture failure of reinforcement, which takes place before reaching the full benefit of frictional resistance which is developed due to increased length of reinforcement. So, the length of reinforcement beyond the edge of footing shouldn't be taken more than 1B so as to get maximum benefit.

In case of isolated and closely spaced square footings, with the increase in size of reinforcing layer, the frictional force increases due to increase in total normal force on the reinforcement area in the lateral moving zone of soil. Figures 49 and 52 show that with the increase in L_x/B or L_y/B, p_r increases and the effect is more pronounced in case of small size footings when pullout failure is predominant. It is due to the increase in overburden pressure on reinforcing layers, which in turn, increase the soil-reinforcement frictional resistance. Further, to get the full benefit of reinforcement for field size foundations, a very high strength reinforcement is required. Therefore, reinforcement layer having extension of 1B beyond the edge of footing will be practical and economical in the field.

(iv) Number of layers of reinforcement

In case of isolated footings, the pressure ratio increases at a very low rate after a certain number of layers of reinforcement. The mobilization of friction is dependent on relative movement of soil and the reinforcement. The settlement of footing at the surface causes a vertical settlement of different magnitude at different layer levels, which is true because in granular soils and at large depths, settlement will not be felt. The mobilization of friction becomes almost zero at depth, 2B; the reinforcement provided beyond 2B depth shall not contribute to any increase in the pressure ratio. It was observed that after a depth of 1.5B is reached, the rate of increase of pressure ratio is very small. So the most beneficial depth up to which the reinforcement is provided should be 1.5B.

In case of interfering strip and square footings, the pressure ratio increases with the increase in number of layers of reinforcement. Keeping all other parameters constant, p_r increases at a very slow rate after a certain number of layers.

(v) Depth of reinforcement

As the mobilization of friction decreases with increase in depth due to reduction in settlement of soil, the pressure ratio does not increase if the reinforcement is provided at larger depths. The mobilization of friction becomes almost zero at depth, 2B; the reinforcement provided beyond 2B depth does not contribute to increase in pressure ratio. Further, it was observed that after a depth of 1.5B is reached, the increase in p_r rate is very small. So, the most beneficial depth up to which reinforcement is provided should be 1.5B.

(vi) Tensile strength of reinforcement

The soil-reinforcement frictional resistance and tensile strength of reinforcement govern the pressure intensity of a footing on reinforced soil. When the former is too high, the rupture failure of the reinforcement takes place earlier, which gives the low value of p_r. There occurs an increase in average pressure in reinforced soil with increase in tensile strength of reinforcement, keeping all other parameters constant.

(vii) Size of footing

If all other parameters are kept the same in terms of width of footing, the p_r value shall be same for every size of footing provided the rupture failure of reinforcement doesn't take place. It was observed that for reinforcement having safe tensile strength of 40 kN/m, the p_r values remain

same for 0.5 m and 1.0 m footing size. For low strength reinforcement, with the increase in size of footing, the normal force causing frictional resistance increases and rupture failure of reinforcement takes place earlier and hence p_r decreases. Similar trends have been found in interfering footings also.

Field tests on prototype foundations give more realistic results in any geotechnical engineering problem. However, economic considerations and other practical difficulties either eliminate the prototype tests completely or restrict their scope to a greater extent. Thus, the findings of such an analytical study provide useful quantitative data, which can be used subsequently to study the effect of important variables through prototype tests.

Dynamic Elastic Constants of Reinforced Soil

An experimental study was conducted to evaluate the dynamic elastic constants (C_u – coefficient of elastic uniform compression and C_τ – coefficient of elastic uniform shear) of sand (SP, $D_{10} = 0.19$ mm, $C_u = 1.1$) and reinforced sand (Saran and Sharma, 1994; Sharma, 1997; Saran et al., 1994; 1995, 1998). For this purpose, cyclic plate load tests and vertical and horizontal resonance tests were carried out. The sand was reinforced with geogrid (CE-121, $E = 1.86 \times 10^4$ kN/m^2). Cyclic plate load tests were performed on a model footing of size 150 mm × 150 mm on sand placed at two relative densities of 70% and 50% reinforced with different sizes of reinforcement and number of layers. Resonance tests were performed on a block of size 0.8 m × 0.4 m × 0.4 m deep on sand placed at a relative density of 70%. In these tests also, sizes and number of layers of reinforcement were also varied.

Typical test data has been produced below in Tables 10 and 11. Complete results are given elsewhere (Sharma, 1997).

Test results indicated that values of dynamic elastic constants reduce marginally with the increase in the amount of reinforcement. However, significant reduction was observed in resonance amplitude values with the increase of reinforcement (Sharma, 1997).

Conclusion

A. Strength and Deformation Characteristics of Reinforced Soil

i) The reinforced soil behaves like a brittle material in rupture failure and as a ductile material in friction failure. The strain at failure increases as the strength of reinforcement increases.

ii) Horizontal reinforcement in a triaxial test sample causes an increase in the strength of sample which evolves as an increase in angle of

Table 10 : Experimental Values of Coefficient of Elastic Uniform Compression – Cyclic Plate Load Tests

Footing Size 150 mm × 150 mm D_r = 70 %	Observed value of Cu ($kN/m^3 \times 10^5$)					Footing Size 150 mm × 150 mm D_r = 50 %	n = 4	Footing Size 300 mm × 300 mm D_r = 70 %	n = 4
	2	3	4	6	8				
Reinforcement size						Reinforcement size		Reinforcement size	
150 mm × 150 mm	2.22	2.04	1.80	1.58	1.45	150 mm × 150 mm	1.75	300 mm × 300 mm	1.95
300 mm × 300 mm	2.10	2.28	2.18	2.00	1.91	300 mm × 300 mm	1.82	600 mm × 600 mm	1.75
450 mm × 450 mm	2.25	2.10	2.08	2.03	2.02	450 mm × 450 mm	1.75	900 mm × 900 mm	1.63
600 mm × 600 mm	2.17	2.17	2.15	2.10	2.08	600 mm × 600 mm	1.86	1200 mm × 1200 mm	1.57
750 mm × 750 mm	2.35	2.32	2.40	2.36	2.16	750m × 750 mm	1.79	1500 mm × 1500 mm	1.54

n = No. of Reinforcement Layers

TABLE 11 : Experimental Values of Coefficient of Elastic Uniform Compression – Vertical Vibration Tests

Reinforcement Size	$\theta° \rightarrow$	Observed value of C_u ($kN/m^3 \times 10^5$)			
		4	12	20	28
0.8 m × 0.4 m	n = 2	1.17	1.095	1.047	1.000
	3	1.095	1.047	1.024	0.977
	4	1.095	1.000	0.977	0.954
	6	1.047	0.977	0.954	0.909
1.2 m × 0.6 m	n = 2	1.145	1.071	1.024	0.977
	3	1.145	1.047	1.000	0.932
	4	1.095	1.000	0.977	0.954
	6	1.071	1.000	0.954	0.909
1.5 m × 0.75 m	n = 2	1.120	1.024	0.977	0.909
	3	1.095	1.000	0.954	0.909
	4	1.095	1.000	0.954	0.887
	6	1.071	1.000	0.932	0.887
1.0 m × 1.0 m	n = 2	1.047	0.977	0.932	0.887
	3	1.024	0.954	0.909	0.887
	4	1.024	0.954	0.887	0.866
	6	1.000	0.932	0.887	0.866
1.2 m × 1.2 m	n = 2	1.071	0.977	0.954	0.932
	3	1.000	0.977	0.932	0.909
	4	0.954	0.932	0.887	0.866
	6	0.954	0.909	0.887	0.866
1.5 m × 1.5 m	n = 2	1.047	0.977	0.932	0.909
	3	1.000	0.977	0.909	0.887
	4	0.909	0.909	0.887	0.866
	6	0.954	0.909	0.887	0.866

friction when the sample fails due to slippage between soil and the reinforcement and as apparent cohesion when failure is caused by rupture of reinforcement.

B. Interfacial Friction Characteristics between Soil and Reinforcement

i) The coefficient of soil-strip interface friction, f^* decreases with an increase in the height of overburden and with reduced length of strip.

ii) Angle of sliding shear, δ, is more for strips having rough surface (bamboo) in comparison to smooth surface strips (aluminium). Linear relation exists between $\tan\delta/\tan\varphi$ (λ) and relative density (D_r) where φ is the angle of internal friction of sand.

C. Reinforced Soil-Wall

i) The variation of tension in reinforcing strips is non-linear with the maximum tension occurring close to wall face. The average slope of the stress-strain curve increases with reduction in the length of strip due to greater mobilisation of skin friction.

ii) Vertical stress near the face of the wall is close to the overburden stress and does not appear to be influenced by lateral thrust.

D. Wall with Reinforced Backfill

i) Unattached reinforcing strips reduce the lateral pressure intensity on the retaining walls.

ii) The resultant pressure on the wall is a function of the length of strips and the non-dimensional parameter, D_p and reduces with increase in these two parameters. For practical values of D_p, the resultant pressure is reduced to one-third by reinforcing the backfill with strips of length equal to 0.6 times the height of wall, H.

iii) The height of point of action of resultant above the base falls rapidly for reinforcement lengths in excess of 0.5H.

iv) The proposed analysis and design approach is validated by field trials and is recommended for use in appropriate field cases.

E. Footings on Reinforced Soil

i) A method of analysis has been presented for the following cases for calculating the pressure intensity to a given settlement in case of footings resting on reinforced soil : a) Isolated strip, square and

rectangular footings subjected to eccentric-inclined load, b) closely spaced strip/rectangular footings.

The process has been simplified by presenting the results in the form of non-dimensional charts, which can be directly used by practicing engineers.

ii) The results have been validated with small and large scale model tests.

Acknowledgements

This author is indeed very grateful to Indian Geotechnical Society for giving him an opportunity to deliver the prestigious IGS Annual Lecture during IGC-2004.

The matter embodied in this paper has been derived from the research work of Dr. D.V. Talwar, Dr. K.G. Garg, Dr. I.N. Khan, Dr. Z.T. Youssef, Dr. Arvind Kumar, Dr. S.K. Saran, Dr. Satyendra Mittal, Dr. M.M.A. Al-Smadi, Dr. Surendra Kumar, Dr. R.K. Sharma and Mr. V.K. Singh. The author was very closely associated with the work of these investigators.

Dr. K.G. Garg and Dr. Arvind Kumar helped the author in the preparation of the manuscript of the paper. Case history reported in the paper is from the work of Dr. K.G. Garg. Their help is gratefully acknowledged.

Dr. M.N. Viladkar helped in editing the manuscript and gave many fruitful suggestions.

Mr. Ravi Kant Mittal and Mr. K.C. Behera read the final manuscript and did some necessary corrections.

Author is also thankful to all my colleagues who encouraged me for this work and enlighten me from their valuable suggestions. Thanks are due to Sri Rajeev Grover for typing the manuscript, Sri Kameshwar Saini for the preparation of drawings and Sri Jai Prakash and his colleagues in xeroxing the matter from time to time.

References

AAMIR, A.A.A. (1992), "Interference effects on behaviour of footings", *Ph.D. Thesis*, Indian Institute of Technology, Roorkee.

ADAMS, MICHAEL T. and COLLIN, JAMES G, (1997). "Large model spread footing load tests on geosynthetic reinforced soil foundations", *Journal of Geotechnical and Geoenvironmental Engineering*, ASCE, Vol.123, No.1, pp.66-72.

AKINMUSURU, J.O. and AKINBOLADE, J.A. (1981) : "Stability of loaded footings on reinforced soil", *Journal of Geotechnical Engg. Division*, ASCE, Vol.107, No.GT6, pp.819-827.

AL-ASHOU, M.O., SULAIMAN, R.M. and MANDAL, J.N. (1994) : "Effect of number of reinforcing layers on the interference between footings on reinforced sand", *Indian Geotechnical Journal*, Vol.24(3), pp.285-301.

AL-SMADI, M.M.A. (1998) : "Behaviour of ring foundations on reinforced earth slab", *Ph.D. Thesis*, Indian Institute of Technology, Roorkee.

BACOT, J., ITLIS, M., LAREAL, P., PAUMIER, T. and SANGLERT, G. (1978) : "Study of the soil reinforcement friction coefficient", *Proc. Symposium on Earth Reinforcement*, ASCE, Pittsburgh, pp.157-185.

BINQUET, J. and LEE, K.L. (1975a) : "Bearing capacity tests on reinforced earth slabs", *Journal of Geotechnical Engg. Division*, ASCE, Vol.101, No.GT 12, pp.1241-1255.

BINQUET, J. and LEE, K.L. (1975b) : "Bearing capacity analysis of reinforced earth slabs", *Journal of Geotechnical Engg. Division*, ASCE, Vol.101, No.GT 12, pp.1257-1276.

BROMS, B.B. (1977) : "Triaxial tests with fabric reinforced soil", *International Conference on the Use of Fabrics in Geotechnics*, Paris, France, Vol.III, pp.129-133.

BROMS, B.B. (1987) : "Fabric reinforced soils", *Proc. International Symposium on Geosynthetics – Geotextiles and Geomembrane*, Kyoto, Japan, pp.13-54.

CASSARD, A., KERN, F. and MATHIEU, G. (1979) : "Use of reinforcement techniques in earth dams", *C.R. Coll. Int. Reinforcement des Sols*, Paris.

DASH, P.K. (1981) : "Interference between surface footing on purely cohesive soil", *Indian Geotechnical Journal*, Vol.11(4), pp.397-402.

DASH, P.K. (1982) : "Effect of an existing footing on the load carrying capacity of a foundation", *Indian Geotechnical Journal*, Vol.12(2), pp.160-165.

DAS, B.M. and LARBI-CHERIF, S. (1983) : "Bearing capacity of two closely spaced shallow foundations on sand", *Soils and Foundations*, Japanese Society of Soil Mechanics and Foundation Engg., Vol.23, No.1, pp.1-7.

DEMBICKI, E., JERMOLOMICZ, P. and NIEMUNIS, A. (1986) : "Bearing capacity of strip foundation of soft soil reinforced by geotextiles", *Proc. Third Int. Conf. on Geotextiles*, Vienna, Austria, Vol.2A/6, pp.205-208.

DEMBICKI, E., ODROBINSKI, W. and MORZEK, W. (1981) : "Bearing capacity of subsoil under strip foundations", *Proc. 10th Int. Conf. on Soil Mechanics and Foundation Engineering*, Stockholm, Vol.2, pp.91-94.

DESHMUKH, A.M. (1978) : "Interaction of different types of footings on sand", *Indian Geotechnical Journal*, Vol.8(4), pp.193-204.

DIXIT, R.K. and MANDAL, J.N. (1993) : "Bearing capacity of geosynthetic reinforced soil using variational method", *Journal of Geotextile and Geomembranes*, Vol.12(6), pp.543-566.

FRAGASZY, R.J. and LAWTON, E. (1984) : "Bearing capacity of reinforced sand subgrade", *Journal of Geotechnical Engg. Div.*, ASCE, Vol.110, No.10, pp.1500-1507.

GARG, K.G. (1988) : "Earth pressure behind retaining wall with reinforced backfill", *Ph.D. Thesis*, Indian Institute of Technology, Roorkee.

GARG, K.G. and SARAN, S. (1989) : "Earth Pressure on wall with reinforced backfill", *International Workshop on Geotextiles*, November, Vol.1, Bangalore, pp.75-79.

GARG, K.G. and SARAN, S. (1990) : "Evaluation of soil-reinforcement interface friction", *Proc. Indian Geotechnical Conference*, Vol.1, pp.27-31.

GARG, K.G. and SARAN, S. (1991) : "Behaviour of reinforced sand samples in triaxial shear", *Proc. IGC-91*, Vol.1, Surat.

GARG, K.G. and SARAN, S. (1997) : "Effective placement of reinforcement to reduce lateral earth pressure", *Indian Geotechnical Journal*, Vol.27, No.4, October issue, pp.353-376

GARG, K.G. (1998) : "Retaining wall with reinforced backfill – A case study", *Journal Geotextiles and Geomembrances*, Elsevier, Vol.16, pp.135-149.

GRAHAM, J., RAYMOND, G.P. and SUPPIAH, A. (1984) : "Bearing capacity of three closely spaced footings on sand", *Geotechnique*, Vol.34(2), pp.173-182.

GUIDO, V.A., BIESIADECKI, G.L. and SULLIVAN, M.J. (1985) : "Bearing capacity of geotextile-reinforced foundation", *Proc. 11th Int. Conf. on Soil Mechanics and Foundation Engg.*, San Francisco, Calf., Vol.5/c/3, pp.1777-1780.

GUIDO, V.A., CHANG, D.K. and SWEENEY, M.A. (1986) : "Comparison of geogrid and geotextile reinforced earth slabs", *Can. Geotech. J.*, Vol.23, pp.435-440.

HAJI ALI, F. and TEE, H.E. (1988) : "Monitoring of reinforced slope", *Proc. First Indian Geotextile Conf. on Reinforced Soil and Geotextiles*, Bombay, pp.D.9-D.14.

HAUSMANN, M.R. and LEE, K. (1978) : "Rigid model wall with soil reinforcement", *Proc. Symp. on Earth Reinforcement*, ASCE, Pittsburgh, pp.400-427.

HAUSMANN, M.R. (1976) : "Strength of reinforced soil", *Proc. Australian Road Research Board Conference*, Vol.VIII.

HUANG, C.C. and TATSUOKA, F. (1990) : "Bearing capacity of reinforced horizontal sandy ground", *Geotextiles and Geomembranes*, Vol.9, pp.51-80.

INGOLD, T.S. (1984) : "A laboratory investigation of soil-geotextile friction", *Ground Engineering*, November, pp.21-28.

JONES, C.J.F.P. (1978) : "The York method of reinforced earth construction", *Proc. Symposium on Earth Reinforcemeni*, ASCE, Pittsburgh, pp.501-527.

KATE, J.M., RAO, G.V., and TYAGI, S.K. (1988) : "Evaluation of soil reinforcement friction", *Indian Geotechnical Journal*, 18(2), pp.153-160.

KHAN, I.N. (1991) : "A study of reinforced earth wall and retaining wall with reinforced backfill", *Ph.D. Thesis*, Indian Institute of Technology, Roorkee.

KHAN, I.N. and SARAN, S. (1990) : "Influence of some factors on friction characteristics of reinforcing materials", *Proc. Indian Geotechnical Conference*, Vol.1, pp.23-25.

KHADLIKAR, B.S. and VERMA, B.S. (1977) : "Analysis of interference of strip footings by FEM", *Proc. 9th Int. Conf. on Soil Mech. And Found. Engg.*, Tokyo, Japan, Vol.1, pp.597-600.

KHING, K.H., DAS, B.M., PURI, V.K., COOK, E.E. and YEN, S.C. (1992) : "Bearing capacity of two closely spaced strip foundations on geogrid-reinforced sand", *Journal of Geotextiles and Geomembranes*, Vol.12, pp.351-361.

KHING, K.H., DAS, B.M., PURI, V.K., COOK, E.E. and YEN, S.C. (1993) : "The bearing capacity of strip foundation on geogrid reinforced sand", *Journal of Geotextiles and Geomembranes*, Vol.12, pp.351-361.

KHING, K.H., DAS, B.M., PURI, V.K., YEN, S.C. and COOK, E.E. (1994) : "Foundation on strong sand underlain by weak clay with geogrid at the interface", *Geotextiles and Geomembranes*, Vol.13, pp.199-206.

KUMAR, A. (1997) : "Interaction of footings on reinforced earth slab", *Ph. D. Thesis*, Indian Institute of Technology Roorkee, Roorkee, India.

KUMAR, A. and SARAN, S. (2000a) : "Analysis of square footing on reinforced soil foundations", *Proc. Int. Conf. on Construction Industry*, Chandigarh, Vol.III, pp.501-510.

KUMAR, A. and SARAN, S. (2000b) : "Soil-reinforcement friction and tensile strength of geogrid", *Proc. All India Workshop on Ground Improvement*, Kurukshetra, pp.103-109.

KUMAR, A. and SARAN, S. (2000c) : "Isolated strip footing on reinforced soil – A parameter study", *Proc. New HOCE-2000*, December, Vadamavandal (Tamilnadu).

KUMAR, A. and SARAN, S. (2001a) : "Isolated strip footings on reinforced sand", *Journal of Geotechnical Engineering*, SEAGS, Bangkok, Thailand, pp.177-189.

KUMAR, A. and SARAN, S. (2001b) : "Adjacent strip footings on reinforced sand", *Proc. Int. Conf. in Civil Engineering (ICCE-2001)* : IISc., Bangalore.

KUMAR, A. and SARAN, S. (2001c) : "Adjacent square footings on reinforced sand", *Proc. Structural Engg. Convention (SEC-2001)* : An International Meet, Roorkee.

KUMAR, A. and SARAN, S. (2002) : "Isolated square footing on reinforced soil – A parametric study", *Proc. A.I.C.M.-2002*, R.E.C., Hamirpur.

KUMAR, A. and SARAN, S. (2003a) : "Bearing capacity of rectangular footing on reinforced soil", *Journal of Geotechnical and Geological Engineering*, Kluwer Academic Publishers, The Netherlands, Vol.21, pp.201-224.

KUMAR, A. and SARAN, S. (2003b) : "Closely spaced strip footings on reinforced sand", *Journal of Geotech. Engineering*, SEAGS Bangkok, Thailand, Vol.34, No.3, pp.177-189.

KUMAR, A. and SARAN, S. (2003c) : "Closely spaced footings on geogrid reinforced sand", *Journal of Geotechnical and Geoenvironmental Engineering*, ASCE, Vol.129, Number 7, pp.660-664.

KUMAR, A. and SARAN, S. (2003d) : "Closely spaced rectangular footings on sand", *Journal of Civil Engineering Division*, Institution of Engineers, Kolkata, India Vol.84, May 2003, pp.27-32.

KUMAR, A. and SARAN, S. (2004a) : 'Closely spaced rectangular footings on reinforced sand", *Journal of Geotech and Geological.Eng.*, Vol.22, pp.497-524.

KUMAR, A. and SARAN, S. (2004b) : "Parametric study of footings resting on reinforced sand", *Journal of Civil Engineering Division*, Institution of Engineers, Kolkata, India (under review).

KUMAR, S. (2002) : "Behaviour of eccentrically and obliquely loaded footings on reinforced earth Slab", *Ph.D. Thesis*, Indian Institute of Technology, Roorkee.

LONG, N.T., GUEGAN, Y. and LEGEAY, G. (1972) : "Etude de la Tenre Armee a l Appreil Triaxial", *Repport de Recherche du Laboratorie Central Des Ponts et Chaussess*, Paris, No.17.

MALLINDER, F.P. (1978) : "The use of FRP as reinforcing elements in reinforced soil systems", *Ground Engineering*, October, pp.19-22.

MANDAL, J.N. and DIVSHIKAR, D.G. (1988) : "Large scale shear box tests with inclined reinforcement", *Proc. First Indian Geotextiles Conference on Reinforced Soil and Geotextiles*, Bombay, pp.C.73-C.77.

MANDAL, J.N. and MANJUNATH, V.R. (1990) : "Bearing capacity of single layer of geosynthetic sand subgrade", *Proc. IGC-90*, Bombay, India, Vol.1, pp.7-10.

MANDAL, J.N. and SHAH, H.S. (1992) : "Bearing capacity tests of geogrid reinforced clay", Technical Note, *Geotextiles and Geomembranes*, Vol.11, pp.327-333.

MCGOWN, A. and ANDRAWES, K.Z. (1977) : "The influence of non-woven fabric inclusions on the stress-strain behaviour of a soil mass", *Proc. International Conference on the Fabrics in Geotechnics*, Paris, Vol.I, pp.161-166.

MCKITTRIK, D. (1978) : "Design, construction, technology and performance of reinforced earth structures", *Proc. Symposium on Earth Reinforcement*, ASCE, Pittsburgh, pp.596-617.

MITTAL, S. (1998) : "Behaviour of retaining wall with reinforced c-ϕ soil backfill", *Ph.D. Thesis*, Indian Institute of Technology, Roorkee.

MIYAMORI, T., IWAI, S. and MAKIUCHI, K. (1986) : "Frictional characteristics of non-woven fabrics", *Proc. III Conference on Geotextiles*, Vienna, Austria, Vol.III, pp.701-705.

MURTHY, B.R.S., SRIDHARAN, A. and SINGH, H.R. (1993) : "Analysis of reinforced soil beds", *Indian Geotechnical Journal*,Vol.23(4) : pp.447-458.

MYSLIVEE, A. and KYSELA, Z. (1973) : "Interaction of neighbouring foundation", *Proc. 8th Int. Conf. on Soil Mechanics and Foundation Engg.*, Moscow, Vol.1(3) : pp.181-184.

NARAIN, J., SARAN, S. and TALWAR, D.V. (1981) : "Laboratory behaviour of reinforced earth wall", *Xth International Conference on Soil Mechanics and Foundation Engineering*, Stockholm, Sweden, pp.753-756.

PASLEY, C.W. (1822) : *Experiments on revetments*, Vol.2, Murray, London.

PATANKAR, M.V. and KHADLIKAR, B.S. (1981) : "Nonlinear analysis of interference of three surface strip footings by FEM", *Indian Geotechnical Journal*, Vol.11(4), pp.327-344.

PATHAK, S.P. and DEWAIKAR, D.M. (1985) : "Study of interference of two footings by method of finite strips", *Proc. 2nd Int. Conf. on Computer Aided Analysis and Design in Civil Engineering*, Jan.-Feb., Roorkee, India, Vol.6, pp.39.

POULOS. H.G. and DAVIS, E.H. (1974) : *Elastic solutions for soil and rock mechanics*, John Wiley and Sons. Inc., New York.

PRAKASH, S., SARAN, S. and SHARAN, U.N. (1984) : "Footings and constitutive laws", *Journal of Geotechnicl Engg. Div.*, ASCE, Vol.110, No.10, pp.1473-1487.

RAO, G.V. and PANDEY, S.K. (1988) : "Evaluation of geotextiles – soil friction", *Indian Geotechnical Journal*, 18(1), pp.77-105.

RAO, G.V., KATE, J.M. and SHAMSHER, F.H. (1994) : "Soil improvement with geosynthetics", *XIII ICSMFE*, New Delhi, India, pp.1237-1240.

SAMATANI, N.C. and SONPAL, R.C. (1989) : "Laboratory tests of strip footing on reinforced cohesive soil", *Journal of Geotehnical Engg. Div.*, ASCE, Vol.115 No.9, 1326-1330.

SARAN, S and AGARWAL V.C. (1974) : "Interference of surface footings on sand", *Indian Geotechnical Journal*, Vol.4(2), pp.129-139.

SARAN, S. and AMIR, A.A.A. (1992) : "Interference between surface strip footings on cohesive soil", *IGC-92*, Calcutta, Vol.1, pp.77-81.

SARAN, S., GARG, K.G. and BHANDARI, R.K. (1882) : "Retaining wall with reinforced cohesionless backfill", *Journal of Geotech. Engg.*, ASCE, GT12, 118, 1869-1888.

SARAN, S., TALWAR, D.V. and VAISH, U.S. (1978) : "Some aspects of engineering behaviour of reinforced earth", *Symposium on Soil Reinforcing and Stabilizing Techniques*, Sydney, Australia, October, pp.40-49.

SARAN, S., TALWAR, D.V. and PRAKASH, S. (1979) : "Theoretical earth pressure distribution on retaining wall with reinforced earth backfill", *International Conference on Soil Reinforcement*, Paris, March, pp.139-144.

SARAN, S. and TALWAR, D.V. (1981a) : "Seismic pressure distribution on retaining walls with reinforced earth backfill", *International Conference on Recent Advances in Geotechnical Earthquake Engineering and Soil Dynamics*, St. Louis, MO, USA, pp.709-713.

SARAN, S. and TALWAR, D.V. (1981b) : "Laboratory investigation of reinforced earth slab", *Symposium on Engineering Behaviour of Coarse Grained Soils, Boulders and Rocks*, Hyderabad, December, 21-23, pp.389-394.

SARAN, S. and TALWAR, D.V. (1982) : "Behaviour of reinforced earth wall during earthquake", VII Symp. on Earthquake Engg., University of Roorkee, Roorkee, Vol.I, pp.477-482.

SARAN, S. and TALWAR, D.V. (1983) : "Analysis and design of retaining walls with reinforced earth backfills", *Journal I.E.*, Vol.64, Pt. CI, July, pp.7-14.

SARAN, S., RAO, A.S.R. and SINGH, H. (1985) : "Behaviour of eccentrically loaded footings on reinforced earth slab", *IGC Conference – 1985*, Vol.I, University of Roorkee, Roorkee, pp.117-122.

SARAN, S. and KHAN, I.N. (1988) : "Analysis of inclined retaining wall having reinforced cohesionless backfill with uniformly distributed surcharge", *Indian Geotechnical Journal*, Vol.28(3), pp.250-269.

SARAN, S. and KHAN, I.N. (1989a) : "Evaluation of frictional characteristics of earth reinforcing materials", *IGC-89*, Vol.1, Vishakhapatnam, pp.455-458.

SARAN, S. and KHAN, I.N. (1989b) : "A study on reinforced earth retaining wall", *International Workshop on Geotextiles*, November, Vol.1, Bangalore, pp.63-67.

SARAN, S. and KHAN, I.N. (1990) : "Seismic design of reinforced earth wall", *Ninth Symposium on Earthquake Engg.*, University of Roorkee, Roorkee, Vol.1, pp.563-582.

SARAN, S., GARG, K.G. and BHANDARI, R.K. (1992) : "Retaining wall with reinforced cohesionless backfill", *ASCE*, Geot. Engg. Division, Vol.118, No.12, December issue, pp.1869-1888.

SARAN, S. and SHARMA, R.K. (1994) : "Dynamic characteristics of reinforced earth", *Indian Geotechnical Society*, Terzaghi-1994, 2nd October.

SARAN, S., SHARMA, R.K. and LAVANIA, B.V.K. (1994) : "Horizontal vibration characteristics of geogrid reinforced sand beds", *Tenth Symposium on Earthquake Engineering*, November, University of Roorkee, Roorkee.

SARAN, S., SHARMA, R.K. and LAVANIA, B.V.K. (1995) : "Cyclic plate load tests on reinforced sand", *Third International Conference on Recent Advances in Geotechnical Earthquake Engineering and Soil Dynamics*, St. Louis, Missouri (USA) : April 2-7.

SARAN, S. and AGNIHOTRI, A. (1996) : "Evaluation of bearing capacity of strip footing resting on reinforced earth slab-theoretical analysis", *Conference on Civil Engg. Practices*, University of Roorkee, Vol.III, pp.1614-1619.

SARAN, S. and KUMAR, A. (1996) : "Interaction of surface strip footings on geogrid – reinforced sand", *Conference on Problematic Subsoil Conditions*, Terzaghi-96, Kakinada, pp.157-169.

SARAN, S. and GALAV, B. (1998) : "Behaviour of ring footings on reinforced sand under vertical and lateral loads", *G.E.N.-1998*, Allahabad.

SARAN, S. (1998) : "Behaviour of footings on reinforced sand", *Invited Lecture*, National Workshop on Reinforcement of Gravel and Slopes, Kanpur, August.

SARAN, S., LAVANIA, B.V.K. and SHARMA, R.K. (1998) : "Equivalent value of Cu of reinforced earth", *11th Symposium on Earthquake Engg.*, University of Roorkee, Roorkee, pp.333-342.

SARAN, S., GARG, K.G. and MITTAL, S. (2001) : "Model studies on retaining wall with reinforced cohesive backfill", *Proc. of Int. Conf. on Geotechnical and Environmental Challenges in Mountaineous Terrain*, Nepal Engg. College, Nepal, Nov. 6-7, pp.110-120.

SARAN, S. and AL SMADI, M.M.A. (2002) : "Model tests on ring footings on reinforced sand", *Indian Geotechnical Journal*, Vol.32, No.2, pp.173-186.

SARAN, S., YOUSSEF, Z.T. and BHANDARI, N.M. (2004) : "Stress strain characteristics of soil / reinforced soil and their modelling", *Indian Geotechnical Journal*, 34(1) : pp.64-79.

SARAN, S.K. (1998) : "Seismic earth pressures and displacement analysis of rigid retaining walls having reinforced backfill", *Ph.D. Thesis*, Indian Institute of Technology, Roorkee.

SCHLOSSER, F. and LONG, N.T. (1970) : "Compartment de I a Terre Armee a I Appareil Triaxial", *Rapport d active du Laboratories Cntral des Ponds et Chciusses*, Amee, Paris.

SCHLOSSER, F. and ELIAS, V. (1978) : "Friction in reinforced earth", *Proc. Symposium on Earth Reinforcement*, ASCE Pittsburgh, pp.735-761.

SHANKARIAH, B. (1991) : "Effect of size and type of reinforcement on bearing capacity of reinforced sand subgrade", *ICE-91*, Surat, India, pp.95-98.

SHARAN, U.N. (1977) : "Pressure settlement characteristics of surface footings from constitutive laws", *Ph.D. Thesis*, Indian Institute of Technology Roorkee, India.

SHARMA, R.K. (1997) : "Dynamic response of block foundation on reinforced earth slab", *Ph.D. Thesis*, Indian Institute of Technology, Roorkee.

SINGH, A., PUNMIA, B.C. and OHRI, M.C. (1973) : "Interference between adjacent square footings on cohesionless soil", *Indian Geotechnical Journal*, Vol.3(4) : pp.275-284.

SINGH, H.R. (1988) : "Bearing capacity of reinforced soil beds", *Ph.D. Thesis*, Indian Institute of Science, Bangalore.

SINGH, V.K. (1991) : "Strength and deformation characteristics of sand reinforced with geotextiles", *M.E. Thesis*, Indian Institute of Technology, Roorkee.

SIVA REDDY, A. and MOGALIAH, G. (1996) : "Interference between surface strip foundations on soil exhibiting anisotropy and non-homogeneity in cohesion", *J. Inst. of Engineers*, India, Vol.57, pp.7-13.

SIVA REDDY, A. and MANJUNATHA, K. (1996) : "Interference of strip footings on anisotropic sand", *Indian Geotechnical Journal*, Vol.26(2) : pp.152.

SREEKANTIAH, H.R. (1990) : "Loaded footing on geotextile reinforced sand bed", *IGC-90*, Bombay, India, Vol.1, pp.73-77.

SRIDHARAN, A. and SINGH, H.R. (1988) : "Effect of soil parameters on the friction coefficient in reinforced earth", *Indian Geotechnical Journal*,Vol.18, No.4,pp.322-339.

SRIDHARAN, A., Murthy, B.R.S. and Singh, H.R. (1988) : "Shape and size effects of foundations on the bearing capacity of reinforced soil beds", *IGC-88*, Allahabad, Vol.1, pp.205-210.

STUART, J.G. (1962) : "Interference between foundations with special reference to surface footings in sand", *Geotechnique*, Vol.12 (1), pp.15-23.

TALWAR, D.V. (1981) : "Behaviour of reinforced earth in retaining structures and shallow foundation", *Ph.D. Thesis*, Indian Institute of Technology, Roorkee.

TALWAR, D.V. and SARAN, S. (1983) : "Triaxial performance of a reinforced sand", *IGS Conference*, IIT Madras, December, pp.I.13-I.19.

TALWAR, D.V., SARAN, S. and SINGH, A. (1987) : "Reinforced earth-design principles and applications", *Current Practices in Geotechnical Engg.*, International Overviews, ISSN 0253-5122, Vol.4, pp.55-100.

VERMA, B.P. and CHAR, A.N.R. (1978) : "Triaxial tests on reinforced sand", *Proc. Symposium on Soil Reinforcing and Stabilising Techniques in Engg. Practice*, Sydney, Australia, October 16-19.

VERMA, G.S. and SARAN, S. (1987) : "Interference effects on the behaviour of footings", *9th South-East Asian Geotehnical Conference*, Bangkok, pp.229-239.

WALTER, P.D. (1978) : "Performance comparison of ribbed and smooth strips", *Symposium on Soil Reinforcing and Stability Techniques*, Sydney, Australia, pp.221-231.

YETIMOGLU, T., Wu, J.H. and Saglamer, A. (1994) : "Bearing capacity of rectangular footings on geogrid reinforced sand", *J. Geotehnical Engg.*, ASCE, Vol.120, No.12, pp.2083-2099.

YOUSSEF, Z.T. (1995) : "Investigations of plane frame-footings-reinforced soil interaction", *Ph.D. Thesis*, Indian Institute of Technology, Roorkee.

YONG, Z. (1972) : "Strength and deformation characteristics of reinforced sand", *Ph.D. Thesis*, University of California, Los Angeles.

Notations

B	=	Width of foundation
c	=	Cohesion
C_1, C_2, C_3, C_4	=	Constants
C_u	=	Uniformity coefficient
d_R	=	Depth of bottom most layer of reinforcement
D_{10}	=	Effective grain size
D_{50}	=	Mean grain size
D_p	=	Spacing coefficient
e_{min}	=	Minimum void ratio
e_{max}	=	Maximum void ratio
f_e	=	Mobilised frictional coefficient
f^*	=	Coefficient of apparent friction
FOS	=	Factor of safety

h_l = Depth at which spacing is required

H = Height of wall

H_r = Height of point of application P_r

H_q = Height of point of application P_q

I_F = Interference factor

K_γ = Coefficient of active earth pressure due to weight of backfill

K_q = Coefficient of active earth pressure due to surcharge

l' = Effective length of reinforcement

L = Length of reinforcing strip, Length of footing

L_x = Extension of reinforcement beyond the either edge of footing, for discontinuous reinforcement and extension of reinforcement beyond the outer edge of footing in x-direction, for continuous reinforcement

L_y = Extension of reinforcement beyond the either edge of footing in y-direction

N_q = Terzaghi's bearing capacity factor

N_R = Number of layers of reinforcement

p_θ = Uniform reaction intensity

p_y = Pressure intensity

p_r = Pressure ratio

P_γ = Total earth pressure due to backfill

P_q = Total earth pressure due to surcharge

q = Intensity of uniformly distributed surcharge on the soil surface, Average contact pressure of the same footing on reinforced soil

q_o = Average contact pressure on unreinforced soil

q_u = Ultimate bearing capacity of footing on unreinforced soil

q_{ur} = Ultimate bearing capacity of footing on reinforced soil

S = Clear spacing between the footings

S_V = Vertical spacing between the reinforcement layers

S_x = Horizontal spacing between reinforcing strips

S_z = Vertical spacing between reinforcement layers

t = Intensity of tension in the reinforcing strip

T = Maximum pull out load, Permissible tensile strength/m length of reinforcement

T_D = Vertically acting tensile force

T_{fx} = Soil-reinforcement frictional force in x-direction

T_{fy} = Soil-reinforcement frictional force in y-direction

T_{max} = Maximum tension

U = Depth of first layer of reinforcement from the base of footing

W = width of reinforcing strip

Z = Depth of reinforcing strip below soil surface

Z_1, Z_2, Z_3 = Distances measured from top of retaining wall

σ_3 = Confining pressure

σ_v = Normal pressure intensity at reinforcing strip level, vertical stress in soil

σ_z = Normal stress

γ = Unit weight of soil

ϕ = Angle of internal friction

γ_d = Dry density of soil

θ = Wedge angle

θ_γ, θ_q = Wedge angles

ξ_q = Interference factor

ϕ_f = Soil-reinforcement friction angle

$\tau_{z\ max}$ = Maximum shear stress

θ_{cr} = Critical rupture wedge angle

q_a = Allowable soil pressure

k_a = Coulomb's active earth pressure coefficient

T_f = Pull out frictional resistance per unit length of strip footing of depth Z

C_u = Coefficient of elastic uniform coefficient

C_τ = Coefficient of elastic uniform shear

E = Young's modulus